Studies of the physiological states of cross-striated muscle with the aim of understanding the underlying processes of the changes from one state to another

Thesis

STUDIES OF THE PHYSIOLOGICAL STATES OF CROSS-STRIATED MUSCLE WITH THE AIM OF UNDERSTANDING THE UNDERLYING PROCESSES OF THE CHANGES FROM ONE STATE TO ANOTHER

Linking narrative with selected publications submitted for the degree of Doctor of Sciences at the Open University by

Else Marie Bartels, PhD

Open University

Feb 1990

Date of submission: 22 February 1990

Date of award: 17 June 1990

LIST OF CONTENTS

Studies of the physiological states of cross-striated muscle with the aim of understanding the underlying processes of the changes from one state to another.

Over the years I have studied aspects of muscle contraction in preparations ranging from intact live muscle in vitro to gels made up of single muscle proteins, along the lines of Natori's (1986) pattern of decomposition and reconstruction. My objective has been to try to understand the underlying processes which make a muscle change from relaxation to rigor or from relaxation to contraction, and thereby shed some light on the excitation-contraction process and on contraction itself.

My PhD studies were on latency relaxation in muscles (Copenhagen 1974). This interesting phenomena appears as a drop in isometric tension preceding the contraction, and it is sarcomere length dependent. At the time, all possible models for the origin of the latency relaxation were linked to theories of excitation-contraction coupling (Sandow, 1966; D.K. Hill, 1968). It was therefore clear to me that I should continue my latency relaxation studies to clarify the link between the excitation and the start of the contraction.

In E.M. Bartels, J.M. Skydsgaard and O. Sten-Knudsen (1979) the time course of the latency relaxation in frog muscle, where the cisternae from the sarcoplasmic reticulum are located at the Z-line, was compared with the time course of the latency relaxation in rat muscle, where the cisternae are located at a fixed distance from the Z-line and in the overlap zone for the A- and I-filaments. The study showed that the amplitude of the latency relaxation is dependent on overlap between the A- and I-filaments, so in the case of no overlap, there is no latency relaxation. The biggest drop in tension was seen around a sarcomere length of 3.1 µm in both frog and mammalian muscle.

The time course in mammalian muscle was independent of sarcomere length up to the length where the cisternae are placed outside the A-I overlap zone, while the time course in frog muscle was dependent on sarcomere length at all lengths. The onset of the latency relaxation was found to be independent of sarcomere length in all skeletal muscles studied. This points towards a link with the Ca^{2+} release from the cisternae, and since the onset did not happen at the moment of stimulation, Ca^{2+}-binding to the I-filament must take some time. My conclusion on this piece of work was that latency relaxation is probably caused by a conformational change of the tropomyosin molecule as Ca^{2+} binds to the troponin in the I-filament (Haselgrove 1973), and this change causes an elongation of the I-filament (Haugen and Sten-Knudsen 1976).

A further study of the relation between latency relaxation, twitch and Ca^{2+} was carried out in hypertonic conditions, E.M. Bartels and P. Jensen (1982). Hypertonic conditions causes an osmotic shrinkage of the muscle cell (Dydynska and Wilkie 1963, Blinks 1965) and thereby a decrease in free cell water and in the diffusion constant for Ca^{2+}. The aim was to see if the latency relaxation showed the same dependency on sarcomere length in normal and in hypertonic conditions and to see how the changed Ca^{2+} diffusion constant would affect the time course of the latency relaxation. The hope was to see whether the latency relaxation was caused by a slackening of the sarcoplasmic reticulum membranes as suggested by Sandow (1966) or if it was, as mentioned, linked to an elongation of the I-filament. Both twitch and latency relaxation were found to decrease linearly with increasing hypertonicity, but the sarcomere length dependency did not change. The latency relaxation time course was extended in a way which suggested that Ca^{2+}-release itself was delayed (onset of the latency relaxation), but the major factor in the extended time course seemed to be the slower diffusion of Ca^{2+} and probably slower binding of Ca^{2+} to the I-filaments. The study confirmed the results of my electron microscopy studies (1979), which suggested that the origin of the latency relaxation is in the contractile system itself, as was earlier suggested by D.K. Hill (1968), and Haugen and Sten-Knudsen (1976).

So far all my research was concerned with studies of whole muscles, sometimes down to single fibres, but never down to closer studies of the processes inside the cell. As my interest for the next step after the excitation-contraction coupling, the actual contraction, grew, I joined Professor Elliott's research group in Oxford to look into the contractile system in preparations which could be classified as more or less 'pure' contractile systems in the form of glycerinated and skinned muscle preparations. The measuring methods were microelectrode techniques to measure Donnan potentials in the various regions of a muscle cell, and from the Donnan potentials to calculate the protein charge concentration. X-ray and laser diffraction techniques were used to define the volume of the contractile apparatus so as to be able to relate charges to filaments or protein molecules. The charge measurements were based on the interesting and pioneering microelectrode studies of glycerinated muscle by Collins and Edwards (1971) and Pemrick and Edwards (1974), and the theoretical considerations given by Elliott (1973).

Although the work began in the spirit of adventure, to try to validate and extend the estimate of protein charge that had been made by Collins and Edwards (1971) and also by Elliott (1973), as it has continued, it has become clear that my objective must be to generate a major change in the paradigm of muscle research. The muscle research community has for more than twenty years been looking for changes in the orientation of the myosin S1 crossbridge when attached to actin during the contractile process, and has failed to find unequivocal evidence of this change. My own studies have convinced me that only when the paradigm is enlarged to include the

electrical environment, the electrical double layer that must exist between the actin and myosin filaments, will we find a modified model for crossbridge behaviour that will be seen to be physically satisfactory. To this end I have continued to make electrical measurements on skinned muscle fibres, and to try to convince the muscle research communities of the relevance of these measurements.

When one uses a technique which is novel and uncommon, it is necessary first to validate the method beyond question. To make sure that it was appropriate to use microelectrodes to measure Donnan potentials, and from these measurements to calculate protein fixed charge concentration, the theoretical and practical aspects of using KCl-filled microelectrodes in muscle treated as an extended polyelectrolyte gel were considered in G.F. Elliott and E.M. Bartels (1982). The conclusion of this paper was that the potential measurements can indeed be interpreted to give the fixed electric charge on the protein filament lattice in the manner introduced earlier by Collins and Edwards (1971) and modified and extended by Elliott *et al* (1978). This is true within the experimental regime whether the microelectrode senses the local potential average or the local average of the free ionic concentrations. A further discussion of the acceptability of the method was given in G.F. Elliott, E.M. Bartels, P.H. Cooke and K. Jennison (1984), where the Donnan potential measurements for calculating fixed electric charges on the A- and I-filaments were defended against a challenge from Godt and Baumgarten's (1984) ion-selective electrode measurements at different pH's, ionic strengths and physiological states. Godt and Baumgarten's measurements confirmed data from both Collins and Edwards (1971) and Bartels and Elliott (1980, 1981, 1982) and were shown to be explicable from Donnan theory. With this establishment that the method applied was acceptable the detailed muscle studies could begin.

If the volume of the filament lattice stays constant in a skinned muscle fibre a protein charge concentration measurement will be useful in discussing the function of the contractile apparatus, since it will be directly related to the charges on the protein filaments. In most practical cases, it is important also to describe the volume changes between states to take them into account when comparing charge changes. In all our muscle experiments the volumes of the filament lattice were measured with a combined laser and X-ray diffraction method.

Our first muscle full-length paper on the experimental measurements was G.R.S. Naylor, E.M. Bartels, T.D. Bridgman and G.F. Elliott (1985). In this paper only A-band charges were studied and these only in the rigor state, to characterize the A-band charges' dependency on sarcomere length, ionic strength and pH. The results showed that the potentials were independent of sarcomere length, which indicates that the protein charge concentration is constant in any given condition, that the A-band charge increased with increasing ionic strength up to μ = 0.071 M after which it started to decrease. The

A-band charge is higher than could be expected from the amino acid sequence of myosin at all ionic strengths beyond μ = 0.015 M and increases linearly with ionic strength up to μ = 0.071 M. A result like this points towards ion binding to the filaments, possibly chloride and phosphate binding. The binding considered is a binding in 'Saroff' sites i.e. extended charged side-chain networks between the myosin chains or molecules. (See Saroff, 1973; Bartels and Elliott, 1985).

The A-band charge was also found to be strongly dependent on pH (as Collins and Edwards had seen in their 1971 study). The isoelectric point varied with ionic strength, and below the isoelectric point the potentials were found to be positive. This gave a further confirmation of the credibility of the measuring methods, since the pH data confirmed titration data on purified myosin (Sarkar, 1950).

Theoretically, it seems trivial to measure Donnan potentials in the A- and the I-bands separately with microelectrodes, because the area the electrode tip is sampling is small enough to separate the two bands. In reality it is not so easy, especially at lower sarcomere lengths, because it is difficult to line the electrode up and have contrast enough to see the position of the electrode tips in the A- and the I-bands clearly. After some experimenting, I succeeded in setting up a system with high power light microscopy (400 X) and phase and polarization contrast which at the same time allowed easy movement of the microelectrode. This effort was necessary because there was no reason to believe that the protein charge concentration in the A- and the I-band is the same in all conditions or states. To look into this problem, A- and I-band charges were studied in both the rigor and the relaxed state, in glycerinated muscle, the 'pure' contractile system, and in chemically-skinned muscle, where the internal S.R. membranes in the cell are intact. The results were described in E.M. Bartels and G.F. Elliott (1985). In rigor the negative fixed charge in the A-band was higher than the negative fixed charge in the I-band, while the A- and the I-band had the same fixed electric charge in a relaxed muscle. When looking at the glycerinated muscle, the relaxed muscle showed a drop in negative fixed charge from the rigor muscle, and the largest charge change was seen in the A-band. This charge change happened whether or not the myosin heads were cross-linked to the I-filaments and is possibly created by a binding of ATP (and certain other ligands like PP_i) to the myosin molecule which again causes a disseminated change that modifies the ion-binding capacity of the myosin rods or parts of them. In skinned muscle preparations the same charge pattern as in glycerinated muscle was seen between rigor and relaxed state, except that it looked as if an extra charge was added along the whole length of the contractile apparatus. A possible candidate for this extra charge is ATP bound to the sarcoplasmic reticulum membranes. This was confirmed in E.M. Bartels, G.F. Elliott and R. S. Wall (1987), where we studied pellets of sarcoplasmic reticulum membranes in rigor and relaxed condition and showed that ATP does indeed cause a rise in negative fixed electric charge on the sarcoplasmic reticulum membranes.

Since the most dramatic charge changes were found in the A-band, a study of the A-filaments was started and especially a study of the main A-band protein myosin. In G.F. Elliott, E.M. Bartels and R.A. Hughes (1986) a physical-chemical approach was taken to the myosin filament in the various physiological states and the overall significance of the work was discussed in relation to current muscle thinking.

In both muscle A-bands and in myosin gel threads ATP caused a drop in fixed electric charge which will be described in detail later. The basic idea is that ATP binding must change the structure of the myosin molecule enough to change the ion-binding properties of the molecule. The effect was seen in purified myosin rod gel as well, so the most likely binding site for ATP (or PP_i which has the same effect) is the tail end of the myosin molecule. It is still not clear if the effect is caused by stripping off negative ions or by binding of more positive ions.

The observed charge changes were related to other effects which are relevant to the function of muscle. In agreement with Millman and Nickel (1980), our earlier work (Elliott and Bartels, 1982) confirmed that the calculated electrostatic repulsive force does not increase beyond a certain level with filament charge, and there is a charge saturation effect. The X-ray spacing between the muscle filaments is sensitive to the myosin charge and the X-ray data at low ionic strength showed that here the interfilament repulsive forces are not charge saturated in rigor or in relaxation.

Our data suggested that the muscle force could be generated by some ion-led change located in the S-2 link between the myosin head and the filament backbone. A specific model using a hypothetical change in this region was suggested by Harrington (1979). Another model could be ionic swelling in the filament lattice as the force producing factor, where the crossbridges function as dragging anchors to transform the transversal force into a longitudinal force. This model derives from Elliott, Rome and Spencer (1970), modified by Elliott *et al* (1978). Probably neither of these models are correct, and radical new thinking may be necessary within the enlarged paradigm which I mentioned earlier in this account.

Recent studies by Spudich and co-workers (Toyoshima *et al* 1987) showed that myosin (S1) heads are able to drive actin filaments in vivo in a system where actin-filaments move over a surface of myosin heads bound to a nitrocellulose film. These heads were produced in three different ways with three slightly different end-products which differed in length. The average speed of the actin was slower over all three types of heads compared to the movement over HMM or myosin, but the movement clearly happened. If the charge change that we see in myosin rod with ATP is directly linked with contraction and movement of the filaments, there is a discrepancy between the observations of Spudich and co-workers and our own experiments. Charge measurements on Spudich's myosin head preparations are not possible with our microelectrode

techniques, but might be possible using fluorescence techniques, which we are setting up in our laboratory at present. These charge measurements would show whether the end of Spudich's S1 preparation contained the part of the myosin rod which carry the charge changing site. My unpublished data on LMM showed no charge changes on the LMM part of myosin, so the charge changing site is on the rod towards S1. If the charge change in ATP is not found in Spudich's S1 preparation, and therefore is unlikely to be the force-generating event, it will be interesting to consider whether the speed of movement is related to the presence of the rod part of the myosin molecule. It has been shown that actin moves with the same speed over HMM and myosin (Toyoshima *et al* 1989), and it is clear that the polarity of the actin filament decides the direction of the movement. The charge change on the myosin rod with ATP cannot therefore be involved in directing the movement, but it may regulate the flexibility of the rod-head junction and thereby influence the speed of the movement, since the bidirectional movement of actin filaments over HMM in the Spudich experiments demands 180° rotational freedom for the myosin heads. Further data from the Spudich group may answer this question.

My own studies of myosin and myosin rod were a real challenge because for our experimental methods to be reliable, we required a completely pure gel of myosin and another of myosin rod. The protein concentration of these gels had to be close to that in the A-band of a muscle cell, and the gel had to be uniform, to make it possible to relate Donnan potentials to charges on an individual protein molecule. The preparations were described in detail in P.H. Cooke, E.M. Bartels, G.F. Elliott and R.A. Hughes (1987).

Myosin was produced in the form of a pure, solid, cylindrical gel which at low ionic strength (0.030 M), had a diameter of 550 µM and a concentration of 125 mg/ml. The gel threads swelled when adding ATP and/or raising the ionic strength, and electron microscopy showed that the threads were based on typical reconstituted myosin filaments. The filaments were grouped into an axially oriented trabecular network of bundles, where each bundle contained a staggered arrangement of filaments, numbering from 5-10 filaments in a section of the small bundles to upwards of 50 filaments in large bundles. Most filaments in most bundles were within ± 15° of the fibre axis, and this was confirmed by the X-ray patterns from the myosin gels. The ATPase activity of myosin in these gels were found to be normal under the conditions studied.

The myosin rod gels were structurally different although they were of the same size and protein concentration. The uniform gel consisted of a geodesic network of tactoids which look like the tactoids seen in rod suspensions. The rod gels showed very little swelling (< 10%) following all changes.

Having achieved enough knowledge about the two protein preparations and after deciding they did fulfil the criteria outlined in the design of the preparations, the charge measurements began. Our results have been communicated to the Physiological Society (E.M. Bartels, P.H. Cooke, G.F. Elliott and R.A. Hughes, 1984), and showed the same charge change in both myosin gel and myosin rod gel as was seen in glycerinated muscle when changing from rigor to relaxed state. The numerical values are different in the three preparations,

which suggests that the underlying phenomenon is dependent on the molecular organization within the filament backbone since the two gels differ from each other structurally and again is different from the structure in a muscle cell filament. The presence of internally located RNA in the myosin filament (A. Carter and A.J. Rowe, 1990) may also explain the higher charge values in intact muscle. The effect must be caused by the ATP binding to a site on the myosin backbone, and on myosin rod, not in the head region.

Although the situation in relaxed state compared to rigor indicates something about the underlying processes for contraction, the question was still what happens during an actual contraction? To study contraction it was necessary to go back to the full contractile apparatus, either in the form of glycerinated or in the form of skinned muscle cells. Studies of both glycerinated and skinned preparations have been communicated (E M Bartels and G F Elliott, 1984), and the data are in general agreement with our data on rigor and relaxed muscle. As the muscle produced force, the negative electric charge concentration increased to a value higher than was seen in rigor. This may be due to a charging up of the myosin head as well as the rod. As the force decreased, the charge concentration decreased to a value lower than measured in relaxed state. This was to be expected since Ca^{+}-ions still were present, and the charge concentration went back to the relaxed value when the contraction solution was exchanged with the relaxing solution.

It can be argued that contraction cannot be considered as a steady state, so the measurements are not valid. Although to a certain extent this must be true, this would only affect the maximum negative charge value seen during contraction. The overall direction of the observations is certainly valid.

There have been some problems in interesting the muscle audience in the work on purified muscle proteins. It is a new way of thinking, and to some referees it did not appeal and was characterised as 'uninteresting for muscle contraction'. These studies are therefore not yet out as a full report because we were at first reluctant to abandon the muscle community and to publish in physical chemical journals. This lack of interest in charge changes inside muscle cells has also affected the full publication of our work on contracting muscle.

When a successful measuring technique is to hand, it is always interesting to apply this method in other fields. I had two linked methods available, light microscopy at high (400 X) magnification and at high contrast and charge concentration measurements with microelectrodes. I decided to look into medical research and recently I have studied diseased human muscles to see whether the microscopic picture was different from normal, and to see whether the charge values were different from normal, questions I have always been interested in. If there were a discrepancy in protein charge concentration between the diseased and the normal muscle, there would be an indication of structural differences between the muscle filaments in the two muscles.

Fibrositis muscle was my first choice, and an extremely interesting finding of abnormal elastic-band-like structures around some of the muscle fibres and inter-connecting threads between the fibres lead to a breakthrough in diagnosing the disease (E M Bartels and B Danneskiold-Samsøe, 1986). Further work is at present in progress with the Danish medical research group to set up the microscopy necessary to make it a safe diagnostic tool in anybody's hand.

The fibrositis muscle showed no abnormalities in charge values, but another disease, polymyositis, showed changes related to the state of the muscle (E M Bartels *et al*, 1989). All polymyositis patients show muscle weakness and breakdown of muscle cells, and the A- and I-band charges are much lower than the values found in normal, healthy muscle. The disease is treated with steroids, and the treatment is not always successful and in unsuccessful cases directly damaging. My measurements demonstrated that a patient not responding to treatment showed a drop in A- and I-band charge values over a year. This makes the charge measurements a possible new and easy way to study response to treatment in these very ill patients. Further studies of polymyositis muscle are planned, both to develop the charge measurements for clinical use, and to study the effects of various forms of drug treatment.

References

E.M. Bartels and G.F. Elliott (1980). Donnan potential measurements in the A- and the I-bands of cross-striated muscles, and calculation of the fixed charge on the contractile proteins. J. Muscle Res. Cell Motil. 1_4 452.

E.M. Bartels and G.F. Elliott (1981). Donnan potentials from the A- and I-bands of skeletal muscle, relaxed and in rigor. J. Physiol. 317 85-87P.

E.M. Bartels and G.F. Elliott (1981). Donnan potential measurements in the A- and the I-bands of barnacle muscle fibers under various physiological conditions. J. Gen. Physiol. 78_6 12a-13a.

E.M. Bartels and G.F. Elliott (1982). Donnan potentials in rat muscle: Differences between skinning and glycerination. J. Physiol. 327 72-73P.

J.R. Blinks (1965). Influence of osmotic strength on cross-section and volume of isolated single muscle fibres. J. Physiol. 177 42-57.

A. Carter and A. J. Rowe (1990) A small RNA (tf RNA) found in myofibrils, located in the thick filaments, and inducing auto parallel packing of myosin monomes. J. Muscle Res. Cell Motil (in press).

E.W. Collins and C. Edwards (1971). Role of Donnan equilibrium in the resting potentials in glycerol-extracted muscle. Am. J. Physiol. 221 1130-1133.

M. Dydynska and D.R. Wilkie (1963). The osmotic properties of striated muscle fibres in hypertonic solutions. J. Physiol. 169 312-329.

G.F. Elliott (1973). Donnan and osmotic effects in muscle fibers without membranes. J. Mechanochem. Cell Motil. 2 83-89.

G.F. Elliott, E.M. Rome and M. Spencer (1970). A type of contraction hypothesis applicable to all muscles. Nature 226 No. 5244 417-420.

G.F. Elliott, G.R.S. Naylor and A.E. Woolgar (1978). Measurements of the electric charge on the contractile proteins in glycerinated rabbit psoas using microelectrode and diffraction effects. In: Ions in Macromolecular and Biological Systems (Colston Papers No. 29) D.H. Everett and B. Vincent, editors, Scientechnica Press, Bristol, United Kingdom. 329-339.

R.E. Godt and C. M. Baumgarten (1984) Potential and K^+ activity in skinned muscle fibers. Evidence for a simple Donnan equilibrium under physiological conditions. Biophys. J. 45, 375-382.

W.F. Harrington (1979). On the origin of the contractile force in skeletal muscle. Proc. Natl. Acad. Sci. USA 76_{10} 5066-5070.

J.C. Haselgrove (1973). X-ray evidence for conformational change in the actin-containing filaments of vertebrate striated muscle. Cold Spring Harb. Symp. Quant Biol. 37 341-352.

P. Haugen and O. Sten-Knudsen (1976). Sarcomere lengthening and tension drop in the latent period of isolated frog skeletal muscle fibres. J. Gen. Physiol. 68 247-265.

D.K. Hill (1968). Tension due to interaction between the sliding filaments in resting striated muscle. The effect of stimulation. J. Physiol. 199 637-684.

A. F. Huxley (1957) Muscle structure and theories of contraction. Proc. Biophys. Biophys. Chem. 7, 255-318.

B.M. Millman and B.G. Nickel (1980). Electrostatic forces in muscle and cylindrical gel systems. Biophys. J. 32 49-63.

R. Natori (1986). Skinned fibres of skeletal muscle and the mechanism of muscle contraction. Jikeikai Med. 33. 33 Suppl. 1 1-74.

S.M. Pemrick and C. Edwards (1974). Differences in the charge distribution of glycerol extracted muscle fibres in rigor, relaxation and contraction. J. Gen. Physiol. 64 551-567.

A. Sandow (1966). Latency relaxation: A brief analytical review. MCV Quarterly 2 82-89.

Sarkar (1950). The effect of ions and ATP on myosin and actomyosin. Enzymologica 14 237-245.

H.A. Saroff (1973). Action of hemoglobin, the energy of interaction. Biopolymers 12 599-610.

Y.Y. Toyoshima, S.J. Kron, E.M. McNally, K.R. Niebling, C. Toyoshima and J.A. Spudich (1987). Myosin subfragment-1 is sufficient to move actin filaments in vitro. Nature 328 536-539.

Y. Y. Toyoshima, C. Toyoshima and J. A. Spudich (1989) Bidirectional movement of actin filaments along tracks of myosin heads. Nature 341, 154-156.

List of papers submitted for consideration by The Open University for DSc Degree

E.M. Bartels, J.M. Skydsgaard and O. Sten-Knudsen (1979). The time course of the latency relaxation as a function of sarcomere length in frog and mammalian skeletal muscle. Acta Physiol. Scand. 106 129-137.

E.M. Bartels and P. Jensen (1982). Latency relaxation in frog skeletal muscle in hypertonic conditions. Acta Physiol. Scand. 115 165-172.

G.F. Elliott and E.M. Bartels (1982). Donnan potential measurements in extended hexagonal polyelectrolyte gels such as muscle. Biophys. J. 38 195-199.

E.M. Bartels, P.H. Cooke, G.F. Elliott and R.A. Hughes (1984). Donnan potential changes in rabbit muscle A-bands are associated with myosin. J. Physiol. 358 80P.

E.M. Bartels and G.F. Elliott (1984). Donnan potentials from contracting muscle. J. Muscle Res. Cell. Motil. 5_2 227-228.

G.F. Elliott, E.M. Bartels, P.H. Cooke and K. Jennison (1984). A reply to Godt and Baumgarten's 'Potential and K^+ activity in skinned muscle fibers: Evidence for a simple Donnan equilibrium under physiological conditions. Biophys. J. 45 487-488.

G.R.S. Naylor, E.M. Bartels, T.D. Bridgman and G.F. Elliott (1985). Donnan potentials in rabbit psoas muscle in rigor. Biophys. J. 48_1 47-60.

E.M. Bartels and G.F. Elliott (1985). Donnan potentials from the A- and I-bands of glycerinated and chemically-skinned muscles, relaxed and rigor. Biophys. J. 48_1 61-76.

E.M. Bartels and B. Danneskiold-Samsoe (1986). Histological abnormalities in muscle from patients with certain types of fibrositis. The Lancet 8484 755-757.

G.F. Elliott, E.M. Bartels and R.A. Hughes (1986). The myosin filament: charge amplification and charge condensation. From: Electrical double layers in biology, Editor M. Blank, Plenum Publication Corporation, New York, 277-285.

E.M. Bartels, G.F. Elliott and R.S. Wall (1987). Donnan potential measurements from the sarcoplasmic reticulum of rabbit muscle under rigor and relaxed conditions. J. Physiol. 388 34P.

P.H. Cooke, E.M. Bartels, G.F. Elliott and R.A. Hughes (1987). A structural study of gels in the form of threads of myosin and myosin rod. Biophys. J. 51 947-957.

E.M. Bartels, S. Jacobsen, L. Rasmussen and B. Danneskiold-Samsoe (1989). Patients with polymyositis show changes in muscle protein charges. J. Rheum. 16.

E. M. BARTELS, J. M. SKYDSGAARD and O. STEN-KNUDSEN

The time course of the latency relaxation as a function of the sarcomere length in frog and mammalian muscle

Reprint from

Acta Physiologica Scandinavica, Vol. 106, No. 2

Acta Physiol Scand 1979, 106: 129–137

The time course of the latency relaxation as a function of the sarcomere length in frog and mammalian muscle

E. M. BARTELS, J. M. SKYDSGAARD and O. STEN-KNUDSEN

Department of Biophysics, The Panum Institute, University of Copenhagen, Denmark

BARTELS, E. M., SKYDSGAARD, J. M. & STEN-KNUDSEN, O.: The time course of the latency relaxation as a function of the sarcomere length in frog and mammalian muscle. Acta Physiol Scand 1979, 106: 129–137. Received 10 Oct. 1978. ISSN 0001-6772. Department of Biophysics, Panum Institute, University of Copenhagen, Denmark.

In a comparative study the isometric twitch tension and the latency relaxation were correlated to the sarcomere length in frog and mammalian muscle, the latter only in the length range from 2.4 to 3.1 μm since at higher degrees of stretch the sarcomere lengths became increasingly non-uniform along the fibres. The location of the triads in mammalian muscle fibres was examined by means of electron microscopy. During stretch the location of the triads was gradually changed from the overlap zone at sarcomere lengths below 2.6 to 2.7 μm to the I-band at sarcomere lengths above 3.0 to 3.1 μm, their centres (T-tubules) being equally distributed between the overlap zone and the I-band at sarcomere lengths around 2.9 μm. In both types of muscle the maximum amplitude of the latency relaxation (of about equal relative size) occurred at a sarcomere length of about 3.1 μm; and both twitch tension and latency relaxation were dependent upon the presence of a zone of overlap between the thin and thick filaments. In neither of the two types of muscles did the time, t_1, from stimulation to the onset of tension drop depend upon the sarcomere length. At room temperature (22°C) t_1 was about 1 ms in mammalian muscle and 2 ms in frog muscle. In mammalian muscle the time, t_2, from the stimulus to the maximum drop in tension and the time, t_3, to positive tension development were both substantially uninfluenced by changes in sarcomere length in the range 2.4 to 2.9 μm, whereas in frog muscle both t_2 and t_3 increased linearly with increasing sarcomere length in the above range. These findings are discussed in the light of the different locations of the triads in frog and mammalian muscle. It is concluded that the theory of Sandow (1966)—extended by Mulieri (1972)—and that of Haugen & Sten-Knudsen (1976), which both have the virtue of being able to account for the increase of the latent period with stretch in frog muscle, also would be applicable to mammalian muscle provided that a time lag of 0.5 to 1.0 ms exists from the time of the binding of Ca^{2+}-ions to the troponin molecules inside the zone of overlap until the attached cross bridges start to move and develop tension.

Key words: Latency relaxation, mammalian muscle, triads

Latency relaxation (Sandow 1944) is the small tension drop which under isometric conditions precedes the development of contraction force proper. The underlying cause of latency relaxation is still unknown but it is generally considered as a reflection of some event in the excitation–contraction process. Recently Haugen & Sten-Knudsen (1976) observed that concomitant with the tension drop there is a small elongation of the sarcomeres. They put forward the hypothesis that this elongation was caused by a minute lengthening of the thin filaments as a result of the conformational change upon the binding of the calcium ions to the troponin molecules (Haselgrove 1973). According to this hypothesis the falling phase of the latency relaxation should reflect the diffusion process of the Ca^{2+}-ions from their time of liberation upon activation of the T-tubules until they reach the zone of overlap between the thin and thick filaments. In frog skeletal muscles T-tubules are located adjacent to the Z-lines and, accordingly, the distance the Ca^{2+}ions liberated have to travel by diffusion to reach the zone of overlap increases when the sarcomere length is increased by stretching the muscle. The hypothesis of Haugen & Sten-Knudsen (1976) therefore accounts for the well established

observation that in frog skeletal muscle the time from the stimulation to the first drop in tension is independent of the sarcomere length whereas the time to the maximum drop in tension is a linear function of the sarcomere length, s, at least in the range $2.2\ \mu m < s < 3.1\ \mu m$ (Guld & Sten-Knudsen 1960, Mulieri 1972, Haugen & Sten-Knudsen 1976). In mammalian muscles the T-tubules are known to be located near the zone of overlap (Porter & Palade 1957). The distances which the Ca^{2+}-ions have to travel in these muscles to reach the zone of overlap are shorter, and do not depend upon the sarcomere length in the same way as in the frog muscles. According to the hypothesis of Haugen & Sten-Knudsen (1976) one should therefore expect that the time course of the latency relaxation depended differently upon the sarcomere length in mammalian and in frog muscles. Therefore, to put the above-mentioned hypothesis to a test we have examined the dependence of the latency relaxation upon the sarcomere length in mammalian muscles. As we were not able to prepare single fibres from mammalian muscles the investigation was carried out as a comparison between whole muscles of almost equal size from frog and mice or on rat fibre bundles. A preliminary report of this investigation was given at a meeting in Bressanone, 1976, held by the European Muscle Club.

METHODS

Preparations

The experiments were performed on fibre bundles or whole muscles with about uniform fibre lengths throughout the specimen at each degree of stretch. While this requirement could be reasonably fulfilled in frog muscle at sarcomere lengths between 2.3 and 3.4 μm, non-uniformity of sarcomere lengths developed in mammalian muscle preparations at sarcomere lengths above 3.1–3.2 μm.

Both fibre bundles and whole muscles were prepared. Fibre bundles can be fixed rapidly for electron microscopy and were used for the examination of the location of the triads at various sarcomere lengths in mammalian muscle. The bundles were also used for the investigation of the latency relaxation, but the length range in which the sarcomeres had uniform lengths was not wider in fibre bundles than in whole muscles. Therefore small undamaged whole muscles were considered more reliable for the study of latency relaxation as a function of sarcomere length.

Whole muscle

1. From the frog (*Rana temporaria*) the M. extensor long. dig. IV (toe muscle) was isolated and both tendons were fitted with light steel hooks for attachment to the transducers. The dissection and the experiments were carried out in a Ringer's solution containing (mM): NaCl 116, KCl 2, $CaCl_2$ 1.8, Na_2HPO_4 0.9, KH_2PO_4 0.2 (pH 7.2). *d*-Tubocurarine 1 $\mu g/cm^3$ was added to the solution.

2. *The M. gracilis anticus* from the mouse including neighbouring tissues and the portions of tibia and pelvis to which the muscle inserts were removed under microscope and transferred to a special chamber for final trimming. The fascia was removed as completely as possible without damaging any fibres. For transducer attachment a loop of platinum wire (diameter 0.2 mm) was fixed to the fragment of tibia, and a silk loop was fixed to the fragment of pelvic bone. The final preparation appeared as a transparent rectangular strip, about 0.5 mm thick, 1.5–2 mm broad, and 15–18 mm long at the resting length.

M. gracilis and the fibre bundles described in the following were dissected and investigated in a Ringer's solution containing (mM): NaCl 140, KCl 5, $CaCl_2$ 3.2, $MgCl_2$ 1.1, Na_2HPO_4 1.1, NaH_2PO_4 0.4 (pH 7.4), glucose 4.5. The Ringer's solution was oxygenated during the dissection, and *d*-Tubocurarine 1 $\mu g/cm^3$ was present during the experiments.

Fibre bundle preparations

1. Narrow fibre bundles from *M. semitendinosus* or *M. adductor long.* in the rat were prepared at full length and fitted with silk loops tied to the tendinous ends. A few superficial fibres were always damaged in this type of preparation.

These bundles functioned for about two hours before the maximum isometric twitch began to decline. They were used for both electron microscopy (see below) and for registration of the latency relaxation at various sarcomere lengths.

2. *Portions—about 1.5 cm long—of fibre bundles* in rat gracilis muscle could be prepared and isolated after ligation without any damage to the isolated fibre portions, taking advantage of the divisions occurring naturally in the muscles. The ligature was placed outside but very close to the dissected portion, the ends of the portion thus being protected by neighbouring fibres and connective tissue. These bundle portions had uniform sarcomere lengths in the range from 2.5 to 3.5 μm, and they were suited for an examination of the degree to which sarcomere lengths estimated by the laser diffraction technique agreed with sarcomere lengths estimated by light microscopy (see below).

Experimental procedure

All experiments were carried out at 20–22°C using a technique described earlier in detail (Bartels et al. 1976). The preparation was mounted between two strain gauge transducers for simultaneous recording of the positive tension (resting tension and isometric force) and the latency relaxation. The muscle length was altered by moving the arm of the manipulatior holding the tension transducer. At each muscle length the sarcomere length was measured, and the preparation was then given an overall stimulation (transversely) with a diphasic current pulse usually of 0.5 ms duration.

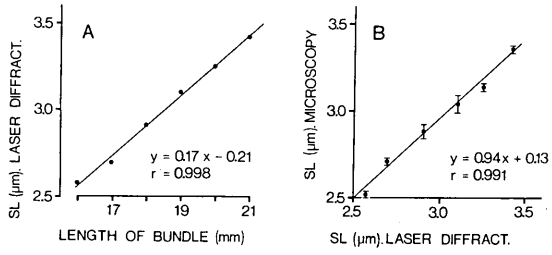

Fig. 1. Example of a fibre bundle from rat gracilis muscle where sarcomere length is linearly related to the fibre length over the range of sarcomere lengths of 2.5 to 3.5 μm. (A). The sarcomere length (SL) measured from laser diffraction as a function of the length of the fibre bundle. (B) Correlation between values of sarcomere lengthmeasured from laser diffraction and values of sarcomere length measured by light microscopy (average ± S.D., 3–5 measurements along the bundle). The equations obtained by linear regression are given in each diagram. *r*, correlation coefficient.

Estimation of the sarcomere length

The estimation of the sarcomere length in frog toe muscle by means of laser diffraction technique has been described (Bartels et al. 1976). The method could be used also in mammalian muscle. Fig. 1 shows comparisons between values obtained by the laser diffraction technique and values obtained by means of light microscopy of fibre bundle portions (cf. fibre bundle preparation 2). A linear relationship between fibre length and sarcomere lengths was seen in the range between 2.4 and 3.6 μm. The light microscopy was performed as follows: Using a Zeiss Standard WL microscope provided with a water immersion lens (Zeiss, 40×, N.A. 0.75) microphotographs were taken of 3–5 spots along the living fibre bundles at each examined length. The sarcomere length was determined by measuring in a "Recordak" aperture card reader the length of 20–30 sarcomeres in series and calculating the average length using for comparison a photograph of a calibrated scale (100 divisions per mm).

Electron microscopy of rat muscle

Fibre bundles from M. semitendinosus of the rat were dissected in oxygenated Ringer's solution. The bundles were stretched to various lengths, and each bundle was maintained at a fixed length by a Teflon holder during fixation in glutaraldehyde (2.5%, 120 min) and osmium tetroxide (2%, 90 min, 20°C) both buffered in 0.1 M sodium cacodylate at pH 7.4. After dehydration in a graded series of ethanol followed by propylene oxide and propylene oxide plus Epon, the preparation was embedded in Epon and cut by an LKB Ultratome I in 50–190 nm sections. The specimens were poststained by 4% zinc uranyl acetate according to Weinstein et al. (1963) at 60°C for 20 min and 0.4% lead citrate at room temperature for 3 min. For electron microscopy an AEI-Corinth 275 electron microscope was used.

RESULTS

1. *The distribution of sarcomere lengths in frog and mammalian muscles at various degrees of stretch*

It was essential for this investigation that the sarcomere lengths were fairly uniformly distributed along the fibres at each muscle length. To find the range of muscle lengths where this requirement was fulfilled the preparation was scanned along its length with the laser beam at each degree of stretch. The measurements of the sarcomere lengths were taken during consecutive stretches and relaxations of the muscles.

In *the frog toe muscle* the sarcomere length was proportional to the muscle length at sarcomere lengths between 2.3 and 3.4 μm. In this range the differences between the highest and the lowest sarcomere length measured along the muscles were less than 0.1 μm, the fibre ends being excluded (Huxley & Peachey 1961). The muscles showed functional characteristics similar to those found in single fibres by Haugen & Sten-Knudsen (1976). The isometric twitch and the tension relaxation passed through their maxima at sarcomere lengths slightly below 2.4 μm and at 3.10±0.15 μm (S.D., 43 obs. in 12 muscles) respectively, both extrapolating to zero at a sarcomere length about 3.65–3.70 μm.

The *mammalian muscle* preparations were usually slack at sarcomere lengths below 2.4 μm. When the muscles were stretched the sarcomere lengths remained fairly uniformly distributed along the lengths of the muscles up to an average sarcomere length of 3.1 μm (cf. Fig. 2). When stretched further irregularities in the distribution of sarcomere lengths appeared. In fibre bundles the laser beam revealed alternating parts with sharp and disappearing diffraction spectra, when the sarcomere length was above 3.1 μm, and the bundles developed isometric tension which extrapolated to zero at sarcomere lengths varied from 3.7 to above 4.0 μm. A small M. gracilis was superior to the fibre bundles in reproducing the length–tension curves provided the muscles were not stretched to sarcomere lengths above 3.2 μm. Furthermore M. gracilis offered a reasonable explanation to the puzzling finding of tension development in fibre bundles in which several cross-sections had sarcomere lengths far above 3.7 μm. Coincident with an almost abrupt increase of the resting tension, M. gracilis showed an in-

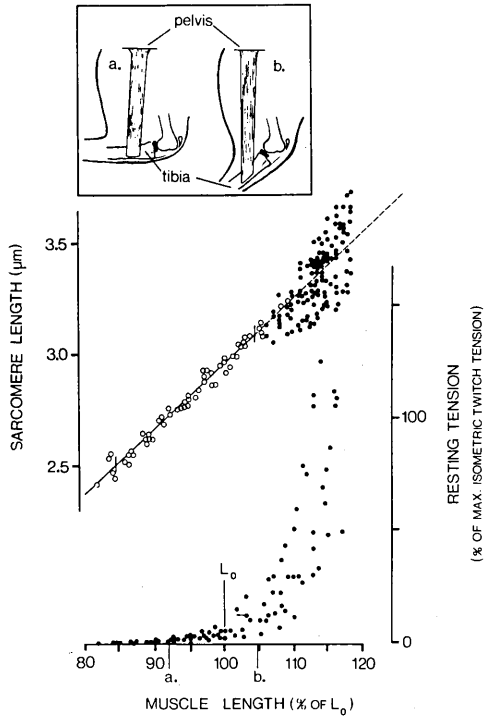

Fig. 2. To illustrate the increasing non-uniformity of the sarcomere lengths with increasing stretch of 9 gracilis muscles from mice. Abscissa, muscle length as a percentage of length L_0, at which maximum isometric twitch tension developed. L_0 corresponds to a sarcomere length of about 2.9 μm. Right ordinate, resting tension as a percentage of maximum twitch tension. Left ordinate, sarcomere length in μm. Open circles indicate that the sarcomere lengths were uniformly distributed. Each point represents the average from three measurements along each muscle. Filled circles, all measurements from the proximal, the middle, and the distal third of each muscle. On the abscissa, (*a*) and (*b*) indicate the approximate limits of muscle length in the intact animals. The appearance of M. gracilis in situ at these limits of length are shown in the insert sketch.

creasing non-uniformity of the sarcomere length when stretched to sarcomere lengths above 3.2 μm (Fig. 2). Simultaneously the isometric twitch, which was maximal at a sarcomere length of about 2.9 μm, decreased linearly with increasing muscle length, and a twitch could still develop when the proximal third of the muscle showed sarcomere lengths up to 4 μm. However, when correlated to the sarcomere length of just the distal third of the muscle, the isometric twitch extrapolated to zero at sarcomere lengths around 3.5–3.6 μm, which suggests that the parallel elasticity (connective tissue etc.) of the extremely stretched fiber fractions acted as a series elastic element between the distal contracting fibre fractions and the proximal tendon. After such stretch beyond 3.2 μm of the shortest sarcomeres, the length–tension curves changed irreversibly, recalling a similar finding of Bahler et al. (1968) on isolated rat gracilis muscle stretched beyond 120% of the resting length. Apparently the connective tissue is woven around the fibres in a way that brings about an inhomogenous strain, the various parts of the fibres not being stretched to the same degree.

The amplitude of the latency relaxation was maximal at a sarcomere length of about 3.1–3.2 μm in mammalian whole muscle. The maximum amplitude was of about the same relative size in both frog and mammalian muscle. The maximum amplitude expressed per thousand of the maximum isometric twitch tension was on average 1.1 in frog muscle, 2.5 in mouse muscle, and 1.7 in rat fibre bundles. At further stretch of mammalian muscle to the lengths with non-uniform distribution of the sarcomere length no consistent pattern of the amplitude as a function of muscle length could be obtained. However, when a linear decline was observed occasionally, both the isometric twitch tension and the amplitude of the latency relaxation extrapolated to zero at about the same muscle length, and a latency relaxation was never observed unless accompanied by a twitch.

If the sarcomere lengths were restricted to the range 2.4–3.1 μm (Fig. 2), the sarcomere length was proportional to the muscle length. The difference between the highest and the lowest sarcomere length observed along the muscles at each length was on the average 0.07 μm (S.D.=$\pm$0.05 μm, 166 obs. in 9 muscles). By transverse scanning with the laser beam it was found that the sarcomere length in M. gracilis at the resting length varied in a regular way, being about 5% higher in the anterior edge than in the posterior edge of the muscle in its rectangular form. A possible explanation is that the muscle—being among others a flexor of the knee—has optimal fibre lengths when it is non-rectangular at stretched knee (Fig. 2, inserted illustration). However, this non-uniformity played a minor role in this investigation, because the time course of the latency relaxation turned out to be almost independent of the sarcomere length in the range 2.4–3.0 μm.

In accordance with these findings the following comparison between frog and mammalian muscle

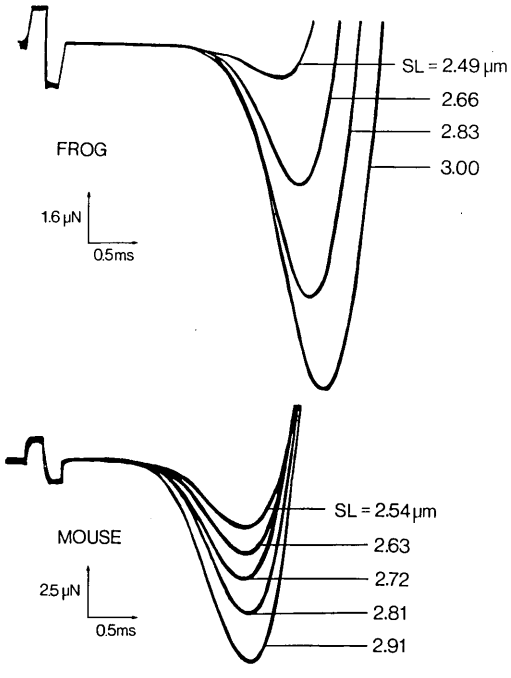

Fig. 3. The time course of the latency relaxation at various sarcomere lengths in whole muscles from the frog (M. ext. long. dig. IV) and the mouse (M. gracilis antic.). Recordings were superimposed at various sarcomere lengths (SL in μm are indicated at each trace. Note the different tension scales in the two sets of recordings).

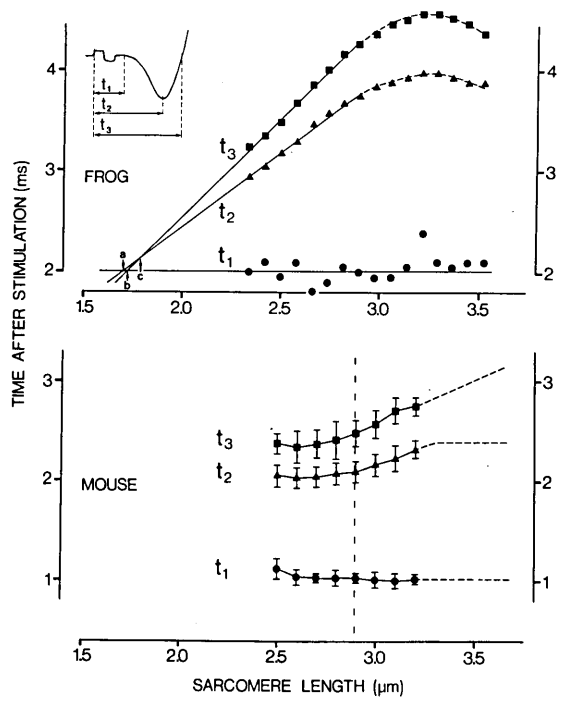

Fig. 4. The influence of the sarcomere length on the time of onset of the latency relaxation, t_1 (filled circles), the time to maximum tension drop, t_2 (triangles), and the time to development of positive tension, t_3 (filled squares), in whole muscles from frog and mouse.

Upper part: results from one frog toe muscle. $a = 1.50 \pm 0.37$ μm: intersection between the mean level for t_1 and the regression line for t_2. $b = 1.55 \pm 0.33$ μm: intersection between the mean level for t_1 and the regression line for t_3. $c = 1.61 \pm 0.37$ μm: intersection between the regression lines for t_2 and t_3. (Average $\pm$ S.D., 43 obs. on 13 muscles.)

Lower part: t_1, t_2, and t_3 (average $\pm$ S.D.) from 9 M. gracilis antic. from mice.

was limited to sarcomere lengths between 2.4 and 3.2 μm. This limited range of sarcomere lengths also had the advantage of being the range in which the resting tension was small, and accordingly changes in the parallel elasticity has a relatively small influence on the time course of the latency relaxation.

2. *The time course of the latency relaxation as a function of the sarcomere length in frog and mammalian whole muscle*

Examples of the superimposed recordings of the latency relaxation at various sarcomere lengths in frog toe muscle and in M. gracilis in the mouse are shown in Fig. 3. All the times were measured from the start of the stimulating pulse. In mammalian muscle the time to the onset of the tension drop was about half of that in frog muscle. However, the main difference between the two sets of recordings was that in mammalian muscle as contrasted to frog muscle, the duration of the latency relaxation was almost uninfluenced by changes in sarcomere length. This is further illustrated in Fig. 4. In agreement with earlier findings (Guld & Sten-Knudsen 1960) the pattern in frog toe muscle was found similar to that in single fibres (Mulieri 1972, Haugen & Sten-Knudsen 1976). While the time, t_1, from stimulation to onset of the tension drop seems uninfluenced by the sarcomere length, both the time, t_2, for maximum tension drop and the time, t_3, for the development of positive tension increased linearly with increasing sarcomere length in the range 2.4–3.2 μm (Fig. 4, upper part). The regression lines for t_2 and t_3 intersected with the mean level for t_1 at a sarcomere length around 1.5–1.6 μm, being close to the length of the thick filament. At sarcomere

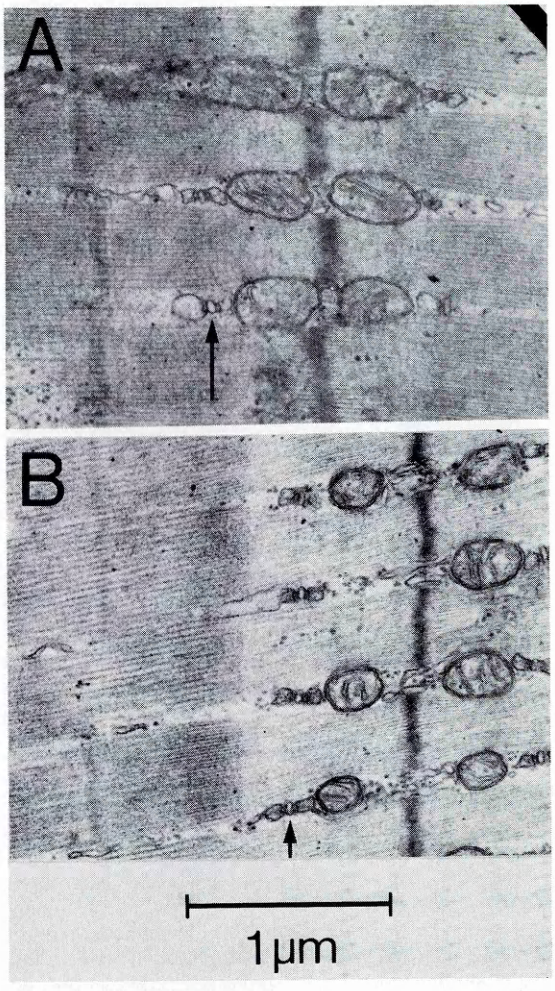

Fig. 5. Electronmicrographs of the rat semitendinosus muscle. Magnification: ×30 000. T-tubules shown by arrows. (A) Sarcomere length 2.3 µm. T-tubules located in the A-band. (B) Sarcomere length 3.3 µm. T-tubules in the I-band.

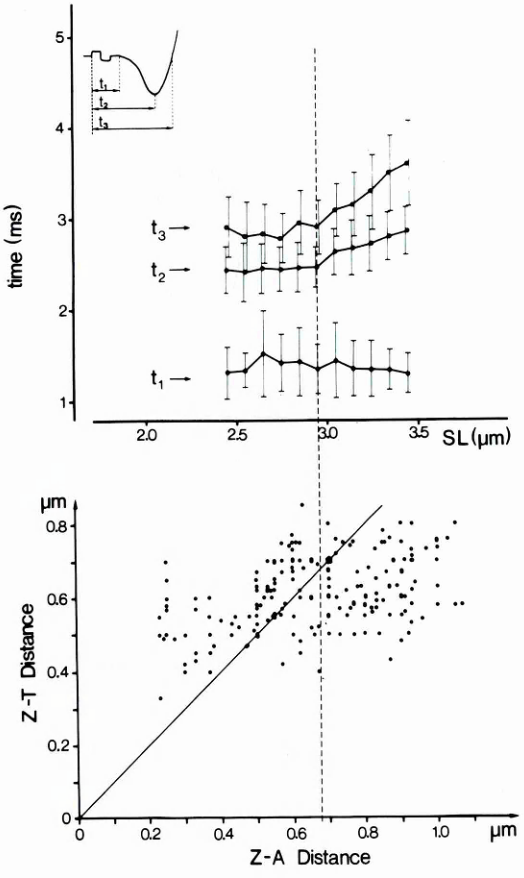

Fig. 6. Duration of the latency relaxation and the location of the T-tubules at various sarcomere lengths in fibre bundles from rat skeletal muscle.

Upper part: The times to onset (t_1), to maximum (t_2), and to termination (t_3) of the latency relaxation as a function of sarcomere length (SL). Ordinate, time (ms). Abscissa, common to upper and lower part, sarcomere length (µm). Average±S.D., 37 obs. in 19 fibre bundles.

Lower part: Location of the T-tubules at various sarcomere lengths. 189 measurements. Ordinate, distance (Z–T) between the Z-line and the T-tubules (µm). Lower abscissa, distance (Z–A) between the Z-line and the myosin filaments (µm). For further explanation see text.

lengths above 3.2 µm both t_2 and t_3 leveled off and could eventually decrease. In mammalian muscle (Fig. 4, lower part, Fig. 6, upper part) the time course of the latency relaxation as a function of sarcomere length differed markedly from the pattern observed in frog muscle in the range of sarcomere lengths from 2.5 to 2.9 µm. Both t_1 and t_2 were found substantially independent of the sarcomere length, and t_3 showed only a slight increase as the sarcomere length was increased from 2.5 to 2.9 µm. At sarcomere lengths from 2.9 µm to about 3.2 µm both t_2 and t_3 tended to increase in mammalian muscle.

3. *The location of the triads at various sarcomere lengths in mammalian muscle*

The location of the triads adjacent to the overlap zone between thick and thin filaments in mammalian muscle is well known (Porter & Palade 1957). To our knowledge there was no information on the displacement of the triads relative to the overlap zone as the sarcomere length changes. Since the possibility of such displacement is important we carried out a systematic examination of the

location of the triads in mammalian muscle fibres at sarcomere lengths from 2.0 to 3.7 μm. The results shown in Figs. 5 and 6 were obtained with rat fibre bundles that were originally used for both the mechanical and the morphological studies of mammalian muscle. The micrographs in Fig. 5 show examples of sarcomeres at two different lengths. At a sarcomere length of 2.3 μm the triads were found in the overlap zone between the thick and thin filaments, but at a sarcomere length of 3.3 μm the triads were located in the I-band. This behaviour is further illustrated in Fig. 6 (lower part) showing the results of 189 measurements of the location of the T-tubules at various degrees of stretch. At each sarcomere length the distance between the Z-line and the T-tubule (Z–T Distance) was plotted against the distance between the Z-line and the A-band (Z–A Distance). The solid line indicates those T-tubules which at each sarcomere length are located at the border of the overlap zone and the I-band. Therefore this line separates the observed T-tubules into two groups: (*a*) those situated in the overlap zone between the thick and thin filaments (region above the line), and (*b*) those situated outside the overlap zone (region below the line). At (Z–A)-distances below 0.5 μm corresponding to a sarcomere length of 2.6 μm practically all T-tubules were found in the overlap zone. At (Z–A)-distances between 0.6 and 0.65 μm corresponding to sarcomere lengths between 2.8 and 2.9 μm about 50% of the T-tubules were situated in the overlap zone. At (Z–A)-distances above 0.75 μm (sarcomere length: 3.1 μm) corresponding to muscle lengths above the maximal length in the intact organism, all T-tubules seemed to have been moved out of the overlap zone. In other words, the T-tubules were found predominantly in the overlap zone at sarcomere lengths below 2.8 μm, and predominantly in the I-band at sarcomere lengths above 2.9 μm.

Fig. 6 (upper part) illustrates that in rat fibre bundles—like in mouse gracilis muscle—t_2 seems to be independent of the sarcomere length in the range 2.4–2.9 μm, and that t_2 tends to increase when the bundles were stretched to sarcomere lengths above 2.9 μm. This means that t_2 tends to increase coinciding with a displacement of the triads away from the overlap zone. It should be kept in mind that neither in the fibre bundles nor in the whole muscle, could the time course of the latency relaxation be correlated to a well defined sarcomere length above sarcomere lengths of 3.1–3.2 μm.

DISCUSSION

Latency relaxation was first observed in mammalian muscles by Goepfert & Schaefer (1942). Their findings were later confirmed by Abbott & Ritchie (1951). None of these investigators made a systematic study of the length dependence of the latency relaxation or did correlate it to sarcomere length. The attempt made in the present investigation to extend the previous works by correlating the time course of the latency relaxation to sarcomere length was only partially successful, since the distribution of sarcomere lengths became increasingly inhomogeneous at higher degrees of stretch. For this reason results usable for the primary purpose of this investigation could only be obtained in the range of sarcomere lengths up to 3.1–3.2 μm. However, by relating the twitch tension to the shortest sarcomeres observed in the muscles under extreme degrees of stretch, contraction did not occur when overlapping between thin and thick filaments no longer existed. Furthermore, the latency relaxation usually came to a maximum at a sarcomere length of 3.1 μm or more and was not observed unless accompanied by a twitch. For these reasons we shall in the following assume that the same basic mechanism is responsible for the latency relaxation in both frog and mammalian muscles.

The main result of the present investigation was the finding of a different correlation in mammalian and in frog muscle between the sarcomere length and the time course of the latency relaxation: In mammalian muscle the time, t_2, from the stimulus to the maximum drop in tension and the time, t_3, to positive tension development, were both substantially uninfluenced by changes in sarcomere length in the range 2.4–2.9 μm, whereas in frog muscle both t_2 and t_3 increased linearly with increasing sarcomere length in the above range, the last result being in agreement with previous observations (Guld & Sten-Knudsen 1960, Haugen & Sten-Knudsen 1976). It is natural to ask whether this difference could most easily be understood in terms of the different location of the triads in frog and mammalian muscle. Among the various proposals put forward to account for the latency relaxation in frog muscle (Sandow 1947, A. F. Huxley 1957, Sandow 1966, H. E. Huxley & Brown 1967, Hill 1968, Peachey 1968, Mulieri 1972, Haugen & Sten-Knudsen 1976) only the theory of Sandow (1966)—extended by Mulieri (1972)—and that of

Haugen & Sten-Knudsen (1976) attempt to account for the increase in the latent period with stretch in frog muscle. Although differing as to the origin of the latency relaxation proper, both theories explain the increasing latent period with stretch by the increasing distance which the Ca^{2+}-ions liberated from the triads upon stimulation have to travel until they reach the overlap zone. Accordingly, both theories would have been invalidated if the time course of the latency relaxation had been found to depend upon the sarcomere length in exactly the same way in frog and mammalian muscle. As it is, the present results are not at variance either with the theory of Sandow (1966) or with that of Haugen & Sten-Knudsen (1976), since in mammalian muscle the distance which the Ca^{2+}-ions must travel to reach the overlapping filaments changes little with sarcomere length and consequently, the time course of the latency relaxation should be almost invariant to changes in sarcomere length. But this also applies to those theories which attribute the origin of the latency relaxation to processes located in the overlap region (Hill 1968, H. E. Huxley & Brown 1967, Wilkie, personal communication). On the other hand these theories do not account for the increase in the latent period with stretch in frog muscle and it seems doubtful whether they will be capable of doing it in a straightforward manner (Haugen & Sten-Knudsen 1976). For this reason we may justifiably examine whether the location of the triads in mammalian muscle is compatible with the appearance of a latency relaxation according only to those theories simply accounting for the increase in latent period with stretch in frog muscle, i.e. the theory of Sandow (1966) and that of Haugen & Sten-Knudsen (1976).

When Ca^{2+}-ions are liberated from the triads in mammalian muscle these ions enter almost simultaneously, depending upon the exact location of the triads, both the A-I filamentary lattice in the overlap zone and the neighbouring thin filaments in the I-band. The last event is immaterial in the Sandow-Mulieri theory, where the latency relaxation is considered to be caused by a change in the compliance of the sarcoplasmatic reticulum resulting from the liberation of the Ca^{2+}-ions. To obtain a latency relaxation of about the same size in both frog and mammalian muscle this theory would require a time delay of about 0.5–1.0 ms from the time the Ca^{2+}-ions enter the filamentary lattice in the overlap zone until the tension developing process starts, i.e. movements of the cross bridges (Fig. 3). Such a time lag is even more urgently needed to preserve the Haugen and Sten-Knudsen theory. According to this theory the origin of the latency relaxation is regarded to be an elongation of the thin filaments resulting from a conformational change in the tropomyosin molecules upon the binding of the Ca^{2+}-ions to the troponin sites (Haugen & Sten-Knudsen 1976). The lengthening of the sarcomere resulting from this elongation is considered mediated by an interfilamentary elastic coupling, probably cross bridges which are attached even in the resting state. Thus, according to this theory the Ca^{2+}-ions entering the I-band are essential in the development of the latency relaxation. To make this theory work also in mammalian muscle and to provide a latency relaxation of about the same size as in the frog it is again necessary that a sufficient time (about 0.5–1.0 ms) exists for the development of the conformational changes in the tropomyosin molecules (Haselgrove 1973) in the I-band before the cross bridges in the overlap zone attach to the I-filaments and start their tension developing movements.

If only the results from mammalian muscles had been available the Haugen & Sten-Knudsen theory would probably have been the last one to be considered if at all. Granted that there is the above-mentioned delay (at least 0.5 ms) the question remains which of the two theories is the more applicable. In this work there is no safe ground to prefer one to the other. However, compared to the Sandow-Mulieri hypothesis that of Haugen & Sten-Knudsen has the advantage of explaining more easily that latency relaxation does not develop unless an overlap exists between the thick and thin filaments.

The authors wish to acknowledge their indebtedness to Miss Elisabeth Krøger for devoting her skill to the preparation of the figures.

REFERENCES

ABBOTT, B. C. & RITCHIE, J. M. 1951. Early tension relaxation during a muscle twitch. J Physiol 113: 330–335.

BAHLER, A. S., FALES, J. T. & ZIERLER, K. L. 1968. The dynamic properties of mammalian skeletal muscle. J Gen Physiol 51: 369–384.

BARTELS, E. M., JENSEN, P. & STEN-KNUDSEN, O. 1976. The dependence of tension relaxation in skeletal muscle on the number of sarcomeres in series. Acta Physiol Scand 97: 476–485.

GÖPFERT, H. & SCHAEFER, H. 1942. Die mechanische Latenz des Warmblütermuskels, nebst Beobachtungen über die Muskelzuckung und den Aktionsstrom. Pflügers Arch Ges Physiol 245: 60–71.

GULD, C. & STEN-KNUDSEN, O. 1960. Correlation of isometric twitch tension and latency relaxation to sarcomere length in frog muscle fibres. Acta Physiol Scand 50, Suppl. 175: 63–65.

HASELGROVE, J. C. 1973. X-ray evidence for conformational changes in actin-containing filaments of vertebrate striated muscle. Cold Spr Harb Symp Quant Biol 37: 341–352.

HAUGEN, P. & STEN-KNUDSEN, O. 1976. Sarcomere lengthening and tension drop in the latent period of isolated frog skeletal muscle fibres. J Gen Physiol 68: 247–265.

HILL, D. K. 1968. Tension due to interaction between the sliding filaments in resting striated muscle. The effect of stimulation. J Physiol (Lond.) 199: 637–684.

HUXLEY, A. F. 1957. Muscle structure and theories of contraction. Progr Biophys 7: 255–318.

HUXLEY, H. E. & BROWN, W. 1967. The low-angle X-ray diagram of vertebrate striated muscle and its behaviour during contraction and rigor. J Molec Biol 30: 383–434.

HUXLEY, A. F. & PEACHEY, L. D. 1961. The maximum length for contraction in vertebrate striated muscle. J Physiol 156: 150–165.

MULIERI, L. A. 1972. The dependence of the latency relaxation on sarcomere length and other characteristics of isolated muscle fibres. J Physiol (Lond.) 223: 333–354.

PEACHEY, L. D. 1968. Muscle. Ann Rev Physiol 30: 401–440.

PORTER, K. R. & PALADE, G. E. 1957. Studies on the endoplasmatic reticulum. III. Its form and distribution in striated muscle cells. J Biophys Biochem Cytol 3: 269–299.

SANDOW, A. 1944. Studies on the latent period of muscle contraction. Method. General properties of latency relaxation. J Cell Comp Physiol 24: 221–256.

SANDOW, A. 1947. Latency relaxation and a theory of muscular mechano-chemical coupling. Ann NY Acad Sci 47: 895–929.

SANDOW, A. 1966. Latency relaxation: a brief analytical review. Med Coll Va Q 2: 82–89.

WEINSTEIN, R., ABBISS, T. & BULLIVANT, S. 1963. The use of double and triple uranyl salts as electron stain. J Cell Biol 19: 74A.

Acta Physiol Scand 1982, 115: 165–172

Latency relaxation in frog skeletal muscle under hypertonic conditions

E. M. BARTELS[1] and P. JENSEN[2]

Department of Biophysics, University of Copenhagen, Denmark

BARTELS, E. M. & JENSEN, P.: Latency relaxation in frog skeletal muscle under hypertonic conditions. Acta Physiol Scand 1982, 115: 165–172. Received 31 Aug. 1981. ISSN 0001-6772. Department of Biophysics, University of Copenhagen, Denmark.

The effect of exposure to hypertonic conditions on latency relaxation (LR), twitch tension and resting tension in frog toe muscle was studied. Measurements were carried out in standard and hypertonic conditions (1 to 3.6 times standard tonicity) and following transversal stimulation. In hypertonic conditions, the LR showed increased duration and decreased amplitude. Both time course and amplitude showed the same dependency on sarcomere length as in standard conditions. The fall in amplitude and extension of the time course was proportional to the increase in tonicity up to 2.2 times the tonicity of the standard. At higher tonicities the time course extended earlier and diverged from the linear dependency, the amplitude falling later with increasing tonicity. The LR was abolished at tonicities exceeding 3 times the standard. In hypertonic conditions the twitch tension was reduced and extended, but showed the same dependency on sarcomere length as in standard conditions. The amplitude showed the same dependency on tonicity as the LR amplitude. The time course extended in a non-linear way with growing tonicity. In hypertonic conditions the resting tension was higher than or the same as in standard conditions, and the dependency on sarcomere length was the same.

A method suitable to investigate the excitation-contraction coupling in muscle was sought in studies of the effect of hypertonic sucrose Ringer's solution on the latency relaxation (LR), the tension drop preceding the isometric twitch tension (Sandow 1944).

LR's time course in standard Ringer's solution depends on sarcomere length in a way which may reflect the diffusion time for Ca^{2+} during the excitation-contraction coupling from the triads to the zone of overlap between the A- and I-filaments (Mulieri 1972, Haugen & Sten-Knudsen 1976). If the LR time course does reflect Ca^{2+} diffusion, then the LR time course would be altered but still dependent on sarcomere length in hypertonic conditions, as the hypertonic solution dehydrates the muscle (Dydynska & Wilkie 1963) and thereby affects the diffusion of Ca^{2+}.

The approach was based on earlier findings by D. K. Hill (1968) and Mulieri (1972). D. K. Hill was not able to measure LR in standard tonicity and Mulieri only investigated lower hypertonicities and did very few experiments. The present study has employed improved measuring techniques and a wide range of tonicities have been studied.

Twitch tension and resting tension were measured parallel to the LR measurements.

METHODS

The experimental set-up was the same as described by Bartels et al. (1976, 1979). The toe muscle (m. ext. long. dig. IV) from the frog *Rana temporaria* was isolated. One end was attached to the transducer to register LR, the other end was attached to the transducer to register isometric twitch and resting tension. The muscle was stimulated transversely to give maximal LR amplitude (Bartels et al. 1976). Before each stimulation the resting tension was recorded, and the sarcomere length was determined by laser diffraction. The twitch tension was measured from base line. All experiments were carried out at room temperature, 20°–22°C.

In each experiment LR, twitch and resting tension were

[1] Present address: The Open University, Oxford Research Unit, Foxcombe Hall, Berkely Road, Boars Hill, Oxford, England.

[2] Present address: Isotope Laboratory, Centralsygehuset, Holstebro, Denmark.

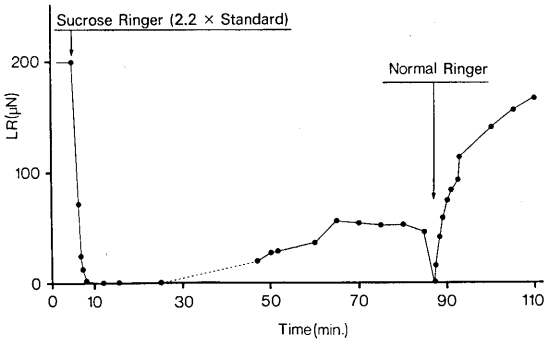

Fig. 1. The effect on the LR amplitude of changing from standard to hypertonic sucrose Ringer's solution (2.2 times standard). When the amplitude of LR obtained a steady, but lower value in hypertonic solution, the muscle was transferred back to standard Ringer's solution.

recorded at a series of sarcomere lengths from 2.2 to 3.5 μm in standard Ringer's solution. The muscle was then adjusted to the sarcomere length which gave maximal amplitude of LR, 3.0–3.1 μm, so that measurements could be compared in different muscles. LR, twitch and resting tension were recorded, and after 5 min rest, the Ringer's solution was changed from standard to hypertonic solution. The changes in LR, twitch and resting tension were recorded as a function of time exposed to hypertonic solution until no more changes were seen; then the three parameters were recorded at a series of sarcomere lengths from 2.2 to 3.5 μm. The muscle was adjusted to the sarcomere length which gave maximal LR amplitude, the hypertonic solution was replaced by the standard solution, and the recovery of the muscle was followed.

The standard Ringer's solution contained (mM): NaCl 116, KCl 2, $CaCl_2$ 1.8, Na_2HPO_4 0.9, KH_2PO_4 0.2; pH 7.2. 1 $\mu g/cm^3$ tubocurarine was added. The tonicity was 225 mOsm.

Hypertonic Ringer's solution was obtained by adding sucrose to the standard solution. The tonicity was varied from 1 to 3.6 times the standard and was determined for each solution by measuring the depression of the freezing point (HI-precision Research Osmometer, Advanced Instruments Ltd., Inc.).

8–12 expts. on different muscles were carried out in each hypertonic solution where a set of averaged results are given (tonicities between 1 and 3 times the standard). 12 expts. in all were carried out at tonicities between 3.2 and 3.6 times the standard. Both twitch and LR were abolished in these solutions, so only data from hypertonicities up to 3 times the standard are given in the results.

RESULTS

The LR amplitude

Fig. 1 shows the LR amplitude as a function of time when changing from standard to hypertonic Ringer's solution (2.2 times the standard). Initially LR was abolished but during the following 30 min LR reappeared, and the amplitude reached a constant value within 30 min from the reappearance. This value was 25% of the amplitude recorded in standard solution. The change in LR amplitude was reversible and the restoration time upon changing back to standard solution was 20–30 min. The example Fig. 1 is representative for tonicities between 2.0 and 3.0 times standard. At tonicities between 1.0 and 2.0 times standard the LR amplitude showed the same pattern as shown in Fig. 1, when changing from standard to hypertonic solution, but instead of being abolished following the change, the LR amplitude was diminished and raised from this lower level to a steady level, lower than the LR amplitude in standard solution. The time from change to hypertonic solution until reach of maximal amplitude after the change, was in this range of tonicities 20 to 50 min and was dependent on the diameter of the muscle (longer time for thicker muscle) with a slight tendency for being shorter in the lower tonicities of the range.

In Fig. 2, the LR amplitude is shown as a function of tonicity. The amplitude is given as a percentage of the amplitude under standard condition and was recorded after a steady value was reached. The fall in amplitude as a function of tonicity is linear up to a hypertonicity of 2.2 times the standard, and a straight line fit (tonicities 1 to 2.2 times the stand-

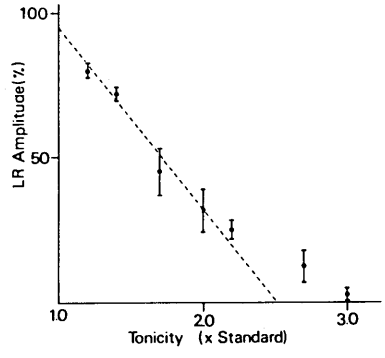

Fig. 2. The LR amplitude as a function of tonicity. The LR amplitude is given after a steady value was reached in the hypertonic solution at the sarcomere length giving maximal amplitude. The amplitude is given as a percentage of the amplitude in standard solution at the same sarcomere length. The tonicity is expressed in factors of the tonicity of standard Ringer's solution. The straight line is the line fitted to the data at tonicities between 1 and 2.2 times the standard.

Table 1. *The LR amplitude in hypertonic solution after reaching a steady level when changing from standard to hypertonic Ringer's solution at 3 different sarcomere lengths*

(SD, n=8). The tonicity is given as factors of the tonicity of standard Ringer's solution. The LR amplitude is given as a percentage of the LR amplitude in standard solution at the same sarcomere length

Sarcomere length (μm)	LR amplitude at tonicity			
	1.2	1.4	1.7	2.0
2.2	95±12	75±7	55±20	46±25
2.4	93±8	73±6	50±16	52±28
2.6	86±9	72±6	46±15	45±16

ard) gives a correlation coefficient of −0.989 for the straight line $y=(158\pm8)-(63\pm5)X$, where the variance of the intercept and the slope is given in terms of SD. At tonicities exceeding 2.2 times the standard the LR amplitude decreased slower with increasing tonicity than the linear fall seen at the lower hypertonicities.

The LR amplitude as a function of sarcomere length showed the same bellshaped curve in standard and in the hypertonic solutions as earlier described (Haugen & Sten-Knudsen 1976). In most experiments the LR amplitude was lower in hypertonic than in standard solution at all sarcomere lengths. In 3 expts., however (one at 1.2, one at 1.7 and one at 2.0 times the standard tonicity) the LR amplitude was just above or the same as the amplitude in standard solution at sarcomere lengths between 2.2 and 2.55 μm, but lower at the longer sarcomere lengths. Table 1 gives the average value of the LR amplitude after a steady value was reached at tonicities between 1.2 and 2.0 times the standard, at sarcomere lengths 2.2, 2.4 and 2.6 μm, to show that the LR amplitude in general was lower in the hypertonic solution than in the standard at the lower sarcomere lengths, as well as at the higher sarcomere lengths. The results in Table 1 are not significantly different from the results shown in Fig. 2.

The time course of the LR

The time course of the LR (inset of Fig. 3A) is characterized by t_1, the time from stimulation to the start of the tension drop, t_2, the time from stimulation to maximal tension drop, and t_3, the time from stimulation to the start of positive tension. The duration of the LR is t_3-t_1.

In hypertonic, as well as in standard Ringer's solution, the time course showed the same dependency on sarcomere length as earlier found (Guld & Sten-Knudsen 1960, Haugen & Sten-Knudsen 1976, Bartels et al. 1979); t_1 was independent of sarcomere length, t_2 and t_3 rose linearly with increasing sarcomere length up to around 3.1 μm and stayed constant with further increase of sarcomere length. Fig. 3 shows an example of the time course as a function of sarcomere length for a muscle in standard solution and in a 2-fold concentration of standard solution. The variation in t_1 in the hypertonic solution is not significant. t_2 and t_3 showed a plateau for sarcomere lengths longer than 3.1 μm, but the plateau always showed a greater variation around the average t_2 and t_3 values in the higher tonicities. The slight rise in this example shows this phenomena.

The time course in hypertonic solution was prolonged, compared to the time course in standard solution, right after the change from standard to hypertonic solution, in the cases where the LR was

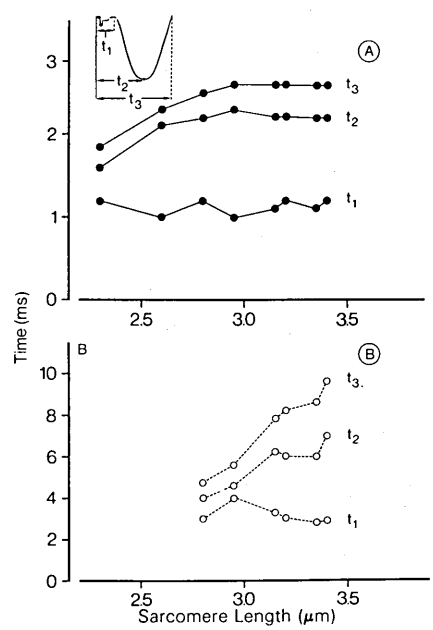

Fig. 3. The dependency on sarcomere length of the time course of LR in the same muscle in standard Ringer's solution (A) and in hypertonic sucrose Ringer's solution (B). (2 times standard.) The time indication t_1, t_2, t_3 (inset) are: t_1 = time from stimulation to the first detectable drop in tension, (onset of LR); t_2 = time from stimulation to maximal drop in tension; t_3 = time from stimulation to start of development of positive (twitch) tension.

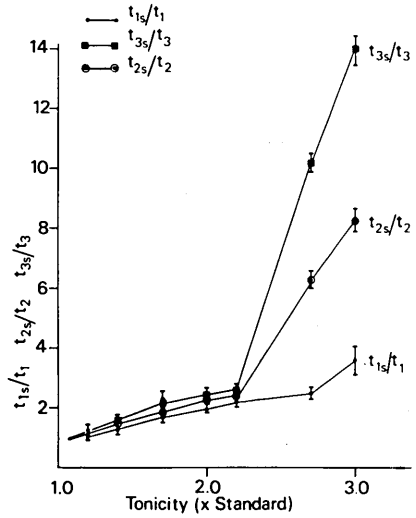

Fig. 4. The LR time course as a function of tonicity. t_1, t_2 and t_3 are the times given Figures 3 A and are measured at the sarcomere length giving maximal LR amplitude. The suffix, s, indicates measurements in the hypertonic sucrose solution. The tonicity is expressed as factors of the tonicity of standard Ringer's solution.

not abolished. At the hypertonicities where LR was abolished after the change, the time course was prolonged as soon as the LR reappeared in the hypertonic solution. The time course of the LR was restored to the time course seen before the exposure to hypertonic solution in 5 to 10 min, when the hypertonic solution was replaced by standard solution. The restoration of the time course of the LR followed the restoration of the LR amplitude.

In the range of 1 to 2.2 times the standard tonicity the time course of the LR increased linearly with increasing hypertonicity (Fig. 4). Straight line fits to the data in the range of 1 to 2.2 times standard tonicity gave for t_{1S}/t_1 as a function of tonicity: $y=-(0.08\pm0.07)+(1.03\pm0.05)X$, correlation coefficient 0.996; for t_{2S}/t_2 as a function of tonicity: $y=-(0.17\pm0.25)+(1.20\pm0.15)X$, correlation coefficient 0.969; for t_{3S}/t_3 as a function of tonicity: $y=-(0.43\pm0.26)+(1.43\pm0.16)X$, correlation coefficient 0.976 (the suffix S indicates values measured in the hypertonic sucrose solution). The variance of the intercept and the slope is given in terms of SD for all line fit.

At tonicities above 2.2 times the standard the increase in t_1 with increasing tonicity only changed slightly, but significantly, from linearity, and t_2 and t_3 showed a dramatic increase with increasing tonicity. The increase in t_3 was higher than the increase in t_2 (Fig. 4).

The twitch tension

The twitch tension decreased to a steady value within 5 to 10 min when a muscle was transferred from the standard to a hypertonic solution. When the hypertonic solution was replaced by the standard, the twitch tension was restored in less than 5 min to the value measured before the exposure to hypertonic solution. This restoration only took place in the cases where the hypertonicity did not exceed twice the standard tonicity or the exposure to hypertonicity did not exceed 90 min. At hypertonicities between 2 and 2.7 times the standard, the twitch tension only restored the value in standard solution after exposures to hypertonicity of at most 90 minutes. At longer exposures the twitch tension started to drop slowly in the hypertonic solution after 90 min of exposure, and a restoration in standard solution never occurred. A restoration of the twitch tension in the standard solution was never seen after exposures to hypertonicities of 3 times the standard or more, even when the exposure was less than 30 min.

The fall in twitch tension as a function of hypertonicity was found to be linear up to a tonicity of 2.2 times the standard (Fig. 5).

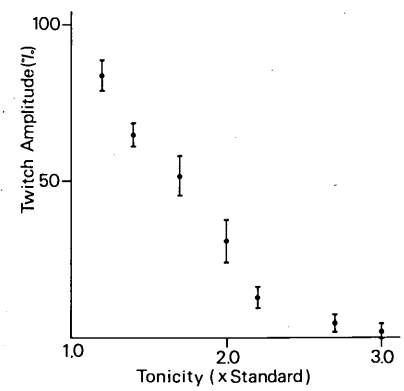

Fig. 5. The amplitude of the twitch tension as a function of tonicity. The amplitude is given after a steady value was reached in the hypertonic solution and as a percentage of the value in standard solution, and at the sarcomere length giving maximal LR amplitude. The tonicity is measured in concentration factors of the tonicity of standard Ringer's solution.

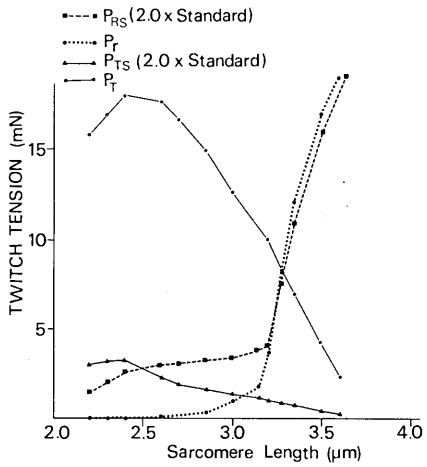

Fig. 6. The twitch tension P_T and resting tension P_R as a function of sarcomere length of a muscle in standard Ringer's solution (no suffix on P_T and P_R) and in hypertonic solution, tonicity twice the standard (P_T and P_R with suffix S).

The twitch tension showed the same dependency on sarcomere length in standard and hypertonic conditions at all tonicities examined, where sarcomere length could be determined (described later). The tension decreased with increasing sarcomere length from a sarcomere length of about 2.3 μm, confirming the findings of Guld & Sten-Knudsen (1960), and those observed during tetanic contraction by Edman (1966). Fig. 6 gives an example of this, showing the twitch tension as a function of sarcomere length in standard solution (twice the standard tonicity).

The time course of the twitch

The twitch was prolonged as soon as a muscle was transferred from the standard to a hypertonic solution. As a measure for the elongation t, the time from stimulation to maximal twitch tension, was chosen. Fig. 7 shows t (after a steady twitch tension was reached in the hypertonic solution) as a function of hypertonicity. The elongation of the twitch increases with increasing hypertonicity and can be described by the polynomial $t=20.3X^3-86.3X^2+129.7X-64.5$, where X is the tonicity. The index of this determination is 0.999, and the standard error for t is 1.04.

The resting tension

The resting tension differed at lower tonicities (up to 1.7 times the standard) from that at higher hypertonicities.

At lower hypertonicities, the resting tension rose in 30–40 min after exposure to the hypertonic solution to a steady value, higher than the value in standard solution. When the hypertonic solution was replaced by standard solution, the resting tension was restored to the value before exposure to hypertonic solution in 2–5 min.

At tonicities above 1.7 times the standard, the tension rose transiently as soon as the muscle was exposed to the hypertonic solution due to a contracture as described by Lännergren & Noth (1973) in single fibres. The contracture lasted for 20–50 min whereafter the tension settled at a value higher than the tension in standard solution, but lower than the tension during the period of contracture. Since tetanic tension was not measured, the size of the contracture has not been related to the tonicity, but in agreement with Lännergren & Noth (1973) the contractures tended to be higher at a tonicity of 2.2 times the standard than at other hypertonicities. When muscles were replaced in standard solution after exposure to hypertonic solutions between 1.7 and 2.7 times the standard concentration, the resting tension recovered to its original value within 4–7 min. After exposure to hypertonicities above 2.7 times the standard, the resting tension did not recover. The muscles seemed to

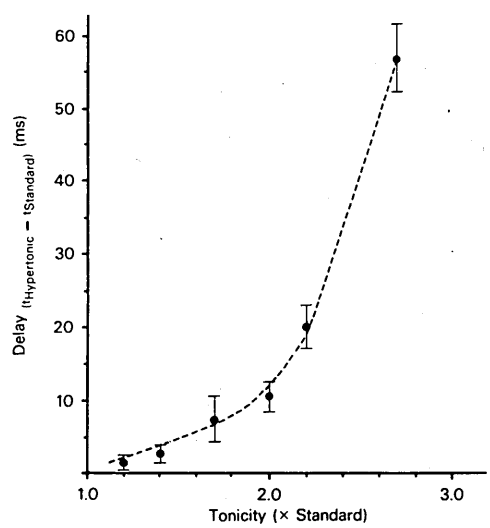

Fig. 7. The delay in time for twitch maximum (at the sarcomere length giving maximal LR amplitude) as a function of tonicity. The polynomial is the polynomial fitted to the data.

suffer when exposed to these highly hypertonic solutions, even though no damage was seen by light microscopy.

The resting tension showed a similar dependency on sarcomere length in standard and hypertonic solution, but the resting tension was only higher than the value in standard solution in hypertonic solution up to a sarcomere length between 3.2 and 3.35 μm after which the resting tension was the same in standard and hypertonic solution or slightly lower in the hypertonic solution as shown in the example Fig. 6. The twitch tension is given in standard and in a two fold concentration of the standard as a function of sarcomere length to show the relation between twitch and resting tension. At hypertonicities up to twice the standard the resting tension in the hypertonic solution was always higher than in the standard at a given sarcomere length.

Extensibility and sarcomere length determination

At tonicities between once and twice that of the standard the laser spectra were clear, and sarcomere length determination was reliable. At tonicities above twice the standard, the laser spectra became increasingly blurred with increasing tonicity, and at 2.5 times standard tonicity, sarcomere length could no longer be determined. A change in extensibility followed the change in the laser spectra. It became more difficult to stretch the muscle at increasing tonicity above twice the standard, and at a tonicity of 2.7 times the standard it was impossible to change the length of the muscle, like trying to stretch a muscle in rigor, so the muscles in hypertonicities of 2.7 and 3.0 times the standard were only studied at the sarcomere length which gave maximal LR. On returning back to standard solution the laser spectra and normal elastic behaviour of a relaxed muscle returned.

As long as sarcomere length could be measured, it remained unaltered when standard solution was replaced by hypertonic solution and vice versa.

DISCUSSION

During the excitation-contraction coupling the time course of the LR in frog muscle fibres depends on sarcomere length in a way which may reflect the diffusion time for Ca^{2+} from the triads to the zone of overlap between the A- and the I-filaments (Mulieri 1972, Haugen & Sten-Knudsen 1976, Bartels et al. 1979). An exposure of a muscle cell to a hypertonic Ringer's solution, and thereby an osmotic shrinkage of the cell (Dydynska & Wilkie 1963, Blinks 1965), causes a decrease in free cell water which decreases the diffusion constant for Ca^{2+}. This can be expected to prolong the LR. We found the time course of the LR to depend on tonicity in a linear way up to a factor of 2.2 times the standard tonicity in agreement with the outlined hypothesis,when assuming that the Ca^{2+} binding to the troponin (Weber & Murray 1973) is not affected by the dehydration. At tonicities exceeding 2.2 times the standard, the vast non-linear increase, particularly in the time t_2, from stimulation until maximal tension drop, and the time t_3, from stimulation until no tension drop is present, with increasing tonicity may be caused by several factors, one being the slower diffusion of Ca^{2+}. Other factors could be slower release of Ca^{2+} from the cisternae due to swollen cisternae at these higher tonicities (Huxley et al. 1963) and a translocation of Ca^{2+} to the longitudinal tubuli (Somlyo et al. 1977). The time t_1, from stimulation until first drop in tension, was relatively less extended compared to t_2 and t_3 in the hypertonicities higher than 2.2 times the standard. Since t_1 is mainly dependent on the time for the first release of Ca^{2+} after stimulation, a slower release of Ca^{2+} from the cisternae would affect t_1, but a translocation of part of the Ca^{2+} from the cisternae to the longitudinal tubuli would not. The effect of the translocation of Ca^{2+} on t_2 and t_3 and not on t_1 may explain the different relative increase in t_1 compared to t_2 and t_3. The only other data on the LR time course are those of D. K. Hill (1968) at 0°C. There is no disagreement between Hill's and our data, since he found the time course to be progressively extended with increasing tonicity, but it is not possible to compare the exact values, since we worked at room temperature.

The amplitude of the LR decreased with increasing tonicity, but depended in the same way on sarcomere length as in standard conditions (Guld & Sten-Knudsen 1960). At a given, sarcomere length the LR amplitude was lower in the hypertonic than in the standard solution. After changing from standard to hypertonic solution the LR either disappeared or the amplitude was smaller than the final in a given solution. This may be due to a lowering or cessation of Ca^{2+} release when the muscle receives the osmotic shock.

Many theories for the origin of the LR have been proposed (Sandow 1947, A. F. Huxley 1957, Sandow 1966, H. E. Huxley & Brown 1967, Hill 1968, Peachey 1968, Mulieri 1972, Haugen & Sten-Knudsen 1976). The theories mainly suggest either that some forcible lengthening change occurs in the contractile substance during the LR or that the LR is the result of a change in either the compliance or the equilibrium length of some elastic structure within the muscle fibre. Our present results for the time course of the LR are not in variance with any of them. The amplitude of the LR showed, on the other hand, dependency on sarcomere length in the same way in standard and hypertonic conditions but the tension drop was dependent on the tonicity in a linear way in the range of tonicities, where the Ca^{2+} diffusion was slowed down in a linear way and this would be accounted for in the theory put forward by Haugen & Stend-Knudsen (1976). According to their hypothesis the origin of the LR is regarded to be an elongation of the thin filaments resulting from a conformational change in the tropomyosin molecules upon the binding of the Ca^{2+}-ions to the troponin sites. If the Ca^{2+} release in hypertonic conditions is lower than in standard conditions (Andersson 1973) some of the Ca^{2+} sites may not be occupied, so no conformational change takes place at these sites. The slower diffusion of Ca^{2+} will at the same time delay the binding of Ca^{2+} to the part of the I-filaments furthest away from the cisternae, so contraction may start in the part closest to the cisternae before the conformational change has taken place in the other parts and overwhelm the tension drop from these parts of the I-filaments.

Mulieri (1972) only studied effects of lower hypertonicities (up to 1.7 times the standard). He found a sarcomere length dependency of the LR emplitude similar to that in our experiment, except that the LR amplitude increased with increasing tonicity up to 1.4 times the standard at sarcomere lengths in the range of 2.0–2.5 μm, no change of amplitude in the range of 2.5–2.8 μm, but a decline of amplitude with growing tonicity at higher sarcomere lengths. The only explanation we can offer is a change in sarcomere length when the solution is changed. Unfortunately, the sarcomere length was not monitored during his experiment.

D. K. Hill (1968) did not find a decrease in the amplitude of the LR with an increase of the tonicity, and the amplitude of the LR was constant and not dependent on sarcomere length in the hypertonic solutions. Since Hill worked at 0°C and used longitudinal stimulation, that may account for the apparent lack of sarcomere length dependency in the hypertonic conditions. Furthermore his set up did not allow him to measure LR at lower hypertonicities and at standard tonicity.

The twitch tension decreased with increasing hypertonicity and was abolished at the same tonicity as the LR was abolished. With increasing hypertonicity the time course became more and more extended. Our result are in agreement with Anderson's (1973), even though it is impossible to compare the absolute value of the time course, since Anderson worked at 1–3°C. D. K. Hill's (1968) results (from two muscles and two tonicities only) are slightly different from Anderson's and ours at higher tonicities, but it is hard to say if this difference is significant. The fall in twitch tension in hypertonic solution may simply be due to the change in ionic strength inside the muscle fibres which alters the mechanical performance of the contractile system (Edman & Hwang 1977). A slower Ca^{2+} diffusion would account for the extended time course of the twitch.

Our findings of a transient rise in resting tension when changing from standard to a hypertonic solution of tonicity higher than about 1.7 times standard and the sustained rise in resting tension in all hypertonic solutions is in agreement with earlier results (Lännergren 1971; Lännergren & Noth (1973) and confirms D. K. Hill's (1968) finding of an increase in resting tension.

As this study was mainly concerned with the effect of hypertonicity on LR, tetanus tension was not monitored, and a comparison of contractile force and resting tension is not possible from our data. The example, Fig. 6, which gives the length-tension diagram for a muscle in standard solution and in a hypertonic solution, twice the standard tonicity, may signify that hypertonicity mainly affects the contractile system. Where it was possible to measure sarcomere length during exposure to hypertonic solution, there was a notable but smaller effect on the resting tension at sarcomere lengths below 3.2 μm. This may be caused by a change in the compliance of the membrane structures due to the dehydration and thereby change in the volume of the muscle cells. The similar dependency on tonicity of the amplitude of the LR and the amplitude of twitch suggests that the origin of the LR is

in the contractile system as proposed by D. K. Hill (1968) and Haugen & Sten-Knudsen (1976).

REFERENCES

ANDERSSON, K. E. 1973. The effect of hypertonicity on the time course of the active state in single skeletal muscle fibres of the frog. Acta Physiol Scand 88: 149–159.

BARTELS, E. M. JENSEN, P. & STEN-KNUDSEN, O. 1976. The dependence of tension relaxation in skeletal muscle on the number of sarcomeres in series. Acta Physiol Scand 97: 476–485.

BARTELS, E. M., SKYDSGAARD, J. M. & STEN-KNUDSEN, O. 1979. The time course of the latency relaxation as a function of the sarcomere length in frog and mammalian muscle. Acta Physiol Scand 106: 129–137.

BLINKS, J. R. 1965. Influence of osmotic strength on cross-section and volume of isolated single muscle fibres. J Physiol 177: 42–57.

DYDNSKA, M. & WILKIE, D. R. 1963. The osmotic properties of striated muscle fibres in hypertonic solutions. J Physiol 169: 312–329.

EDMAN, K. A. P. 1966. The relation between sarcomere length and active tension in isolated semitendinosus fibres of the frog. J Physiol 183: 407–417.

EDMAN, K. A. P. & HWANG, J. C. 1977. The force-velocity relationship in vertebrate muscle fibres at varied tonicity of the extracellular medium. J Physiol 269: 255–272.

GULD, C. & STEN-KNUDSEN, O. 1960. Correlation of isometric twitch tension and latency relaxation to sarcomere length in frog muscle fibres. Acta Physiol Scand Suppl. 175: 63–65.

HAUGEN, P. & STEN-KNUDSEN, O. 1976. Sarcomere lengthening and tension drop in latent period of isolated frog skeletal muscle fibres. J Gen Physiol 68: 247–265.

HILL, D. K. 1968. Tension due to interaction between the sliding filaments in resting striated muscle. The effect of stimulation. J Physiol. 1968. 199: 637–684.

HUXLEY, A. F. Muscle structure and theories of contraction. Prog Biophys 7: 255–318.

HUXLEY, H. E. & BROWN, W. 1967. The low-angle X-ray diagram of vertebrate striated muscle and its behavior during contraction and rigor. J Molec Biol 30: 383–434.

HUXLEY, H. E., PAGE, S. & WILKIE, D. R. 1963:. An electron microscopic study of muscle in hypertonic solutions. J Physiol 169: 325–329.

LÄNNERGREN, J. 1971. The effect of low-level activation on the mechanical properties of isolated frog muscle fibres. J Gen Physiol 1971. 58: 145–162.

LÄNNERGREN, J. & NOTH. 1973. Tension in isolated frog muscle fibres induced by hypertonic solutions. J Gen Physiol 61: 158–175.

MULIERI, L. A. 1972. The dependence of the latency relaxation on sarcomere length and other characteristics of isolated muscle fibres. J Physiol 1972. 223: 333–354.

PEACHEY, L. D. Muscle. 1968. Ann Rev Physiol 30: 401–440.

SANDOW, A. 1944. Studies on the latent period of muscular contraction. Method. General properties of latency relaxation. J Cell Comp Physiol. 24: 221–256.

SANDOW, A. 1947. Latency relaxation and a theory of muscular mechano-chemical coupling. Ann NY Acad Sci 47: 895–929.

SANDOW, A. 1966. Latency relaxation: A brief analtyical review. MCV Quarterly 2: 82–89.

WEBER, A. & MURRAY, J. M. 1973. Molecular control mechanisms in muscle contraction. Physiol Rev 3: 612–673.

DONNAN POTENTIAL MEASUREMENTS IN EXTENDED HEXAGONAL POLYELECTROLYTE GELS SUCH AS MUSCLE

G. F. ELLIOTT AND E. M. BARTELS
Biophysics Group, The Open University, Oxford Research Unit, Boars Hill, Oxford, OX1 5HR, England

ABSTRACT In this paper we reconsider the theoretical and practical aspects of using KCl-filled microelectrodes in extended polyelectrolyte gels such as muscle to measure Donnan potentials, and then calculate protein fixed-charge concentrations. An analytical calculation of the electrical potential function between muscle filaments shows that whether the microelectrode averages the ionic concentration or the local potentials the results are indistinguishable in the practical regime. After consideration of this and other possible sources of error, we conclude that the charge-concentration measurements that have appeared in the literature are legitimate.

INTRODUCTION

During the past decade a number of groups have reported potentials, measured with KCl-filled microelectrodes, from muscle fibers whose membranes have been destroyed or removed by the technique of glycerination (Collins and Edwards, 1971, Pemrick and Edwards, 1974, Elliott et al., 1978) and also by chemical skinning and mechanical skinning (Bartels et al., 1980, Bartels and Elliott, 1980; 1981; Stephenson et al., 1981). Stephenson et al. (1981) used their data largely to work out average ratios between the internal and external concentrations of various ions and other solutes. The other authors have taken the argument one step further, and invoke the principle of electrical neutrality to infer the internal fixed electric charge concentration on the contractile proteins. Bartels and Elliott (1980; 1981), using high-powered light microscopy to observe the position of the microelectrode tip, recorded Donnan potentials from the *A*- and *I*-bands of glycerinated rabbit psoas muscle and mechanically skinned barnacle muscle in rigor and relaxing solutions. They found different *A*- and *I*-band potentials in rigor solutions, and concluded that the fixed-charge concentrations must be different in the two bands under these conditions; in relaxing solutions the *A*- and *I*-band potentials (and therefore the fixed-charge concentrations) were equal.

In making these measurements, all conventional precautions are taken to avoid appreciable tip potentials in the microelectrodes. Attention should be drawn to the effects of KCl diffusion from the microelectrode. This will set up a diffusion (junction) potential to which the modified Nernst equation applies (Geddes, 1972). For 3-M KCl-filled microelectrodes in a solution which is essentially 100 mM KCl this junction potential is ~1.6 mV. Because the internal and external potassium and chloride ion concentrations are similar, the junction potential will be very nearly the same in the internal and external phases (Thomas [1978] remarks that it is both small and stable) and will not affect a measurement of the Donnan potential, because this is the difference between the potentials that the electrode records in the external and internal phases. Kushmerick and Podolsky (1969) have shown that there are no differences of ionic mobility inside and outside the contractile lattice which might make the junction potential inside different from outside. A further effect of KCl diffusion might be to cause an appreciable change in the internal concentrations of the free ions. Fig. 7 in Thomas (1978) shows such an effect, caused by chloride leakage from a KCl-filled microelectrode into a snail neuron, but the time scale (minutes for an appreciable concentration change) is very different from the few seconds which a Donnan measurement requires. Moreover in membraneless systems the internal chloride ion concentration is already approximately 30 times that in a normal cell, so the relative effect of a small leakage should be much reduced. In none of the experiments (see the published time records of Naylor, 1978, and Stephenson et al., 1981) is there any sign of consistent potential drift, on the seconds time scale, which might be caused by bulk diffusion.

Since the distance between muscle filaments is of the order of 40 nm, and the local potential will vary over this distance, while the size of the microelectrode tip used is 100–200 nm (Naylor, 1977), the microelectrode must measure an average potential. The calculation of fixed charge requires a knowledge of how this averaging is done by the microelectrode within the typical dimensions shown in Fig. 2. Our purpose is to reinvestigate this averaging, to

see whether the calculations of charge concentration which have been made in the literature are sensible.

ANALYSIS

Fig. 1, adapted from Alexandrowitz and Katchalsky (1963) represents diagrammatically the extended phase of filaments in a salt solution, in equilibrium with an external salt solution. In the absence of any permselective membrane the small ions are freely diffusible, and in equilibrium. There is a potential minimum midway between the filaments, and a further negative potential (E) between this minimum and the extended potential in the external phase (taken as the zero of potential). For convenience all potentials will be expressed in the reduced form ϕ ($\phi = e\psi/kT$) following the notation of Alexandrowitz and Katchalsky (1963).

Alexandrowitz and Katchalsky (1963; Eq. 5) show that the product $(m_+)_r \times (m_-)_r$ [$= (m_0)^2$] is independent of the position vector r and that the local chemical potential of the salt is therefore constant throughout the system. This means that the system is (at all points) in Nernst-Donnan equilibrium with the surrounding salt solution. Let us imagine that an infinitely small microelectrode, taking the form of a salt bridge connected to a junction reversible to one of the freely diffusable ions, could be placed at radius r. (We can suppose that the negative ions are chloride, and that a [reversible] Ag/AgCl junction is connected via an [irreversible] KCl bridge.) The electrode would detect the Nernst potential for negative (chloride) ions, $\phi_r = \log \{m_{-r}/m_0\}$ relative to an externally placed reference electrode. (We could write alternatively $\phi_r = -\log \{m_{+r}/m_0\}$

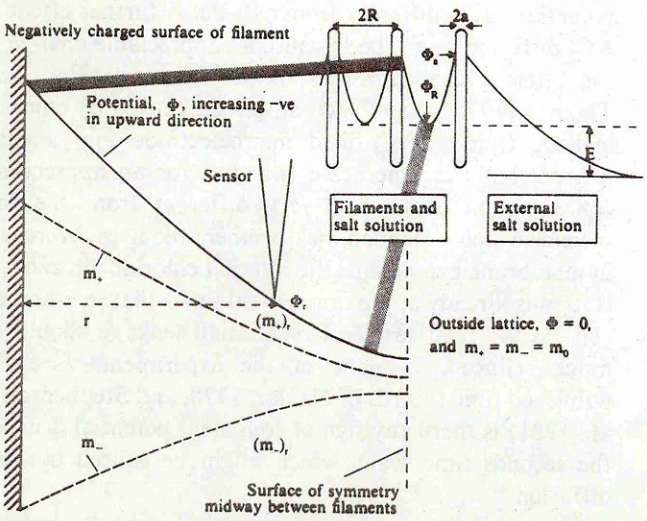

FIGURE 1 The electrical potentials in an extended gel of charged cylindrical filaments, diameter $2a$ and center-to-center separation $2R$, in equilibrium with an external phase containing salt molecules only. The *inset* shows the potential at higher magnification, and the counter and co-ion concentrations, between the filament surface and the sub-volume surface (radius R) where there is a potential minimum between the filaments.

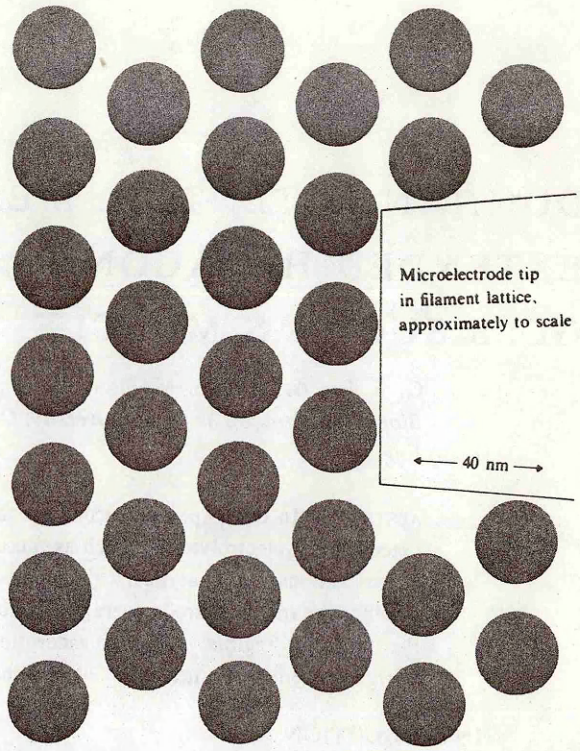

FIGURE 2 A diagramatic cross section of a hexagonal lattice of filaments, radius 15 nm and center-to-center separation 40 nm. The microelectrode tip, ~0.1 μm, is shown to scale.

because of the relationship between the ion concentrations mentioned above: Alexandrowitz and Katchalsky Eq. 5). The microelectrode, however, cannot in practice be made much smaller than the situation shown in Fig. 2. Clearly it must record an average potential, and it seems very likely that the effective averaging will be over the electrically neutral sub-volume between the filament surface and the symmetry plane (Figs. 1 and 2).

It has been suggested to us that the microelectrode might form a vacuole round its tip, and the conditions in this vacuole could be different from the original conditions within the lattice. There seems to be no good reason why this should happen. Once the microelectrode is properly inserted, movement generally causes no further potential changes unless the microelectrode tip can be seen to bend under the (high-powered) microscope or is removed from the lattice. A more sensible view is that the microelectrode does indeed average the existing environment within the filament lattice, and does not make any appreciable disturbance in the lattice ahead of its approach.

There are two ways in which the averaging may occur.

(a) If the microelectrode averages so that ϕ_m (measured) $= -\log \langle m_+ \rangle / m_0$, then $\exp(-\phi_m) = \langle m_+ \rangle / m_0$. (The quantity inside the bracket is positive because ϕ_m is negative.) A similar equation can be written for the negative ions.

$$m_0 \{\exp(-\phi_m) - \exp(+\phi_m)\} = \langle m_+ \rangle - \langle m_- \rangle.$$

The right-hand side represents the charge concentration on the filament surface, because the sub-volume must be electrically neutral. This is the charge calculation introduced by Collins and Edwards (1971) and used in its generalized form by Naylor (1977), Elliott et al. (1978) and Bartels and Elliott (1981). More formally,

$$\phi_m = -\log \frac{\frac{1}{V}\int_V m_0 \exp(-\phi_r)\mathrm{d}v}{m_0},$$

i.e., $\exp(-\phi_m) = 1/V\int_V \exp(\phi_r)\,\mathrm{d}v$, where the integral is taken over the sub-volume. Thus,

$$\exp(\phi_m) = \frac{1}{V}\int_V \exp(\phi_r)\,\mathrm{d}v$$

or

$$\exp(\phi_m) = \langle \exp \phi_r \rangle. \qquad (1)$$

(*b*) If, on the other hand, the microelectrode averages so that

$$\phi_m = -\left\langle \log\left\{\frac{m_0 \exp(-\phi_r)}{m_0}\right\}\right\rangle,$$

then

$$\phi_m = \frac{-1}{V}\int_V \log[\exp(-\phi_r)]\,\mathrm{d}v$$

(the integral is again taken over the sub-volume)

$$= \frac{1}{V}\int_V \phi_r\,\mathrm{d}v,$$

i.e.,

$$\phi_m = \frac{1}{V}\int_V \phi_r\,\mathrm{d}v$$

$$\phi_m = \langle \phi_r \rangle. \qquad (2)$$

Mathematically, Eq. 2 is different from Eq. 1, and might be very different for large values of ϕ_r, so we must ask whether the electrode measures Eq. 1 or 2.

Expanding the exponentials, Eq. 1 can be written

$$1 + \phi_m + (\text{terms in } \phi_m^2, \phi_m^3)$$
$$= 1 + \langle \phi_r \rangle + (\text{terms in } \langle \phi_r^2 \rangle\ \langle \phi_r^3 \rangle).$$

The bracketed terms on the left-hand side converge rapidly (it is rare that the measured potential exceeds 10–15 mV so $\phi_m \leq 0.6$). As long as $\exp(\phi_r)$ is able to be linearized over the inter-filament space, the terms in brackets on the right-hand side may be neglected and Eq. 1 reduces to

$$\phi_m = \langle \phi_r \rangle$$

which is identical to Eq. 2. Thus to a first approximation Eqs. 1 and 2 are equivalent, as long as ϕ_r can sensibly be regarded as linearizable through the interfilament region. We have therefore calculated the potential ϕ_r using the formal approach of Alexandrowitz and Katchalsky (1963) who matched a linearized (Bessel function) solution of the Poisson-Boltzmann equation for an outer region far from the cylinder surface with a nonlinearized solution for an inner region close to the cylinder surface. The nonlinearized solution was obtained (in trigonometric functions) by Fuoss et al. (1951), who assumed that the co-ion concentration is negligible (within the inner region). The two solutions are matched at a radius chosen to minimize the errors caused by neglecting the co-ion density in the inner region, and by neglecting the nonlinear terms for co- and counter-ion density in the outer region. Both these effects increase towards the match point, which is therefore taken at a radius that makes the effects equal in magnitude (Alexandrowitz and Katchalsky, Eq. 25). Alexandrowitz and Katchalsky state that in the worst possible case (zero salt concentration) this procedure introduces an error of <16% in the value of the charge density, and that the potential calculated by numerical integration is 'practically identical' to the analytical solution.

Inasmuch as some of the equations are transcendental in form, we programmed a computer with the calculation

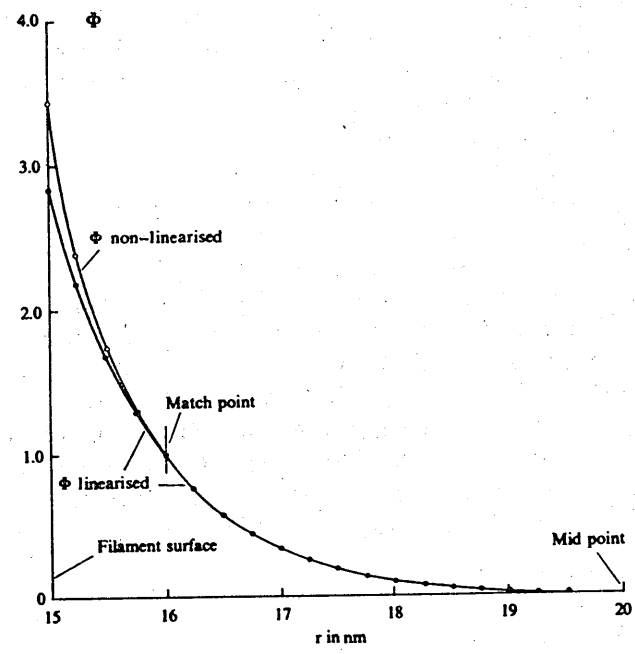

FIGURE 3 The two potential functions, linearized and nonlinearize (expressed in units of $e\psi/kT$) calculated for $K = 1\ \mathrm{nm}^{-1}$, $a = 15$ nm, R 20 nm and charge per unit length = 57 e/nm. The difference between th two functions (cylindrically integrated, see text) is ~5%. Note that in th diagram the zero of potential has been shifted for convenience of plottin so that it is at the sub-volume surface potential minimum. The potenti difference E between this minimum and the external phase is 0.0345 i these potential units (i.e., ~0.86 mV).

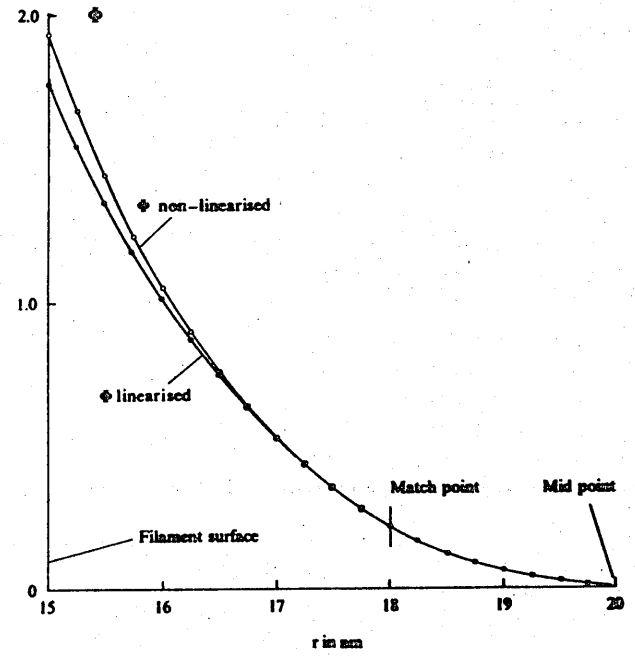

FIGURE 4 As Fig. 3, but with $K = 0.33$ nm^{-1} and charge per unit length = 12 e/nm. The cylindrically integrated difference is ~4%. Here again the zero of potential is at the mid-point for convenience of plotting; $E = 0.94$ or 23.5 mV.

using the (full) procedure suggested in Alexandrowitz and Katchalsky (III.3, p. 3240).[1] Calculated potentials for two typical cases are shown in Figs. 3 and 4. Fig. 3 is for a charge of 57 e/nm, which is about equivalent to the charge measured for the A-filaments in rigor muscle by Bartels and Elliott (1981) and a Debye length ($1/K$) of 1.0 nm, about equivalent to physiological ionic strength. Fig. 4 is for lower (by a factor of 5) charge at lower (by a factor of 10) ionic strength; the conditions shown in these two figures roughly bracket current experimental measurements in our laboratory.

In both figures the linearized potential function is plotted in both the outer and inner regions, and the nonlinearized function is plotted as well inside the chosen match point. It is apparent that in both figures the nonlinearized potential function represents a small correction to the linearized one. An estimate is obtained by an approximate numerical integration, carried out in annular regions to take account of the near-cylindrical symmetry. The difference is ~5% for Fig. 3 and 4% for Fig. 4. In either case this is within the experimental error of measurement of ϕ_m; in a typical experiment with 25 observations the standard error is usually 5–10%. In all cases the integrated potential derived from the linearized potential function is lower than that derived from the nonlinearized analytical solution. Further calculations show that at physiological ionic strength the difference is ~10% if the charge is twice as great (~120 e/nm) and is ~20% if the charge is six times as great (~360 e/nm).

Thus even if the microelectrodes do average as in Eq. 2, no significant error will be introduced under our experimental conditions by treating the data as if the averaging were done in Eq. 1, and calculating the fixed-charge concentration as described in Collins and Edwards (1971) and Elliott et al. (1978).

DISCUSSION

Although it seems to us intuitively sensible that the microelectrode will average the ion concentrations as in Eq. 1, it has been suggested that a significant number of electrophysiologists would disagree and assume Eq. 2 (averaging the local potentials) to be correct. We have demonstrated that the two are equivalent when the potential function can be approximated by linearization, and that this is the case within the experimental regimes used in our laboratory and in Edwards's.

Naylor (1982) has calculated the interfilament potentials independently, and also concludes that the interfilament space is a regime in which the potentials may be treated as simple Donnan averages.

In the course of calculations of the interfilament potential, we have confirmed that this approach predicts the charge saturation effect, which Millman and Nickel (1980) first pointed out, and Naylor (1982) has also shown. For example, at a Debye length of 1 nm the calculations show that however great the filament charge, the potential difference (E) between the potential minimum and the surrounding phase cannot be increased beyond 1.25 mV. This potential, at a constant Debye length, is directly related to the swelling pressure of the gel. For these small values of E the swelling pressure is proportional to E^2 (Alexandrowitz and Katchalsky, 1963; Eq. 14). A similar conclusion was derived by Bell and Levine (1958); see Elliott (1968). Using this relationship, a comparison with the calculations of Millman and Nickel (1980) was made with the cooperation of Dr. B. M. Millman. At a charge density of 100 e/nm, with a Debye length of 1.2 nm, their calculations using numerical integration give a swelling pressure of 3 Torr and the present calculation gives a swelling pressure of 6.5 Torr. Either value is in reasonable agreement with their experimental curves, and the theoretical accord is pleasing considering the different approaches adopted. The value taken for the cylinder radius in this work, 15 nm, is about twice the electron-microscope myosin (thick-filament) backbone radius of ~7 nm. Both Millman and Nickel (1980) and Naylor (1982) have found it necessary to depart from this radius to get reasonable agreement between experimental results and theory. We have calculated the swelling pressure near charge saturation for a cylinder radius of 7.5 nm, and separation of 20 nm, and find it about 10^{-6} times that with 15-nm radius. A similar comparison can be obtained

[1]There are a couple of minor errors in that paragraph, in line nine the second expression should read q/B, and the bracketed expression in the final term of Eq. 33′ should be squared.

by extrapolating Fig. 6 of Millman and Nickel (1980), the factor from their work is $\sim 2 \times 10^{-5}$; once again the agreement is reasonable.

In this paper we have followed Alexandrowitz and Katchalsky (1963) and used ion concentrations rather than ion activities in our equations for the Nernst-Donnan potential. Our justification for this is largely experimental. The experiments of Hinke and Gayton (1971), who measured activities using ion selective microelectrodes and compared these with chemical measurements of the ion concentrations, establish that at least for the major monovalent ions the activity coefficients are about equal inside and outside and thus cancel out in the equations. See for example Figs. 1 and 2 of Hinke and Gayton (1971), where the experimental points for K^+ activity and concentration ratios, both measured, are very similar. There are differences between the measured concentration and activity data for the Cl^- ions, but Hinke and Gayton attribute these to chloride binding to the contractile proteins. We have come to the same conclusion from our microelectrode studies and have discussed it elsewhere (Elliott, 1980).

For barnacle muscle, the internal ion concentrations and fixed charge concentrations have also been measured independently by isotope distribution (Hinke, 1980) and by membrane incorporation (Caillé, 1981). The accord with our Donnan measurements on the same muscle (Bartels and Elliott, 1981) is very reasonable.

CONCLUSION

After a reexamination of the theoretical and practical implications of Donnan potential measurements using KCl-filled microelectrodes in extended hexagonal gels such as muscle, without effective permselective boundary membranes, we conclude that these potential measurements can indeed be interpreted to give the fixed electric charge on the protein filament lattice in the manner introduced by Collins and Edwards (1971) and modified by Elliott et al. (1978).

We are grateful to Drs. G.R.S. Naylor and V.A. Parsegian for helpful discussions and comments, and particularly to Professor B. M. Millman, who would not be satisfied with intuition and insisted on a thorough analysis of this problem.

Received for publication 24 June 1981 and in revised form 15 October 1981.

REFERENCES

Alexandrowitz, Z. and A. Katchalsky. 1963. Colligative properties of polyelectrolyte solutions in excess of salt. *J. Polym. Sci. Part A.* 1:3231–3260.

Bartels, E. M., T. D. Bridgman, and G. F. Elliott. 1980. A Study of the electrical charges on the filaments in striated muscles. *J. Muscle Res. Cell Motil.* 1:194.

Bartels, E. M., and G. F. Elliott. 1980. Donnan potential measurements in the A- and I-bands of cross-striated muscles, and calculation of the fixed charge on the contractile proteins. *J. Muscle Res. Cell Motil.* 1:452.

Bartels, E. M., and G. F. Elliott. 1981. Donnan potentials from the A- and I-bands of skeletal muscles, relaxed and in rigor. *J. Physiol. (Lond.)* 317:86–87 P.

Bell, G. M., and S. Levine. 1958. Statistical thermodynamics of concentrated colloidal solutions. III. *Trans. Faraday Soc.* 54:975–988.

Caillé, J. P. 1981. The myoplasmic fixed charges of the barnacle muscle fiber and the free calcium concentration. *Biochim. Biophys. Acta.* 673:416–424.

Collins, E. W., and C. Edwards. 1971. Role of Donnan equilibrium in the resting potentials of glycerol-extracted muscle. *Am. J. Physiol.* 221:1130–1133.

Elliott, G. F. 1968. Force-balance and stability in hexagonally-packed polyelectrolyte systems. *J. Theoret. Biol.* 21:71–87.

Elliott, G. F. 1980. Measurements of the electric charge and ion-binding of the protein filaments in intact muscle and cornea, with implications for filament assembly. *Biophys. J.* 32:95–97.

Elliott, G. F., G. R. S. Naylor, and A. E. Woolgar. 1978. Measurements of the electric charge on the contractile proteins in glycerinated rabbit psoas using microelectrode and diffraction effects. *In* Ions in macromolecular and biological systems (Colston Papers No. 29). D. H. Everett and B. Vincent, editors. John Wright and Sons Ltd., Bristol. 329–339.

Fuoss, R. M., A. Katchalsky and S. Lifson. 1951. The potential of an infinite rod-like molecule and the distribution of the counter ions. *Proc. Natl. Acad. Sci.* U. S. A. 37:579–589.

Geddes, L. A. 1972. Electrodes and the measurement of bioelectric events. Wiley-Interscience, New York.

Hinke, J. A. M. 1980. Water and electrolyte content of the myofilament phase in the chemically skinned barnacle fiber. *J. Gen. Physiol.* 75:531–551.

Hinke, J. A. M., and D. C. Gayton. 1971. Transmembrane K^+ and Cl^- activity gradients for the muscle fiber of the giant barnacle. *Can. J. Physiol. Pharmacol.* 49:312–322.

Kushmerick, M. J., and R. J. Podolsky. 1969. Ionic mobility in muscle cells. *Science (Wash., D. C.)* 166:1297–1298.

Millman, B. M., and B. G. Nickel. 1980. Electrostatic forces in muscle and cylindrical gel systems. *Biophys. J.* 32:49–63.

Naylor, G. R. S. 1977. X-ray and microelectrode studies of muscle. PhD Thesis. The Open University, Milton Keynes, England.

Naylor, G. R. S. 1978. A simple circuit for continuous recording of microelectrode resistance. *Pflügers Arch. Eur. J. Physiol.* 378:107–110.

Naylor, G. R. S. 1982. On the average electrostatic potential between the filaments in striated muscle and its relation to a simple Donnan potential. *Biophys. J.* 38:201–204.

Pemrick, S. M., and C. Edwards. 1974. Differences in the charge distribution of glycerol-extracted muscle fibers in rigor, relaxation and contraction. *J. Gen. Physiol.* 64:551–567.

Stephenson, D. G., I. R. Wendt, and Q. C. Forrest. 1981. Non-uniform ion distributions and electrical potentials in sarcoplasmic regions of skeletal muscle fibers. *Nature (Lond.)* 289:690–692.

Thomas, R. C. 1978. Ion-selective microelectrodes. Academic Press, Inc London.

[*From the Proceedings of the Physiological Society*, 14–15 *September* 1984
Journal of Physiology, **358**, 80*P*]

Donnan potential changes in rabbit muscle A-bands are associated with myosin

By E. M. Bartels, P. H. Cooke, G. F. Elliott and R. A. Hughes. *Open University Research Unit, Foxcombe Hall, Berkeley Road, Boars Hill, Oxford OX1 5HR*

Donnan potentials recorded from the A-bands of skinned or glycerinated striated muscle fibres show a reversible drop from the rigor to the relaxed state, caused by a drop in the fixed electric charge on the protein matrix (Bartels & Elliott, 1981, 1982, 1983; Elliott & Bartels, 1982). To determine whether this charge drop is related to myosin, the major protein component of the A-band, Donnan potentials have been recorded from fine threads (0·5 mm diameter) of cross-linked synthetic thick filaments and also of myosin rods (derived from purified myosin isolated from rabbit muscle following Offer, Moos & Starr, 1973). The measured concentration of myosin or rod in the threads is typically 100–150 mg ml^{-1}, about the same as in an intact A-band. The experimental apparatus and methods are described in Bartels & Elliott (1981).

Table 1

	Whole-myosin threads	Myosin-rod threads	Myosin in A-band
Rigor solution	112 ± 5 ($n = 33$)	72 ± 8 ($n = 15$)	278 ± 4 ($n = 20$)
Relaxing solution	84 ± 6 ($n = 23$)	46 ± 5 ($n = 13$)	153 ± 4 ($n = 20$)

The charges are expressed in electrons per molecule, with standard errors of the mean. Rigor solution is 50 mM-KCl, 2·5 mM-$MgCl_2$ and 10 mM-phosphate buffer, pH 7. Relaxing solution is the same, with the addition of 2·5 mM-ATP. The number of separate experiments is shown, each includes at least 40 observations of potential. A-band charges are calculated from data given in Bartels & Elliott (1981) assuming each thick filament contains 300 myosin molecules and the charge is due only to myosin, and using X-ray values for interfilament spacings.

The results, given in Table 1, show that the A-band charge-change effect can also be recorded from a thread containing pure myosin filaments or myosin rods so that the effect is evidently related to the myosin filament backbone, rather than to the globular myosin heads which cross-link thick and thin filaments. The numerical values of charge are different in the protein threads and the A-bands, suggesting that the phenomenon depends on the molecular organization within the myosin filament backbone, since it is unlikely that the molecular packing is the same in these protein aggregates as in the native filaments of an intact muscle.

Supported by the S.E.R.C.

REFERENCES

Bartels, E. M. & Elliott, G. F. (1981). *J. Physiol.* **317**, 85–87*P*.
Bartels, E. M. & Elliott, G. F. (1982). *J. Physiol.* **327**, 72–73*P*.
Bartels, E. M. & Elliott, G. F. (1983). *J. Physiol.* **343**, 32–33*P*.
Elliott, G. F. & Bartels, E. M. (1982). *Biophys. J.* **38**, 195–199.
Offer, G., Moos, C. & Starr, R. (1973). *J. molec. Biol.* **74**, 653–676.

fast-fibre preparations (rat and rabbit) the increase in the A- and the I-band potentials during contraction has not been seen, perhaps because of the speed of the contractile processes. With these fast fibres a sustained potential rise during contraction appears in the microscope to have gone into a 'fluffy' state, and when no relaxation can be seen when the muscle is transferred back to relaxing solution. The increase in the Donnan potential during contraction might be due to the heads being locked in an 'on' and electrically charged position. When the heads are released again the potential will drop again and, due to the presence of Ca^{2+}, drop to a lower value than in the relaxed condition. We do not understand why this should affect the I-band potential during contraction. (Supported by the S.E.R.C.)

Donnan potentials from contracting muscle

E. M. Bartels and G. F. Elliott
Biophysics Group, The Open University, Oxford Research Unit, Foxcombe Hall, Boars Hill, Oxford, U.K.

In skinned and glycerinated skeletal muscle, different Donnan potentials were found in the A- and I-bands in rigor. In the relaxed muscle, the A- and the I-band potentials were found to be equal [Bartels & Elliott, *J. Physiol.* 317, 85–7P (1981); *J. Physiol.* 327, 72–3P (1982)]. Recently we have studied contracting skinned muscles. The Donnan potentials are measured with KCl-filled microelectrodes under a high-power microscope so that the position of the electrode tip can be seen during measurements. We have used mechanically skinned barnacle fibres, glycerinated (fast) rabbit psoas and chemically skinned fibre bundles from rat semitendinosus (fast) muscle and rat soleus (slow) muscle. The muscles are stimulated with calcium. In some of the experiments the mechanical force is registered alongside the potential measurements, in other experiments the contraction is followed optically from the changing band pattern.

In all barnacle fibres in good condition (fibres used on the day that the animal is killed) and in most slow fibre rat preparations, the A- and the I-band potentials increase during contraction and then decrease, to a potential lower than the relaxed muscle potential, when no more contraction can be seen. The A- and the I-band potentials are equal during contraction. In

LETTER TO THE EDITOR

A Reply to Godt and Baumgarten's Potential and K^+ Activity in Skinned Muscle Fibers: Evidence for a Simple Donnan Equilibrium Under Physiological Conditions

Dear Sir:

The K^+ ion-selective microelectrode measurements of Godt and Baumgarten (1984) have shown that K^+ is in electrochemical equilibrium at pH 7, which is close to physiological pH (pH 7.21 for crab muscle, Aickin and Thomas, 1975). In this observation they have confirmed the work of Collins and Edwards (1971) for rigor solutions and have extended this to relaxing solutions (in the presence of ATP). They have also confirmed the observation of Bartels and Elliott (1980, 1981, 1982) that the potential observed in the A-band with a 3 M KCl microelectrode is significantly more negative in the absence than in the presence of ATP. (We have noticed that random penetration of muscle fibers at moderate sarcomere lengths is much more likely to monitor the A-band than the I-band potential, so that under the conditions of Godt and Baumgarten's experiments the measured potential very probably arises from the A-band.)

Because we all agree empirically that there is electrochemical equilibrium at physiological pH for K^+, the major counter ion, in the presence of ATP or in its absence, then unless the major coion (Cl^-) is not in electrochemical equilibrium the analyses of Elliott and Bartels (1982) and Naylor (1982) show that it is legitimate to use the 3 M KCl potentials to calculate the fixed charge (i.e., the contractile protein charge) change between rigor and relaxed muscle. Nothing in Godt and Baumgarten's experimental observations vitiates this analysis or this conclusion.

Is it legitimate to assume that Cl^- is in electrochemical equilibrium at pH 7? In the absence of experimental evidence to the contrary, and given that K^+ is in equilibrium at this pH under all observed conditions, it seems highly unlikely that this assumption will be incorrect, but we shall await with interest any experimental reports using Cl^- ion-selective microelectrodes.

If the major counter and coions are in equilibrium and yet for any reason other diffusible ions are not so, will this cause any modifications in the fixed-charge measurements? Godt and Baumgarten give no argument to support such a hypothesis, beyond their sentences "the most likely explanation is that at pH 7 charge transfer associated with the ATPase reaction is fortuitously near balance, whereas at pH 5 it is not. This difference may arise from pH-induced alterations in the relative amounts and/or mobilities of the various diffusing species." But unless their K^+ electrode is sensitive to the diffusing species (and we doubt whether they themselves believe this), the K^+ balance surely shows that the amounts and/or mobilities of diffusing species are negligible at pH 7 compared with the electrochemical equilibrium. In this event, we know no physical principle that suggests that diffusion potentials are other than negligible, so that the situation reduces to an effective Donnan equilibrium, which leads to the fixed charge values that we have published already.

We are aware of the paper of Overbeek (1956) and the statement quoted from that paper. We do not, however, think that deviations from electrochemical equilibrium, which at pH 7 are too small to be measured with ion-selective electrodes, will cause highly significant differences in the potentials observed with 3 M KCl microelectrodes between rigor and relaxation, which we have measured and which Godt and Baumgarten confirm. We shall continue to regard these potentials as Donnan potentials and the calculated fixed-charge differences at physiological pH as real unless Godt and Baumgarten demonstrate theoretically or empirically that this is not the case.

Godt and Baumgarten's results show that under the ionic conditions of their solutions the effective isoelectric point is ~pH 5.8, both with and without ATP. This agrees with similar results for frog muscle by Dewey et al. (1982). In addition, Godt and Baumgarten have made some most interesting observations at low pH. Close to the isoelectric point, but on the alkali side (at pH 6) their results show that K^+ is in equilibrium in the absence of ATP, and very nearly so in its presence. Their results on the acid side of the isoelectric point (at pH 5) again show a K^+ equilibrium in the absence of ATP, but a significant disequilibrium in the presence of ATP. However, we think they should consider some possible perturbation factors before they relate their observation to working muscle. In the first place, working muscle includes a buffering power of 47 slykes (mM H^+ added/pH change produced) that resists change to lower pH (Aickin and Thomas, 1975). The buffering power of 15 mM Tris maleate at pH 5, measured in solutions made up according to the data given in Godt and Baumgarten (1984), is only ~2.5 slykes in the acid direction (this pH is outside the recommended range for the buffer), so that the buffering is unlikely to be very effective at pH 5 under these circumstances (see Murphy and Koss, 1968). It therefore seems possible that H^+ ions produced by ATP splitting might induce appreciable fixed-charge changes and thus cause local K^+ disequilibrium. In the second place, it seems possible that organic compounds, released at low pH from mechanically-skinned fibers in the presence of ATP, might interfere with the K^+ electrode. In this connection Dawson and Djamgoz (1983) have shown that K^+ ion-selective electrodes using the Corning ion-exchanger 477317 resin give abnormal readings in blow fly larval muscle cells (compared with electrodes using the valinomycin-based neutral ion carrier [NIC]). They report that in these muscles the 477317 electrode potentials lead to an internal potassium activity 26% greater than that derived from the NIC electrode potentials (this is a very similar excess to that shown in Godt and Baumgarten's Table III at low pH in the presence of ATP), and they conclude that the 477317 electrodes are sensitive to an organic interfering ion.

Even if both these effects turn out to be negligible, however, we shall still doubt whether phenomena that have been observed close to the isoelectric point or on the acid side of that point are important for the behavior of working muscle at physiological pH. We would prefer to look for an explanation in the work of Sarkar (1950), who measured the effects of ATP and ions on the isoelectric point of myosin, and showed that this point was highly dependent on the added ions, presumably because of specific ion

ɔsorption onto the protein. Dewey et al. (1982) have observed ıifts of isoelectric point in some muscles, and point out that fferent buffers also produce different detailed effects, and they ention ion absorption as a probable explanation. The effects ıat Godt and Baumgarten observe may well be explicable in ıese terms.

eceived for publication 17 June 1983 and in final form 17 ugust 1983.

REFERENCES

ickin, C. C., and R. C. Thomas. 1975. Microelectrode measurement of the internal pH of crab muscle fibres. *J. Physiol. (Lond.).* 252:803–815.

artels, E. M., and G. F. Elliott. 1980. Donnan potential measurements in the A- and I-bands of cross striated muscles, and calculation of the fixed charge on the contractile proteins. *J. Muscle Res. Cell Motil.* 1:452.

artels, E. M., and G. F. Elliott. 1981. Donnan potentials from the A- and I-bands of skeletal muscle, relaxed and in rigor. *J. Physiol. (Lond.).* 317:85–87P.

artels, E. M., and G. F. Elliott. 1982. Donnan potentials in rat muscle: differences between skinning and glycerination. *J. Physiol. (Lond.).* 327:72–73P.

ollins, E. W., and C. Edwards. 1971. Role of Donnan equilibrium in the resting potentials in glycerol extracted muscle. *Am. J. Physiol.* 221:1130–1133.

awson, J., and M. B. A. Djamgoz. 1983. Intracellular potassium activities of blow fly larval muscle cells. Proceedings of the Cambridge Meeting of the Physiological Society, June 1983. *J. Physiol. (Lond.).* 343:30–31P.

Dewey, M. M., D. Colflesh, P. Brink, Shih-fang Fan, B. Gaylinn, and N. Gural. 1982. Structural, functional and chemical changes in the contractile apparatus of *Limulus* striated muscle. *In* Basic Biology of Muscles. B. Twarog, P. Levine, and M. Dewey, editors. Raven Press, New York. 53–72.

Elliott, G. F., and E. M. Bartels. 1982. Donnan potential measurements in extended hexagonal polyelectrolyte gels such as muscle. *Biophys. J.* 38:195–199.

Godt, R. E., and C. M. Baumgarten. 1984. Potential and K^+ activity in skinned muscle fibers. Evidence for a simple Donnan equilibrium under physiological conditions. *Biophys. J.* 45:375–382.

Murphy, R. A., and P. G. Koss. 1968. Hydrogen ion buffers and enzymatic activity: myosin ATPase. *Arch. Biochem. Biophys.* 128:236–242.

Naylor, G. R. S. 1982. Average electrostatic potential between the filaments in striated muscle and its relation to a simple Donnan potential. *Biophys. J.* 38:201–204.

Overbeek, J. T. G. 1956. The Donnan equilibrium. *Prog. Biophys. Biophys. Chem.* 6:57–84.

Sarkar, N. K. 1950. The effects of ions and ATP on myosin and actomyosin. *Enzymologica.* 14:237–245.

G. F. ELLIOTT, E. M. BARTELS, P. H. COOKE, AND K. JENNISON, *The Open University, Oxford Research Unit, Foxcombe Hall, Berkeley Road, Boars Hill, Oxford OX1 5HR, England*

DONNAN POTENTIALS IN RABBIT PSOAS MUSCLE IN RIGOR

G. R. S. NAYLOR, E. M. BARTELS, T. D. BRIDGMAN,* AND G. F. ELLIOTT
Biophysics Group, Open University, Oxford Research Unit, Boars Hill, Oxford, England

ABSTRACT Collins and Edwards (1971, *Am. J. Physiol.*, 221:1130–1133) have shown that a tissue potential can be measured with microelectrodes in glycerinated muscle and that this potential is consistent with a Donnan equilibrium of small ions due to the concentration of net fixed electric charge on the contractile proteins. This approach has been combined with x-ray and light diffraction measurements of the muscle lattice dimensions, and the data are used to determine the thick filament charge and thin filament charge under a variety of different conditions. The thick filament charge is a function of the bathing solution, in particular its pH and ionic composition. These parameters are important in determining the volume of the equilibrium lattice and possibly are involved in the contraction mechanism itself.

INTRODUCTION

The membrane system of striated muscle fibers can be disrupted by storing them in a 50% glycerol-water solution for several weeks at low temperatures (Szent-Gyorgyi, 1949, 1951). Most of the components of the sarcoplasm are leached out (Weber and Portzehl, 1952) but despite this comparatively rough treatment the structure of the contractile system is preserved as seen in the electron microscope (H. E. Huxley, 1957) and by x-ray diffraction (H. E. Huxley, 1953). Because of the absence of ATP the fibers are in rigor, but if they are bathed in a suitable solution containing ATP, they become relaxed and extensible, and if calcium is then added, they will contract and generate a tension similar to the maximum tension produced in live muscle (Weber and Portzehl, 1952, 1954). Thus glycerinated muscle is a simpler system than an intact fiber and is useful for the study of the basic contractile elements, avoiding the osmotic and ion-selective effects imposed by the fiber membrane.

Low-angle x-ray diffraction experiments (Rome, 1967, 1968; Matsubara and Elliott, 1972) in which the spacing of the thick filament lattice is measured in a variety of bathing media suggest that there are significant long-range electrostatic forces between the filaments (see also Elliott, 1967, 1968; Millman and Nickel, 1980). These long-range forces will depend upon the fixed charge on the protein filaments.

Naylor and Merrellees (1964) and Weiss et al. (1967) observed that a negative resting potential could be measured with microelectrodes in glycerinated fibers. Collins and Edwards (1971) showed that this tissue potential behaved as a Donnan phase boundary potential due to the net fixed electric charge on the contractile proteins.

We have considered elsewhere (Elliott and Bartels, 1982; Naylor, 1982) the way in which the measured potential is related to the point-to-point potential between the muscle filaments, and have demonstrated that in the practical regime the average potential can be considered as a simple Donnan average, so that the measured potentials can be used, together with the principle of electrical neutrality, to give the fixed electric charge on the contractile proteins. This is the calculation introduced by Collins and Edwards (1971) and used in its general form by Elliott et al. (1978).

Here the techniques of low-angle x-ray diffraction and electrophysiology are combined to determine the net fixed charge on the muscle filaments in situ. The overall aim is to characterize the net fixed charge for a variety of different conditions of the bathing medium and different physiological states of the muscle. Some preliminary results of this work have already been published (Elliott et al., 1978). The experimental techniques have since been modified, and it is shown that the preliminary results gave artifactually high values for the Donnan potential. Here results are presented for the A-bands of rigor fibers, in experiments varying the pH and ionic strength of the bathing medium. In the following paper the effects of relaxing solutions are considered in both A- and I-bands (Bartels and Elliott, 1985).

METHODS

Basis of the Method

Collins and Edwards (1971) demonstrated that the fixed charge concentration in muscle is due to the contractile proteins, since partial extraction of actin and myosin at high ionic strength reduced the measured potential (and thus the fixed charge concentration) without having any effect on the measured isoelectric point.

*Deceased.
Dr. Naylor's present address is Physics Department, James Cook University, Townsville, Q 4811, Australia.

BIOPHYS. J. © Biophysical Society · 0006-3495/85/07/47/13 $1.00
Volume 48 July 1985 47–59

To go one step further and measure the electric charge per filament, not just the charge concentration, it is necessary to determine the volume associated with the fixed charge, i.e., the volume occupied by each filament. Low-angle x-ray diffraction studies give the lattice spacing of the thick filaments and combining this with laser diffraction, which gives the sarcomere length, determines the volume of the sarcomere. Here specimens were examined by diffraction and microelectrode methods to give information on the actual filament charge rather than the charge concentration.

Specimen Preparation

Psoas muscle from several different rabbits were used for all the experiments. The method of glycerination was similar to that of Rome (1967), the glycerinating solution contained 50% glycerol (by volume) and 50% (by volume) 100 mM KCl, 2 mM $MgCl_2$, 4 mM EGTA, 7 mM KH_2PO_4, 13 mM K_2HPO_4, pH 7.0. Strips of muscle ~4 mm in diameter were stored in this solution for 2 d at 4°C, changing the solution every 8 h, and were then transferred to a freezer at −20°C for 3 wk before use.

Muscle strips were prepared at a wide range of sarcomere lengths by stretching the fresh muscle to different degrees before glycerination. For our sarcomere-length variation experiments specimens were chosen at several sarcomere lengths, measured by light diffraction (see below).

Small strips of muscle, ~1 mm in diameter and 30 mm long, were used in all experiments. They were left to soak in the required solution for 30 min before being transferred to the experimental cell and were then allowed another 30-min equilibration time. In many experiments the specimen was examined in several different solutions and a re-equilibration time of 30 min was found to be sufficient.

Bathing Medium

The standard salt solution used consisted of 100 mM KCl, 5 mM $MgCl_2$, 7 mM KH_2PO_4, 13 mM K_2HPO_4, pH 7.0. The ionic strength of the salt solution was varied by serial dilution of the standard solution to give a set of solutions with KCl contents 100, 50, 20, 10, and 5 mM. The free ion concentration of each species was calculated from the accumulative association constants of Sillén and Martell (1964) and Portzehl et al. (1964) with the computer program described by White and Thorson (1972) and Perrin and Sayce (1967). In experiments where the pH was varied a citric acid/K_2HPO_4 buffer was used from 3.5–6.0 pH; this is one of the few buffers that will act effectively over this range.

X-ray Diffraction

The first two equatorial diffraction maxima, the (1,0) and (1,1) reflections from the hexagonal lattice of myosin filaments were obtained using a modified double Franks camera (Elliott and Worthington, 1963) mounted on a fine-focus rotating anode x-ray generator (Elliott Automation GX-6 GC Avionic Ltd., Boreham Wood, United Kingdom). The camera was aligned to give a vertical line and a spot above it. A specimen to film distance of between 160 and 200 mm was used and measured to an accuracy of ±0.5 mm. An exposure time of 60–90 min gave well-defined patterns. Films were measured with a traveling microscope to an accuracy of 0.01 mm and thus a typical spacing of 40 nm could be determined to an accuracy of ±1 nm.

Light Diffraction

The sarcomere length was measured using light diffraction from a 0.5 mW helium-neon laser (λ = 0.6328 μm) with a beam ~1.5 mm in diameter. Because of specimen inhomogeniety the sarcomere length was determined to an accuracy of ±0.05 μm. Initially the same specimen was used for x-ray diffraction, laser diffraction, and microelectrode observation. Later, as more x-ray data were accumulated, it was found more convenient to make parallel x-ray and microelectrode observations on separate specimens from the same experimental batch, chosen at sarcomere lengths defined by laser diffraction. This change of procedure did not make any significant difference to the gradient of the pooled x-ray data plotted against sarcomere length.

Electrophysiology

Borosilicate glass capillary tubing with an inner fiber (Hildenberg, Glass, Malsfeld, Federal Republic of Germany) and of 1.5 mm outside diameter was used for the microelectrodes (Sato, 1977). It was possible to fill the microelectrodes completely by capillary action with a syringe (Tasaki et al., 1968); the microelectrodes were filled with 3 M KCl. A few microelectrodes were examined in the electron microscope (e.g., Fig. 1). The diameter range of the tips was 0.1–0.2 μm, for microelectrodes with a resistance of 25–30 MΩ. Microelectrodes were connected to a high impedance direct current (DC) amplifier (10^{14} Ω) via a silver-chloride junction (model EH-1S; Transidyne General Corp., Ann Arbor, MI) and the output was displayed on a suitable calibrated meter. The circuit was completed with a calomel reference electrode (Corning Glass Works, Corning Science Products, Corning, NY or Radiometer American Inc., Westlake, OH), and a variable millivolt source was available on the low impedance side for calibration. In each muscle sample, 20 potential readings were taken and averaged; a standard deviation was obtained, typically <1 mV.

Junction Potentials

The amplifier will see the phase potential between the muscle and the bathing fluid, added to two liquid potentials, one at the calomel electrode and one at the microelectrode. As long as these do not change on impalement they can simply be "backed-off." Kushmerick and Podolsky (1969) have shown that the ionic mobilities inside and outside the contractile lattice are unchanged, except for a "tortuosity" factor, which is the same for all ions. This will not affect the liquid junction potentials. Since the free ions are identical inside and outside the lattice, and the concentrations are similar, it is simple to show that the change in junction potential of the microelectrode will be ~0.1 mV, and can thus be disregarded.

In a recent abstract Rehm et al. (1984) have interpreted the potential seen with a 3 M KCl electrode impaling the corneal stroma (an analogous matrix of charged proteins and proteoglycans) as solely due to a junction or diffusion potential. They state that they "interpret the PD as due to the effect of fixed negative charges of connective tissue fibers on the ratio of the K^+ to Cl^- mobilities." However, it is the essence of a Donnan distribution that the local charge distribution is on the average neutral, both inside and outside the charged matrix, and it is difficult to believe that K^+ and Cl^- ions, diffusing out of the microelectrode tip, will be able to differentiate the charges on the matrix from those on the co- and counter-ions in local equilibrium with that matrix. The argument is thus physically implausible and is, moreover, in conflict with the experimental results of Kushmerick and Podolsky (1969) for muscle.

Rehm et al. (1984) and Davis et al. (1970) (and also Viera and Onuchic, 1978, for the stratum corneum) report that the potential measured with their microelectrodes was a function of the electrode filling solution, decreasing to zero when the concentration within the electrode was the same as the solution bathing the tissue. This is not evidence that changes in diffusion potentials are important, as can be seen using the formulation of Teorrell (1953), who considered a situation where two salt solutions were in equilibrium with opposite sides of an ionic membrane, which consisted of a fixed-charge matrix and an aqueous, salt-containing medium. Teorrell showed (Eq. 20:2) that sum of the Donnan potentials at the two surfaces could be expressed as

$$25.6\left(\sinh^{-1}\frac{\bar{X}}{2a_2}-\sinh^{-1}\frac{\bar{X}}{2a_1}\right)\text{mV}.$$

$\bar{X}$ is the concentration of fixed charge in the membrane (typically 50 mM) and a_1, a_2 are the salt concentrations on the first and second sides of the membrane. Taking the first side as the solution in the microelectrode and the second side as the bathing solution in experiments of the type made in

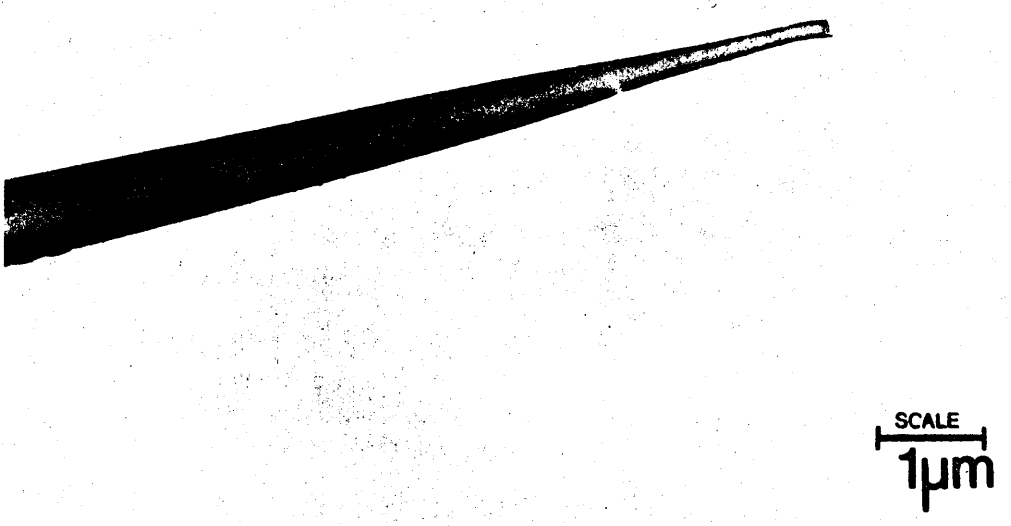

FIGURE 1 Electron micrograph of a typical microelectrode showing the tip diameter.

this paper and in the papers of Davis et al. (1970) and Viera and Onuchic (1978), it is easy to see that this sum will indeed be 0 if $a_1 = a_2$. It is also clear, though, that the second term is unimportant if $a_2 \sim 100$ mM and $a_1 \sim 3{,}000$ mM, which is the case in the experiments made in this paper. Under the conditions of these measurements, a typical experiment decreasing the salt concentration in the microelectrode gives, $E = (-9.3 \pm 0.7)$mV with 3 M KCl electrodes, (-9.4 ± 0.6)mV with 1 M KCl electrodes, and (-9.3 ± 0.6)mV with 0.5 M KCl electrodes.

Teorrell (1953) also considered a third component of potential, a diffusion potential between the two surfaces of the ionic membrane. This potential he expressed in Eq. 26:2, for the special case where a 1-1 valent salt is diffusing, as

$$25.6 \times \frac{u - v}{v + v} \ln \frac{a_1(r_1 u + v/r_1)}{a_2(r_2 u + v/r_2)} \text{ mV}.$$

Here u,v are the mobilities of the diffusing cations and anions, respectively, and r_1,r_2 are the Donnan ratios at the first and second surfaces, which can be shown to be 1.00 and 0.78, for a fixed charge concentration of 50 mM, using Teorrell's Eq. 8:2. Apart from the extra terms in the brackets, this diffusion potential is the same in form as the conventional (Henderson) expression for the diffusion potential from an electrode containing a filling solution of concentration a_1 into a solution of concentration a_2. Taking the usual values for K^+ and Cl^- mobilities, the terms in the brackets give a modifying factor of 0.97 to the logarithmic term. The logarithm is 3.40 in the absence of this factor and 3.37 in its presence, so that the diffusion potential changes by ~1%, which underlines the statement made in the first paragraph under this subheading.

Tip Potentials

The tip of a microelectrode may also produce a potential of 10 mV or more, larger than that predicted from a liquid junction; this potential is called the "tip potential" of the microelectrode (Adrian, 1956). The tip potential depends on the tip diameter, the composition of the glass used, and the concentration, composition, and pH of the solutions both inside and surrounding the tip (Adrian, 1956; Kostyuk et al., 1968; Lavallee, 1964; Lev, 1968; Szabo, 1966). Adrian showed that the major determinants of changes in tip potential (which is the important factor in these experiments) were different ions in the solutions (i.e., going from a sodium-rich Ringer's solution to a potassium-rich cytoplasmic solution) and different concentrations of these ions. In the experiments described in this paper the ions are the same inside and outside the lattice, and the changes in concentrations are small, so that large changes in any tip potential would not be expected. Nevertheless the tip potential was routinely measured (compared to a broken and blunt microelectrode) and electrodes where this potential was >1 mV were discarded.

A resistance meter described elsewhere (Naylor, 1978) was added to the circuit to enable the resistance of the microelectrode to be monitored continuously during impalement. Schanne et al. (1968) showed that the resistance of the microelectrode changes at the same time as the tip potential. By monitoring the tip resistance during impalement, it is possible to avoid situations where the resistance changes dramatically due to partial blockage with a possible change in tip potential. Readings where the resistance varied by >10% were discarded as a matter of routine. It was found (see Results) that a yet more stringent test was needed, so high power light microscopy (Bartels and Elliott, 1981, 1982, and 1985) was used to observe the tip of the microelectrode during impalement. On some impalements where the resistance change was <10% some mechanical deformation of the tip was visible (e.g., a slight bending of the electrode). Careful examination revealed that these impalements gave artifactually high readings (Results, Fig. 2). Light microscopy was subsequently used routinely to avoid this artifact, and all the microelectrode experiments were repeated, giving smaller values for the averaged potentials than in the first report (Elliott et al., 1978).

Depth of Impalement

It is important that the electrode is far enough inside the lattice of filaments that edge effects are minimized. The depth of impalement of

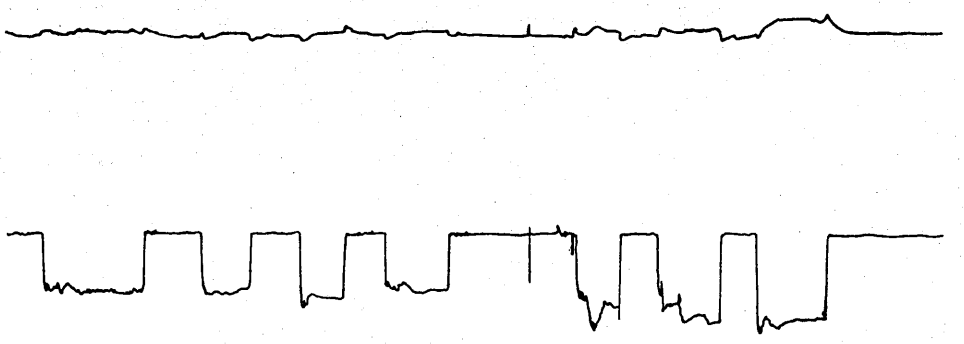

FIGURE 2 Potential and resistance traces of microelectrode insertions in a two-times diluted solution, based on 50 mM KCl. The first four insertions are normal, the next three are inserted too hard (see the section entitled Experiments in the Results).

the microelectrodes was measured by two methods, first by observation in the field of view of the microscope, and second by noting the change in the readings on the vernier scale used for impalement. Typical impalements without electrode deformation, measured by both methods, are 10–15 μm in depth. Since the unit cell in the filament lattice is of the order of 0.04 μm, the tip of the microelectrode is several hundred unit cells from the edge of the specimen. This is sufficiently far from that edge for edge effects on the potential and ion distribution to be ignored.

RESULTS

Initial Experiments

Fig. 2 shows a voltage and resistance trace of an experiment (made in a solution based on 50 mM KCl) under microscopic observation, which illustrates the problems with earlier data taken without microscopic observation. The first four impalements were made with the microelectrode seen in the microscope just to enter the A-band; the potential change is clear and apart from small transient changes, the resistance of the microelectrode does not vary outside the 10% previous criterion. The average of these impalements is about −7.5 mV. The next three impalements were made with a firmer touch on the micromanipulator. In the microscope the A-band could be seen to deform slightly, and in the last of these impalements the microelectrode could be seen to bend as impalement went deeper; these three readings are considerably higher than the earlier readings (average (~12 mV) and yet the resistance change of the microelectrode is still within the 10% criterion.

It seems clear that without microscopic observation of the electrode tip the observed potentials are higher than they would otherwise be and all the microelectrode experiments from the initial work have therefore been repeated. To see whether the history of a particular specimen would affect the measured potential or the measured x-ray spacing, it was necessary to study the effect of previous solutions on the specimen. (For example, when using several solutions is the order in which the solutions are used important?) These preliminary experiments were described in Naylor (1977). The conclusion was that the potentials and x-ray spacings measured are the same for a given specimen in a given solution as long as sufficient time is allowed for equilibration. The order in which solutions are used is unimportant.

Effect of Ionic Strength

Strips of muscles were studied in the set of serially diluted solutions with varying ionic strength and at different sarcomere lengths to find out the effect of sarcomere length. In agreement with the results of the preliminary investigation (e.g., Fig. 4 in Elliott et al., 1978), the observed potentials are independent of sarcomere length. Fig. 3 shows potential measurements plotted as a function of sarcomere length in four solutions of different ionic strength. The least-squares fit gradients of the straight lines, from the most concentrated to the most dilute solution in order, are −0.05, +0.34, +0.014, and −0.15 mV μm^{-1}. The largest gradient represents a change of only 0.48 mV over the range of lengths and this is within the standard deviation of the measurements. Since in addition these small gradients are two positive and two negative there is no consistent length effect, and the results from all sarcomere lengths have therefore been averaged in Table I. (See also the section entitled Absence of Sarcomere-Length Dependence: Further Details).

X-ray data were collected in the same solutions, giving the interfilament spacings $d(1,0)$ corresponding to the microelectrode data. A typical plot showing the variation of $d(1,0)$ as a function of sarcomere length for a particular solution is given in Fig. 4. As Rome (1967) observed, $d(1,0)$ and sarcomere length appear to be linearly related, with the spacing decreasing as the sarcomere is increased. The data were fitted to a straight line using a least-squares method and the equations so obtained are given in Table I.

Effect of pH

To study the effect of pH a set of four solutions was used — centered around the anticipated isoelectric point, pH = 4.5 (predicted from a minimum in the x-ray equatorial spacing [Rome, 1968] and a reversal in the sign of the Donnan potential [Collins and Edwards, 1971]). No x-ray pattern could be observed below pH = ~3.5, which was therefore chosen as the lowest pH. As far as possible one simple

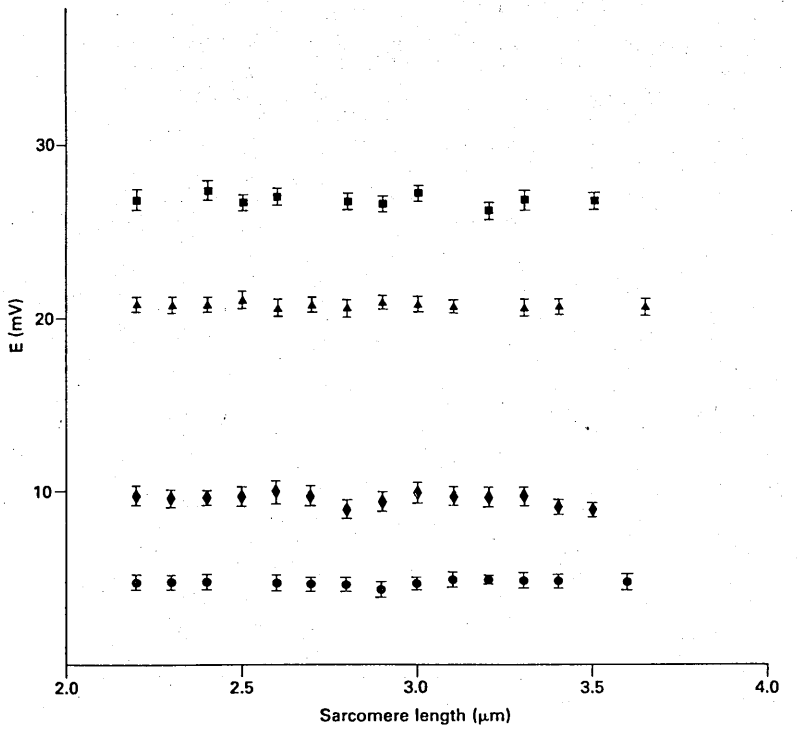

FIGURE 3 Potentials in four standard solutions, plotted as a function of sarcomere length. Circles, standard rigor solution; diamonds, two-times diluted triangles, five times diluted; squares, ten times diluted.

buffer system was used to avoid any possible effect of different binding affinities of different buffers to the filaments; a citric acid–K_2PO_4 buffer was chosen, allowing a maximum of pH 6.0. The data obtained at pH 7.0 in the previous section can be included with the results, though these were obtained with a different buffer system (phosphate) and may therefore not be strictly comparable.

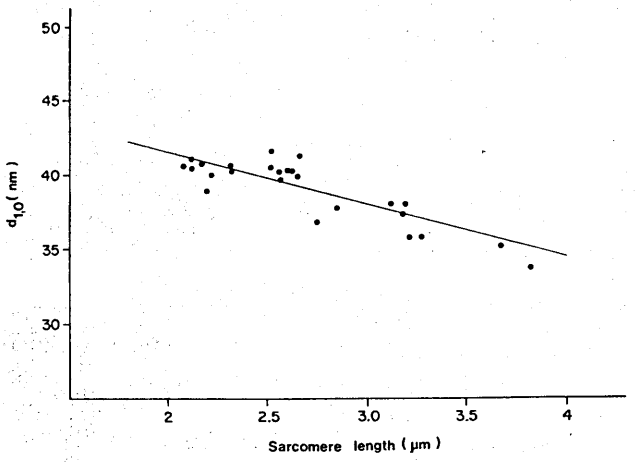

FIGURE 4 A plot of the x-ray spacing, $d_{1,0}$ as a function of sarcomere length S for the solution in the serial dilution set with [KCl] = 50 mM. The straight line shows the least-squares fit for all the data. Notice, however, that between S = 2.0 and ~2.6 μm there is no clear gradient in the observed data and only from S = 2.6–4 μm is there an appreciable change in side spacing (see Discussion, third paragraph).

pH Effect at Low Ionic Strength, [KCl] = 10 mM. Both x-ray and microelectrode techniques were used at a variety of different sarcomere lengths. Once again the potentials are independent of sarcomere length. The dependence of the potential changes sign and becomes positive, indicating a change in sign of the net electric charge on the filaments as shown in Fig. 5. This is effectively an in situ titration curve, and gives an isoelectric point of pH 4.5.

A summary of the corresponding x-ray data is also given in Table II, A. At the three higher pH's the x-ray lattice spacings decrease with decreasing pH but the least-squares straight lines for pH = 3.5 and pH = 4.0 intersect so that at short sarcomere lengths the spacing continues to decrease, whereas at long sarcomere lengths a minimum is observed. These results agree well with Rome (1968) who found a minimum spacing at pH 4.7 for long sarcomere length data (S = 3.15 μm) but observed no minimum spacing at short sarcomere lengths. Thus the pH behavior of the spacing of the myosin lattice unperturbed by the actin (at long sarcomere length) appears to reflect directly the charge on the thick filaments.

pH Effect at High Ionic Strength [KCl] = 50 mM. To see the effect of ionic strength on the titration curve and the isoelectric point the experiment was repeated at a higher ionic strength. The potentials were again independent of sarcomere length and the average potentials are also plotted as a function of pH in Fig. 5. This

TABLE I
SUMMARY OF RESULTS OF VARIATION OF IONIC STRENGTH

Solution	E	[Pr]	X-ray data	σ_m/σ_a	σ_m	σ_a
	mV	*mM*			*e/nm*	*e/nm*
100 mM KCl 5 mM $MgCl_2$ 20 mM phosphate buffer pH 7.0 μ = 0.14M	−4.7 ± 0.6 n = 400	52 ± 7	d^* = (47.2 ± 1.6) −(3.0 ± 0.5) × S‡ n = 31	7.1	47	6.5
2 × dilution, 50 mM KCl, etc. μ = 0.071 M	−9.7 ± 1.1 n = 400	56 ± 7	d = (48.1 ± 1.1) −(3.4 ± 0.5) × S n = 43	6.1	45	7.4
5 × dilution, 20 mM KCl, etc. μ = 0.029 M	−20.8 ± 1.1 n = 400	56 ± 4	d = (56.1 ± 1.5) −(6.3 ± 1.2) × S n = 28	2.7	40	15
10 × dilution, 10 mM KCl, etc. μ = 0.015 M	−26.8 ± 1.2 n = 400	40 ± 3	d = (59.6 ± 1.8) −(7.0 ± 1.5) × S n = 21	2.5	30	12
20 × dilution, 5 mM KCl, etc. μ = 0.0074 M	−34.6 ± 1.8 n = 40	31 ± 3	d = (68.9 ± 2.0) −(9.6 ± 2.7) × S n = 14	1.7	22	13

σ_m and σ_a are the linear densities, the thick and thin filaments, respectively. All potentials and the associated [Pr] are given as a mean and standard deviation. The x-ray data are shown as the least-squares straight line fit to the experimental data, with standard errors calculated in the normal manner. The charge ratios in column 5 have a precision of about ±50%, the thick filament linear charge in column 6 of about ±25%, and the thin filament linear charge in column 7 (much less precise for reasons given in the text; see Analysis) of about ±75%.

*d is measured in nanometers.

‡S is measured in microns.

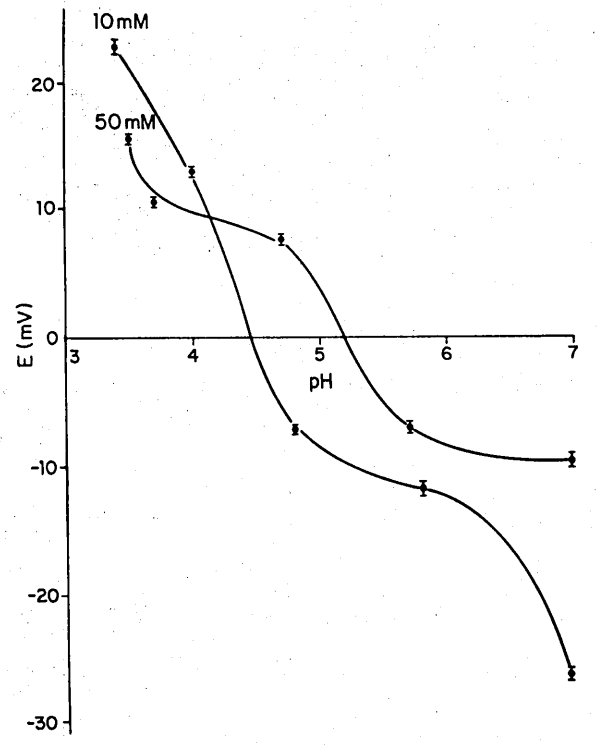

FIGURE 5 A plot showing the variation of the Donnan potential E as a function of pH. (*a*) [KCl] = 10 mM (*b*) [KCl] = 50 mM. The error bars show the standard error of the mean. Note that the measurements at pH 7 were obtained with a different buffer (phosphate) and may not therefore be strictly comparable with the other points, in citrate buffer.

shows an isoelectric point of pH = 5.2, so that the in situ isoelectric point has shifted to a higher pH on increasing the ionic strength. The corresponding x-ray data are also summarized in Table II, B. At pH = 6.0 and 5.0 the dependence of the $d(1,0)$ spacing on sarcomere length is less pronounced than in the low ionic strength solution.

Absence of Sarcomere-Length Dependence: Further Details

We have made extensive investigations of the measured potentials at different sarcomere lengths in an attempt to discover any sarcomere length dependence of the potentials. In no case was such an effect observed either in rigor solutions of different ionic strength (Elliott et al., 1978), rigor solutions of different pHs, or of different magnesium concentrations, or in relaxing solutions (Naylor, 1977; Bartels and Elliott, 1985), and the measured potentials are independent of sarcomere length in all the solutions that have been investigated.

In the preliminary experiments (Elliott et al., 1978) it had been concluded that in rigor muscle there were different charge concentrations in the A-bands and I-bands and therefore there should be different potentials arising from those bands. It therefore seemed possible that two families of potentials might be seen at longer sarcomere lengths, when the chance of hitting an I-band ought to be greater. Accordingly, a series of observations were made without light microscopy, recording large numbers (~150)

TABLE II
SUMMARY OF RESULTS OF VARIATION OF pH

Solution	E	[Pr]	X-ray data	σ_m/σ_a	σ_m	σ_a
A.	*mV*	*mM*			*e/nm*	*e/nm*
10 mM KCl	−11.8 ± 0.8	−11 ± 1	d^* = (55.4 ± 2.0)	2.3	7	3
0.5 mM $MgCl_2$			−(6.4 ± 1.6) × S‡			
0.8 mM phosphate/citric-acid buffer						
pH 5.8						
μ = 0.013 M	n = 100		n = 17			
As above	−7.2 ± 0.5	−6 ± 1	d = (50.6 ± 2.2)	3.6	4	1.1
pH 4.8			−(5.0 ± 1.2) × S			
μ = 0.014 M	n = 100		n = 18			
As above	12.9 ± 0.7	14 ± 1	d = (49.2 ± 1.8)	2.5	7	2.8
pH 3.95			−(5.7 ± 1.4) × S		net positive charge	net positive charge
μ = 0.014 M	n = 100		n = 17			
As above	22.7 ± 0.7	27 ± 1	d = (32.3 ± 1.7)	−42	21	0.5
pH 3.4			+(0.5 ± 0.05) × S		net positive charge	
μ = 0.014 M	n = 100		n = 14			
B.						
50 mM KCl	−7.1 ± 0.5	−32 ± 3	d = (38.5 ± 1.6)	32.2	29	0.9
2.5 mM $MgCl_2$			−(0.6 ± 0.1) × S			
4 mM phosphate/citric-acid buffer						
pH 5.7						
μ = 0.071 M	n = 100		n = 19			
As above	7.5 ± 0.8	42 ± 5	d = (36.9 ± 1.4)	25.9	33	1.3
pH 4.7			−(0.8 ± 0.2) × S		net positive charge	net positive charge
μ = 0.069 M	n = 100		n = 20			
As above	10.6 ± 0.7	60 ± 4	d = (34.6 ± 1.4)	30.5	58	1.9
pH 3.7			−(0.9 ± 0.2) × S		net positive charge	net positive charge
μ = 0.071 M	n = 100		n = 17			
As above	15.5 ± 0.6	92 ± 4	d = (33.7 ± 1.3)	73.3	66	0.9
pH 3.5			−(0.5 ± 0.03) × S		net positive charge	net positive charge
μ = 0.073 M	n = 100		n = 18			

*d is measured in nanometers.
‡S is measured in microns.

of potentials observed by random penetration in preparations at a range of sarcomere lengths in the rigor solution based on 20 mM KCl (fivefold dilution) and plotting the results in the form of histograms. These are shown in Fig. 6 *a–d*). It will be seen that at the longer sarcomere lengths (3.0 and 3.3 μm) the distribution is skewed at the lower potential end, while at the shortest sarcomere length (2.2 μm) the histogram shows a more nearly symmetrical distribution. It was not possible, however, to distinguish two separate peaks in experiments of this type with glycerinated rabbit muscle at long sarcomere lengths. The best-fit Gaussian curves are also seen in Fig. 6 *a–d*, and it will readily be appreciated that the mean potentials did not vary outside the experimental error, as was apparent also from the other experiments. Notice that the skewing of the histograms in Fig. 6 is not due to a sarcomere length effect on the A-band potential, which is eliminated by the data shown in Fig. 3. It is the result of the convolution of the A-band potential with the I-band potential, which is more likely to be observed in random observations at long sarcomere length. In experiments under optical control, where the location of the electrode is known, the data are not skewed in this manner.

It seems, therefore, that random penetration experiments, made without light microscope back-up, record the A-band potential in glycerinated rabbit muscle. In the subsequent paper further observations relevant to this point will be reported.

What Is the Effect of the H-Zone?

Although there is, in rigor glycerinated rabbit psoas muscle, a clear difference between the observed A- and I-band potentials (Bartels and Elliott, 1981, 1985) no effect has been seen experimentally in these muscles that needs be assigned to a manifestation of different potential regions in the overlap region of thick and thin filaments and in the H-zone of nonoverlap at the center of the A-band. Now there clearly is a different potential regime in the overlap and nonoverlap regions of the A-band, and if the experi-

EACH X = 0.33 PERCENT
a
EACH X = 0.23 PERCENT
b
EACH X = 0.26 PERCENT
c
EACH X = 0.26 PERCENT
d

mental method were sufficiently sensitive, it might be possible to detect the Donnan effects of these two different potential regions. This has not been observed here, nor has it been observed in the experiments of Aldoroty and April (1984) and Aldoroty et al. (1985) who have made similar measurements on crayfish muscle, where the A-band is three times longer than in rabbit or rat and where it therefore would be easier to detect the H-zone region when placing the microelectrode.

A possible reason for this inability to detect different H-zone potential is that the region over which the microelectrode senses an average is of the order of a 1-μm diameter sphere. This would tend to average both H-zone and overlap zone in an A-band of 1.6 μm in length. Whatever may be the reason, Fig. 3 shows that there is no sarcomere length on the observed A-band potential, as might have been expected from an H-zone effect.

ANALYSIS

The concentration of all ions in the external solution can be calculated from the Perrin program. Therefore, when the Donnan potential has been determined, the application of the Nernst equation gives the concentrations of all these diffusible ions inside the filament lattice. Since the lattice must maintain electrical neutrality, the protein charge concentration [Pr^-] in millimolar units is given by: $[Pr] = \Sigma c_i^+ z_i^+ - \Sigma c_i^- z_i^-$, where c_i^+ and z_i^+ are the internal millimolar concentrations and valencies of the diffusible cations and c_i^- and z_i^- are the internal concentrations and valencies of the diffusible anions. Normally, with a negative Donnan potential this equation expresses the concentration of net negative charge on the protein filaments. Since the concentrations are all expressed in millimolar quantities it is simplest to express [Pr] in millimoles of univalent charge, because the valency of the charged matrix is unknown.

The working hypothesis for the interpretation of the preliminary results was that a microelectrode inserted randomly in glycerinated muscle in rigor recorded the higher A-band potential rather than the lower I-band potential (Elliott et al., 1978). Experimentally, this A-band potentials is indepedent of sarcomere length. In the present experiments microelectrode measurements have been combined with direct observation of the microelectrode tip under a high-powered light microscope and under these circumstances it is possible to differentiate between A- and I-band potentials, see Bartels and Elliott (1985).

Using the A-band potential alone, however, combined with the x-ray data, it is possible to calculate the charge on the thick and thin filaments. At long sarcomere lengths the A-band is composed solely of thick filaments, and one unit cell contains exactly one thick filament. Thus σ_m, the net charge on the thick filament (per unit length) is given by: σ_m = [Pr] × (volume occupied by unit length of the filament) × N_o, where N_o is Avogaradro's number. But volume occupied by the filament per unit length is $d_{3,8}^2/\sin 60°$. (Adopting the notation $d_{3,8}^2$ for the square of the value of d[1,0] evaluated at S = 3.8 μm). Hence $\sigma_m = 6.95 \times 10^{-4} \times [Pr] \times d_{3,8}^2$. It is assumed that the myosin filaments are 1.6 μm in length and the actin filaments are 1.1 μm in length, reasonable values for mammalian muscle, so that 3.8 μm is the point of zero overlap. If d is nanometers, and [Pr] is millimolar, σ_m is in electrons per nanometer.

At the short sarcomere length (S = 2.2 μm), where the thin filaments just meet, a unit cell in the A-band contains exactly one thick filament and two thin filaments. Thus the net charge (per unit length) on the thin filament σ_a is given by: $2\sigma_a + \sigma_m = 6.95 \times 10^{-4} \times [Pr] \times d_{2,2}^2$ (where $d_{2,2}^2$ is the square of the value of d[1,0], evaluated at S = 2.2 μm). Combining this expression with the expression evaluated above for σ_m, $\sigma_a = 3.48 \times 10^{-4} \times [Pr] \times (d_{2,2}^2 - d_{3,8}^2)$ and the charge ratio, $\sigma_m/\sigma_a = 2\, d_{3,8}^2/(d_{2,2}^2 - d_{3,8}^2)$. Notice that this ratio does not depend on the value of [Pr], and thus of the value of the measured potential, but only on the parameters of the x-ray data. It does depend on the experimental fact that the A-band potential is independent of the sarcomere length, and thus that the A-band charge concentration is the same at all sarcomere lengths (see also Elliott, 1973).

σ_a and σ_m are given in Table I for the experiments varying ionic strength and in Table II for the experiments varying pH. In the calculations we used the values for the spacings d(1,0) that are predicted from the least-squares fit. The values calculated for σ_a are inherently of low precision because of the subtraction of two large and nearly equal numbers, $d_{2,2}^2$ and $d_{3,8}^2$.

DISCUSSION

Veracity of the Method

The electrophysiology of the Donnan potential measurements has been discussed by Elliott and Bartels (1982) and in the Methods section here. Two additional points may be made.

(*a*) First, Aldoroty and April (1984) have performed elegant model experiments using agar gels, and have shown that the measured Donnan potentials behaved as expected when the concentration of the agar was varied. In other experiments the potential was unchanged when the tip diamenter was varied, when the concentration of KCl in the electrode was varied, and when the bathing solution was changed from potassium chloride to the same concentration of potassium propionate. They report that the absence of significant variation under these conditions, where diffusion potentials would be expected to change,

FIGURE 6 Histograms of a large number (150+) of potential readings taken in the same solution (the five times diluted solution based on 20 mM KCl) at different sarcomere lengths (*a*) 2.2 μm, (*b*) 2.6 μm, (*c*) 3.0 μm, and (*d*) 3.3 μm.

demonstrates that artifactual diffusion potentials do not contribute significantly to the measurements. (*b*) Second, the A-band of a rabbit muscle fiber contains proteins whose amino-acid sequence data are known, and whose charge can therefore be calculated (Appendix). At zero overlap none of the thin filament proteins contribute to the A-band charge. The volume can be measured with precision by a combination of x-ray and light diffraction. Under low ionic strength conditions, where ion binding would be expected to be minimal, the measured thick filament charge by the methods used here is 22 electrons (e) nm^{-1}. The calculated charge range (Appendix) is 9–26 e nm^{-1} (depending on the degree of ionization of the histidine residues) with a mean at ~ 18 e nm^{-1}. The accord between these two values is pleasing, and gives added confidence in the veracity of the method.

Discussion of the Experimental Results

The approximate linear behavior of the x-ray lattice spacing as a function of sarcomere length is similar to that observed by Rome (1967, 1978). In Rome's study of the effect of ionic strength the results are in good agreement with ours at short sarcomere length; at long sarcomere lengths (3.2 μm) she found that the spacing decreased with increasing dilution (opposite to the effect at short sarcomere length, S = 2.9 μm). This effect was not observed in our experiments at S = 3.2 μm but is clearly seen at S = 3.8 μm (i.e., at zero overlap). Thus at long sarcomere lengths the behavior of the lattice spacing in the myosin lattice unperturbed by actin filaments follows the electric charge on myosin (see Table I). Compare this with the similar pH behavior (see Results).

(In collaboration with Professor B. M. Millman of Guelph University [Guelph, Canada] a computer data bank has been established of all the available published and unpublished x-ray equatorial data on muscle, collected by several different investigators, in several different laboratories, over the last two and a half decades. The least-squares fit straight lines of the x-ray data in Table I agree closely with the collations of all this data. This is particularly true for the 100-mM solution, where the data bank contains a total of 226 individual observations.)

We are aware that it is only approximately correct to treat the x-ray data as a linear function of sarcomere length, and that the experiments of Shapiro et al. (1979) and Magid and Reedy (1980) show nonlinear behavior. (Indeed some of the present x-ray data show similar nonlinearity, see Fig. 4.) For the present purposes however, the precision of this approximation is sufficient for the analysis presented.

The trend of our observations of potential as a function of ionic strength agrees with that of Collins and Edwards (1971) who studied glycerinated frog ventricle and sartorius, and found that the fixed charge concentration increased with [KCl]. The major result of these experiments is that the net charge on the thick filament varies considerably with ionic strength, even taking into account the volume changes due to the swelling of the lattice. The thin filament charge, in comparison (although its determination is less accurate) seems to be less dependent on the ionic composition of bathing solution.

There are two effects that might account for the variation in the thick filament charge.

(*a*) First, hydrogen ions themselves will be distributed across the phase boundary according to the Donnan equilibrium and thus the pH of the medium surrounding the filaments will not be the same in the various solutions. For the experiment varying the total ionic strength the internal pH varies from 6.8 to 6.2, the lower ionic strength giving the lower internal pH.

At this point the effect of the changing internal pH on the thick filament charge will be considered in more detail. It is well known that the range pH 6–7 probably contains the effective *pK* of the histidine residues in proteins. Fig. 5 shows that there are definite changes in potential over this range of pH and there must be a similar change in fixed charge also. Is this sufficient to account for the effects seen in Table I? It is shown in the Appendix that there are 82 histidine residues on myosin and its associated light chains. If all these histidine residues became ionized the myosin filament charge would decrease from 26–9 e nm^{-2} (Appendix). The measured values lie from 47–22 e/nm. Put in another way, the change in myosin charge concentration would be less than the existing amount, i.e., 12 mM (Appendix), and the observed change is from 56–30 mM. The histidine effect seems insufficient to account for this even if allowance is made for a change of the actin charge to take account of its histidine content, 8 per monomer from the data of Collins and Elzinga (1975). (Tropomyosin and the troponins have negligible amounts of histidine according to the sequence data mentioned in the Appendix.) It is interesting though that on the interpretation given here the thick filaments, which contain the larger amount of histidine per unit length, are also those that seem to have ion-binding properties (see *b* below) and it might be speculated that one effect may perhaps be involved in the other.

(*b*) Second, the effect of ion binding must be considered. The major effect is due to the binding of a negative ion since on dilution the binding is presumably reduced and it is seen experimentally that the negative charge is reduced. There are therefore three possibilities for this binding, either chloride ions or phosphate ions or both of these ions together. The present experiments do not distinguish between these possibilities, although note that the chloride ions are present at much higher concentrations. In other experiments, to be reported in a subsequent paper (Bridgman, T. D., E. M. Bartels, and G. F. Elliott, manuscript in preparation; see also Elliott, 1980), it has been shown that either chloride or phosphate in the absence of the other is sufficient for this effect, that both appear able to bind at the same time, but that the binding of phosphate ions is interactive with the level of free magnesium ions, so that an increase of the magnesium causes a fall in Donnan poten-

tial, and therefore of protein charge concentration, if there are phosphate ions present.

The term ion binding is used here to refer to ions that are associated with the fixed-charge matrix of the total system and are thus not freely diffusible in and out of the system. This does not imply that these are necessarily covalently bound. Probably they are associated electrostatically with the matrix, and possibly it would be better to use the older term adsorbed ions.

In the Appendix expected thick and thin filament charges have been calculated on the basis of sequence data for the contractile proteins. The measured values for the thin filament charge, in the range 6–15 e nm^{-1}, agree well with the calculated value considering that the error of measurement is large. The measured values for the thick filament charge are up to two and a half-times the calculated value, though they drop to the calculated value as the ion concentration approaches zero, Table II. It is this fact that leads to the postulation of negative ion binding as an important characteristic of intact thick filaments in glycerinated psoas muscle. The total of all the calculated charge concentrations is <30 mM, the measured values range from 30–60 mM, and increase with ionic strength. This strongly suggests that negative ion binding must occur somewhere in the contractile system. Moreover the same conclusion can be drawn from the data of Collins and Edwards (1971) and Pemrick and Edwards (1974) if their values of charge concentration are recalculated using all the ions in their solutions and not just the KCl concentrations as they have done.

The experiments varying the pH of the bathing solution confirm and extend the earlier results of Collins and Edwards (1971) who showed a reversal in the sign of the measured potential at low pH. The data also confirm the x-ray results of Rome (1968), i.e., that the interfilament spacing decreases with decreasing pH and that at long sarcomere lengths there is a distinct minimum of the interfilament spacing at low pH. The fact that the potential changes sign at this point is very strong evidence that the potential being measured is related to the Donnan potential since it follows the sign of the net charge on the filaments, changing on passing through the isoelectric point. The graph of the potential vs. the pH represents the titration curve of the proteins, probably essentially the titration curve of the thick filaments because the A-band at long sarcomere lengths is composed solely of thick filaments, which contain mainly myosin but also a small amount of other components, notably C-protein (Offer, 1973). The change is slope of the curves near pH 7.0 is in the histidine *pK* region, which appears to depend on the ionic strength.

The experimental data have been analyzed on the hypothesis that the measured potential is a Donnan potential, and is the average of the potential well between the filaments (see Elliott and Bartels, 1982; Naylor, 1982). This hypothesis has been substantiated by previous workers (Collins and Edwards, 1971; Pemrick and Edwards, 1974), who showed that the potential increased on decreasing the ionic strength and behaved in the expected manner on different sides of the isoelectric point of the muscle proteins. These experiments have been repeated and extended with a similar outcome and there seems to be no difference between the behavior of the experimental tissues. Using this hypothesis a detailed analysis of the data yields a self-consistent set of results that are in agreement with other data. In this respect the experiments varying pH are important; these results show that the titration curve and the isoelectric point of myosin are a function of the ionic composition of the bathing medium.

APPENDIX

Charge Values from Sequence Data

The data of Barlow and Thornton (1983, and personal communication) established that at least 85% of the ion-pairs in known protein structures are accessible to the solvent, and that the unpaired ionic groups are also so accessible. Rashin and Honig (1984) put the proportion even higher, >95%. It is therefore reasonable to predict the net protein charge on any protein from the amino acid or sequence data.

Such an attempt to predict filament charges, and hence muscle charge concentration was made by Elliott (1973). The major problem at that time was that the amide NH_3 is difficult to measure with accuracy and had largely been left unmeasured by workers more recent than Kominz et al. (1954). A secondary problem was that the number of myosin molecules in a myosin filament was a matter of controversy. Using a myosin charge value of 15 electrons per 10^5 daltons (or ~75 e for the whole molecule) from Kominz et al. (1954), which agreed with the titration data of Milhayi (1950), Elliott (1973) calculated a thick filament charge of ~20 e nm^{-1}. (This calculation assumed Huxley's [1960] figure of 432 myosin molecules per filament.) Pepe's (1967) model for the myosin filament has ~400 molecules, similar to Huxley's number, so that the calculated filament charge using Pepe's model does not differ appreciably from Elliott's calculation. Squire's (1973) model has ~300 molecules, giving a figure of ~15 e nm^{-1}. These filament-charge figures ignored the C-protein (Offer, 1973) but this is unlikely to cause more than a 10% error. They also ignored the myosin light chains, see below.

The recent complete myosin sequence data of McLachlan and Karn (1982) and Karn et al. (1983) for nematode myosin, gives 90 e/molecule of which 94 e is on the myosin rod and 2 e^+ on each myosin head. Each myosin molecule in rabbit fast muscle has four light chains associated with it, two to each myosin head, and the sequence data on these are given by Grand (1982). These add 19 e to each myosin head, making a total charge on myosin heavy and light chains of 128 e. (Notice in passing that the light-chain charge makes a considerable difference to the myosin head charge, as might be appropriate for a control function. Equal occupancy of LC_1 and LC_3 has been assumed).

In these calculations it has been assumed that none of the histidine residues are ionized at physiological pH. There are a total of 82 histidine residues on the molecule and its light chains (34 on the rod, 21 on each head, and 3 on the light chains associated with each head). If all these were ionized the 128 e would fall to 46 e.

It is now clear that the myosin filament is three stranded (Kensler and Stewart, 1983) so that there are 300 myosin molecules in a rabbit or frog thick filament. The total range for the myosin filament charge from amino acid sequence and structural data is thus 9–26 e nm^{-1}, a rather wide range that includes the 1973 estimate. Taking the average value ~18 e nm^{-1}, and a sarcomere volume at $S = 3.8$ μm of 4×10^{-15} ml in the solution with 100 mM KCl (from the data given in Table I), the charge concentration in the whole sarcomere due to the myosin filaments is ~12 mM, which is close to the value (12.1 mM) given by Pemrick and

Edwards (1974) who approached the same problem from bulk protein-concentration measurements.

For the thin filaments, Elliott (1973) calculated ~10 e nm^{-1}. This also can now be modified since the actin sequence data of Collins and Elzinga (1975) give a precise figure, 7 e, for the actin molecule charge, the tropomyosin sequence data of Stone and Smillie (1978) gives 50 e for tropomyosin, the sequence data of Collins et al. (1977) for troponin C gives 29 e for that protein, the sequence data of Pearlstone et al. (1977) gives 9 e^+ for troponin T and the sequence data of Wilkinson and Grand (1975) gives 9 e^+ for troponin I. The total net molecular charge on the troponins is thus 11 e (negative). From these figures the thin filament charge is 2.5 e nm^{-1} due to actin, 2.4 e nm^{-1} due to tropomyosin, and 0.5 e nm^{-1} due to the troponins, and the total calculated thin filament charge is 5.4 e μm^{-1}. The charge concentration in the whole sarcomere due to actin is 4.6 mM, considerably less than Pemrick and Edwards (1974) figure (19.2 mM); this is due to their using an actin charge (24 e) that is untenable in the light of the sequence data. The other values (4.4 mM due to tropomyosin and 5.7 due to the troponins) are not appreciably different from those given by Pemrick and Edwards (1974).

We are grateful to Professor B. M. Millman and Drs. Tony Angel, Charles Edwards, David Gayton, Suzanne Pemrick, Mark Shoenberg, and Tony Woolgar for help, advice, and useful discussions during the course of this work.

We would particularly like to acknowledge the students of the Open University course S321, "The physiology of cells and organisms," whose work on experiments of this type over eight years in successive summer schools has shown us the reality of the phenomena that we observe.

Received for publication 28 March 1984 and in final form 19 November 1984.

REFERENCES

Adrian, R. H. 1956. The effect of internal and external potassium concentration on the membrane potential of frog muscle. *J. Physiol. (Lond.)*. 133:631–658.

Aldoroty, R. A., and E. W. April. 1984. Donnan potentials from striated muscle liquid crystals. A-band and I-band measurements. *Biophys. J.* 46:769–779.

Aldoroty, R. A., N. B. Garty, and E. W. April. 1985. Donnan potentials from striated muscle liquid crystals. Sarcomere length dependence. *Biophys. J.* 47:89–96.

Barlow, D. J., and J. M. Thornton. 1983. Ion-pairs in proteins. *J. Mol. Biol.* 168:867–885.

Bartels, E. M., and G. F. Elliott. 1981. Donnan potentials from the A- and I-bands of skeletal muscle, relaxed and in rigor. *J. Physiol. (Lond.)*. 317:85–87P.

Bartels, E. M., and G. F. Elliott. 1982. Donnan potentials in rat muscle: difference between skinning and glycerination. *J. Physiol. (Lond.)*. 327:72–73P.

Bartels, E. M., and G. F. Elliott. 1985. Donnan potentials from the A- and the I-bands of glycerinated and chemically skinned muscles, relaxed and in rigor. *Biophys. J.* 48:61–76.

Collins, E. W., and C. Edwards. 1971. Role of Donnan equilibrium in the resting potentials in glycerol-extracted muscle. *Am. J. Physiol.* 221:1130–1133.

Collins, J. H., and M. Elzinga. 1975. The primary structure of actin from rabbit skeletal muscle. *J. Biol. Chem.* 250:5915–5920.

Collins, J. H., M. L. Greaser, J. D. Potter, and M. J. Horn. 1977. Determination of the amino acid sequence of troponin C from rabbit skeletal muscle. *J. Biol. Chem.* 252:6356–6362.

Davis, T. L., J. W. Jackson, B. E. Day, R. L. Shoemaker, and W. S. Refrew. 1970. Potentials in frog cornea and microelectrode artefact. *Am. J. Physiol.* 219:178–183.

Elliott, G. F. 1967. Variations of the contractile apparatus in smooth and striated muscle. *J. Gen. Physiol.* 50 (Pt. 2):171–184.

Elliott, G. F. 1968. Force-balances and stability in hexagonally-packed polyelectrolyte systems. *J. Theor. Biol.* 21:71–87.

Elliott, G. F. 1973. Donnan and osmotic effects in muscle fibers without membranes. *J. Mechanochem. Cell Motil.* 2:83–89.

Elliott, G. F., and E. M. Bartels. 1982. Donnan potential measurements in extended hexagonal polyelectrolyte gels such as muscle. *Biophys. J.* 38:195–199.

Elliott, G. F., and C. R. Worthington. 1963. A small-angle optically focusing x-ray diffraction camera in biological research. Part I. *J. Ultrastruct. Res.* 9:166–170.

Elliott, G. F., G. R. S. Naylor, and A. E. Woolgar. 1978. Measurements of the electric charge on the contractile proteins in glycerinated rabbit psoas using microelectrode and diffraction effects. *In* Ions in Macromolecular and Biological Systems. (Colston Papers No. 29). D. H. Everett and B. Vincent, editors. Scientechnica Press, Bristol, United Kingdom. 329–339.

Grand, R. J. A. 1982. The structure and function of myosin light chains. *Life Chem. Rep.* 1:105–160.

Huxley, H. E. 1953. X-ray analysis and the problem of muscle. *Proc. R. Soc. Lond. B. Biol. Sci.* 141:59–62.

Huxley, H. E. 1957. The double array of filaments in cross-striated muscle. *J. Biophys. Biochem. Cytol.* 3:631–648.

Huxley, H. E. 1960. Muscle cells. *In* The Cell. J. Brachet and A. E. Mirsky, editors. Academic Press, Inc., New York. 365–481.

Karn, J., S. Brenner, and L. Barnett. 1983. Protein structural domains in the *Caenorhabditis elegans unc*-54 myosin heavy gene chain are not separated by introns. *Proc. Natl. Acad. Sci. USA.* 80:4253–4257.

Kensler, R. W., and M. Stewart. 1983. Frog skeletal muscle thick filaments are three-stranded. *J. Cell. Biol.* 96:1797–1802.

Kominz, D. R., A. Hough, P. Symonds, and K. Laki. 1954. The amino acid composition of actin, myosin, tropomyosin and the meromyosins. *Arch. Biochem. Biophys.* 50:148–159.

Kostyuk, P. G., Z. A. Sorokina, and Yu. D. Kholodova. 1968. Measurement of activity of hydrogen, potassium and sodium ions in striated muscle fibers and nerve cells. *In* Intracellular Glass Microelectrodes. M. Lavallee, O. F. Schanne, and N. C. Herbert, editors. John Wiley & Sons, Inc., New York. 322–348.

Kushmerick, M. J., and R. J. Podolsky. 1969. Ionic mobility in muscle cells. *Science (Wash. DC)*. 166:1297–1298.

Lavallee, M. 1964. Intracellular pH of rat atrial muscle fibres measured by glass micropipette electrodes. *Circ. Res.* 15:185–193.

Lev, A. A. 1968. Electrochemical properties of so-called incompletely sealed cation sensitive microelectrodes. *In* Intracellular Glass Microelectrodes. M. Lavallee, O. F. Schanne, and N. C. Herbert, editors. John Wiley & Sons, Inc., New York. 76–94.

Magid, A., and M. Reedy. 1980. X-ray diffraction observations of chemically skinned frog skeletal muscle processed by an improved method. *Biophys. J.* 30:27–40.

McLachlan, A. D., and J. Karn. 1982. Periodic charge distributions in the myosin rod amino acid sequence match cross-bridge spacing in muscle. *Nature (Lond.)*. 299:226–231.

Matsubara, I., and G. F. Elliott. 1972. X-ray diffraction studies on skinned single fibers of frog skeletal muscle. *J. Mol. Biol.* 72:657–669.

Milhayi, E. 1950. The dissociation curves of crystalline myosin. *Enzymologica.* 14:224–236.

Millman, B. M., and B. G. Nickel. 1980. Electrostatic forces in muscle and cylindrical gel systems. *Biophys. J.* 32:49–63.

Naylor, G. R. S. 1977. X-ray and microelectrode studies of glycerinated rabbit psoas muscle. Ph.D. thesis, The Open University, Milton Keynes, England. 147 pp.

Naylor, G. R. S. 1978. A simple circuit for automatic continuous recording of microelectrode resistance. *Pfluegers Arch. Eur. J. Physiol.* 378:107–110.

Naylor, G. R. S. 1982. On the average electrostatic potential between the filaments in striated muscle and its relation to a simple Donnan potential. *Biophys. J.* 38:201–204.

Naylor W. G., and N. C. R. Merrellees. 1964. Some observations on the fine structure and metabolic activity of normal and glycerinated ventricular muscle of toad. *J. Cell. Biol.* 22:533–550.

Offer, G. 1973. C-protein — the periodicity in the thick filaments of vertebrate skeletal muscle. *Cold Spring Harbor Symp. Quant. Biol.* 37:87–93.

Pearlstone, J. R., P. Johnson, M. R. Carpenter, and L. R. Smillie. 1977. Primary structure of rabbit skeletal muscle troponin T. *J. Biol. Chem.* 252:983–989.

Pemrick, S. M., and C. Edwards. 1974. Differences in the charge distribution of glycerol extracted muscle fibers in rigor, relaxation, and contraction. *J. Gen. Physiol.* 64:551–567.

Pepe, F. H. 1967. The myosin filament 1. Structural organization from antibody staining observed in electron microscopy. *J. Mol. Biol.* 27:203–225.

Perrin, D. D., and I. G. Sayce. 1967. Computer calculation of equilibrium concentrations in mixtures of metal ions and complexing species. *Talanta.* 14:833–842.

Portzehl, H., P. C. Caldwell, and J. C. Ruegg. 1964. The dependence of contraction and relaxation of the muscle fibers from the crab Maio Squinado on the internal concentration of free calcium ions. *Biochem. Biophys. Acta.* 79:581–591.

Rashin A. A., and B. Honig. 1984. On the environment of ionizable groups in globular proteins. *Mol. Biol.* 173:515–521.

Rehm, W. S., M. Schwartz, and G. Carrasquer. 1984. Microelectrode artefact and the Donnan potential. *Biophys. J.* 45(2, Pt. 2):139*a* (Abstr.)

Rome, E. 1967. Light and x-ray diffraction studies of the filament lattice of glycerol-extracted rabbit psoas muscle. *J. Mol. Biol.* 27:591–602.

Rome, E. 1968. X-ray diffraction studies of the filament lattice of striated muscle in various bathing media. *J. Mol. Biol.* 37:331–344.

Sato, K. 1977. Modifications of glass microelectrodes: a self-filling and semi-floating microelectrode. *Am. J. Physiol.* 232:C207–C210.

Schanne, O. F., M. Lavallee, R. Laprade, and S. Gagne. 1968. Electrical properties of glass microelectrodes. *Proc. IEEE* (*Inst. Electr. Electron. Eng.*) 56:1072–1082.

Shapiro, P. J., K. Tawada, and R. J. Podolsky. 1979. X-ray diffraction of skinned muscle fibers. *Biophys. J.* 25:(2, Pt. 2):18*a*. (Abstr.)

Sillén, L. G., and A. E. Martell. 1964. Stability constants of metal-ion complexes. Special Publication No. 17, The Chemical Society, London.

Squire, J. M. 1973. General model of myosin filament structure. *J. Mol. Biol.* 77:291–323.

Stone, D., and L. B. Smillie. 1978. The amino acid sequence of rabbit skeletal α-tropomyosin. *J. Biol. Chem.* 253:1137–1148.

Szabo, G. 1966. Etude des phenomenes d'amplilfication ionique dans des membranes artificielles. Master's thesis, Universite de Montreal, Montreal, Canada.

Szent-Gyorgyi, A. 1949. Free-energy relations and contraction of actomyosin. *Biol. Bull.* (*Woods Hole*). 96:140–161.

Szent-Gyorgyi, A. 1951. The Chemistry of Muscular Contraction. Academic Press, Inc., New York. 162 pp.

Tasaki, K., Y. Tsukahara, and S. Ito. 1968. A simple, rapid and direct method for filling microelectrodes. *Physiol. Behav.* 3:1009–1010.

Teorell, T. 1953. Transport processes and electrical phenomena in ionic membranes. *Progr. Biophys.* 3:305–369.

Vieira, F. L., and M. I. Onuchic. 1978. Biological and artificial ion exchanges: Electrical measurements with glass microelectrodes. *Membr. Biol.* 40:157–164.

Weber, H. H., and H. Portzehl. 1952. Muscle contraction and fibrous muscle proteins. *Adv. Protein Chem.* 7:161–252.

Weber, H. H., and H. Portzehl. 1954. The transference of the muscle energy in the contraction cycle. *Prog. Biophys. Biophys Chem.* 4:60–111.

Weiss, R. M., R. Lazzara, and B. F. Hoffman. 1967. Potentials measured from glycerinated cardiac muscle. *Nature* (*Wash. DC*). 215:1305–1307.

White, D. C. S., and J. Thorson. 1972. Nonlinear dynamics of muscle. *J. Gen. Physiol.* 60:307–336.

Wilkinson, J. M., and R. J. A. Grand. 1975. Amino acid sequence of troponin I from rabbit skeletal muscle. *Biochem. J.* 149:493–496.

DONNAN POTENTIALS FROM THE A- AND I-BANDS OF GLYCERINATED AND CHEMICALLY SKINNED MUSCLES, RELAXED AND IN RIGOR

E. M. BARTELS AND G. F. ELLIOTT
Biophysics Group, Open University Research Unit, Oxford OX1 5HR, England

ABSTRACT Using a combination of microelectrode measurements and high-power microscopy we have demonstrated that different Donnan potentials can be recorded from the A- and I-bands of glycerinated and chemically skinned muscles in rigor, so that the A-band fixed charge concentration exceeds the I-band fixed charge concentration in the rigor condition. In relaxation the two potentials, and therefore the two charge concentrations, are equal in the two bands. X-ray data are presented for relaxed and rigor rat semitendinosus muscle, chemically skinned, and actin and myosin filament charges are calculated under a variety of conditions. Our conclusions are that (*a*) the fixed (protein) charge is different in the A- and I-bands of striated muscle in the rigor state; (*b*) the fixed charges are equal in the A- and I-bands of relaxed muscle; (*c*) the largest charge change between relaxation and rigor is on the thick filament. This occurs whether or not the myosin heads are cross-linked to the thin filaments. (*d*) Possibly an event on the myosin molecule, the binding of ATP (or certain other ligands) causes a disseminated change that modifies the ion-binding capacity of the myosin rods, or part of them.

INTRODUCTION

The experiments reported in the preceding paper (Naylor et al., 1985) convinced us that different Donnan potentials should arise from the A- and I-bands of glycerinated rabbit psoas muscles in rigor, but that it was impossible to demonstrate these different potentials clearly by "random insertion" microelectrode methods. Here the optical methods used to show these different A- and I-band potentials directly are described, and the observations are extended to glycerinated rabbit muscle in relaxing solution and to glycerinated and chemically skinned rat muscle, both relaxed and in rigor. We wished to investigate possible differences between glycerinated and chemically skinned preparations, and since one of us had experience with rat muscle (Bartels et al., 1979) this was an obvious choice, because it is comparatively easy to dissect small bundles in a relaxing solution without glycerination, a protocol that we found difficult with the classical rabbit psoas muscle.

Here the changes in A- and I-band potentials between relaxed (ATP and EGTA present) and rigor muscles are described. The differences, in a single muscle, between specimens prepared by glycerination and by chemical skinning are also investigated. Preliminary reports of some of these experiments have appeared before (Bartels et al., 1980; Bartels and Elliott, 1980, 1981*a*, *b*, 1982, 1983).

METHODS

Preparations

Chemically Skinned Rat Muscle. Experiments were carried out on the rat semitendinosus muscle. A portion of a fiber bundle, 0.25–0.5 mm in diameter and 10–15 mm in length, was dissected as described for the gracilis muscle by Bartels et al. (1979) in (rat) Ringer's solution, containing (in millimoles per liter): 140 NcCl; 5 KCl; 3.2 $CaCl_2$; 1.1 $MgCl_2$; 4.5 D-glucose; 1.5 phosphate buffer, pH 7. After dissection, the bundle was transferred to relaxing solution, containing (in millimoles per liter): 150 KCl; 5 $MgCl_2$; 5 Na_2ATP (BDH); 4 EGTA; 10 imidazole buffer, pH 7, for 5 min before final transfer to the skinning solution, which was the relaxing solution with the addition of 50 μg saponin ml^{-1}. After 25 min in the skinning solution, the muscle was washed in relaxing solution for 30 min and then transferred to the experimental solution. The fiber bundle was tied into a perspex cell, the sarcomere length was adjusted to the chosen length (using laser diffraction), and the muscle was left to equilibrate for 30 min in the experimental solution before the start of the experiment. The experiments were carried out at a fixed sarcomere length in the range 2.5–3.4 μm, and the sarcomere length was checked at 3–4 points along the length. At longer sarcomere lengths rat muscle does not always show a uniform sarcomere length distribution along the muscle, but in this paper all the results are from preparations with a uniform sarcomere length distribution.

Glycerinated Rat Muscle. Fiber bundles, 1–2 mm in diameter and as long as possible (1–2 cm), were dissected and tied to perspex rods and glycerinated following the procedure for rabbit muscle described by Naylor et al. (1985). Bundles of 2–10 fibers were attached either in a perspex cell or in a petri dish and left to equilibrate in the experimental solution for 30 min before start of the experiment.

Glycerinated Rabbit Muscle. Fiber bundles from the psoas muscle were dissected and glycerinated as described by Naylor et al. (1985) and the experimental procedures were the same as for glycerinated rat muscle.

Experimental Chambers/Cells

A circular perspex chamber was used for all the diffraction experiments and for some of the potential measurements in the chemically skinned rat muscle. The chamber had moveable muscle attachments that made it possible to stretch the specimens when required. The rat specimens were

typically 12 mm long and the chamber had a 9-mm diameter Mylar window in the base, so that diffraction measurements could in principle be made over most of the specimen length. Some of the microelectrode measurements were made in the same chamber, the size was adequate (~26 mm in diameter, 5 mm deep) for an ample volume of bathing solution to be present. As a precaution, if more than two or three microelectrodes were broken in the course of the measurements, the bathing solution was replaced to avoid any possibility of concentration change due to small amounts of 3 M KCl released.

All potential measurements in the glycerinated preparation and in some of the skinned ones were performed in a petri dish. The bottom of the disk was filled to a depth of 2–3 mm with a casting resin (Sylgard-184 [silicone]; Dow Corning Corp., Midland, MI), which when solidified has the consistency of a firm jelly and is biologically inert. A suitable slot (3–4 mm wide, 2 cm long) was cut in this resin, and the single fiber or fiber bundle was stretched between the sides and held by pushing its ends into slots cut in the resin with razor blades.

Solutions

Two series of solutions were used, a rigor series and a relaxing series. The rigor solutions were the same as in Naylor et al. (1985) (see Table I), these are a set of serially diluted ATP-free rigor solutions with decreasing ionic strength. For relaxed muscles the solutions were modified to contain suitable amounts of ATP and also EGTA to chelate calcium ions (Table II). We also made some measurements in solutions of varying pH, keeping the ionic strength constant (Table III). In all our solutions, the concentrations of the free ions were calculated using the Perrin program, see Naylor et al. (1985). The calculated ionic strengths are given in Table I–III.

Microelectrode Measurements

Donnan potentials were measured with the microelectrode techniques described by Naylor et al. (1985). The microelectrodes were filled with 3 M KCl, and the resistance of the microelectrode was monitored at all times using a modification of Naylor's (1978) circuit; readings were discarded if the steady resistance changed by >5% inside the impaled tissue. The microelectrodes resistances were in the range of 14–25 MΩ, which implies that the tip diameters of the electrodes were ~0.1–0.2 μm. Tip potentials were also measured routinely, as described by Naylor et al. (1985), and electrodes with tip potentials >1 mV were discarded. Because we wished to see whether two separate (A- and I-band) potentials could be detected from rat muscles examined by random insertion, some experiments were made by this technique, and the results were displayed as histograms of numbers of readings against observed potentials. Most of our experiments, however, were made under optical observations as described in the next paragraph.

Optical Arrangements

The petri dish or experimental cell with the muscle specimen was placed on the stage of an inverted microscope (model 405; Carl Zeiss, Inc., Thornwood, NY), overall magnification 400 times. A simultaneous combination of phase contrast and polarization contrast was possible with the Zeiss instrument and this was used in all the experiments reported here. Under these conditions of illumination and contrast and with the single fibers, or bundles of a few fibers, there was no difficulty in identifying the A- and I-band regions from the different appearances of the Z-line and H-zone structures at moderate sarcomere lengths.

The method of obtaining contrast proved to be successful with skeletal muscle and the practical resolution was so good that it was possible with confidence to see the position of the microelectrode tip in the A-band or the I-band of slightly stretched muscle fibers (sarcomere length 2.6 μm and above) (Fig. 1), particularly since it was possible to focus up and down to help in locating the tip. At sarcomere lengths ~2.5 μm it was not so easy to locate the tip but it was still just possible. At lower sarcomere lengths it became extremely difficult to see exactly where the tip was placed. Most of our experiments were therefore carried out at sarcomere lengths >2.7 μm, after we had checked that the Donnan potentials were independent of sarcomere length in a particular solution.

The microelectrode was carried on a micromanipulator, which was not mounted on the microscope stage or on the microscope itself, so that the microelectrode could be moved independently of the experimental cell or chamber. The impalement was made using the microscope stage to move the speciment onto the microelectrode, rather than moving the microelectrode into the specimen. The whole apparatus was at ground floor level, and mounted on a massive concrete bench to minimize vibration.

Diffraction Techniques

The methods for x-ray and laser diffraction were as in Naylor et al. (1985). X-ray data for the glycerinated rabbit muscle were taken from their results, but equatorial spacings were measured for the skinned rat muscles. A suitable lid with a second Mylar window was fitted to the specimen cell, which was mounted directly on the x-ray or laser diffraction apparatus as required. When a petri dish was used for microelectrode experiments, sarcomere lengths were determined with a vertically oriented laser beam.

TABLE I
COMPOSITION OF THE RIGOR SOLUTIONS

Rigor solution	KCl	$MGCl_2$	Phosphate buffer, pH 7	Tris-HCl-buffer, pH 6	Ionic strength
	mM	*mM*	*mM*	*mM*	*M*
Standard	100	5	20	—	0.141
2× diluted	50	2.5	10	—	0.072
5× diluted	20	1	4	—	0.030
10× diluted	10	0.1	2	—	0.015
Low pH	50	2.5	—	4	0.074

TABLE II
COMPOSITION OF THE RELAXING SOLUTIONS

Relaxing solution	KCl	$MGCl_2$	Phosphate buffer, pH 7	Na_2ATP (BDH)	EGTA	Ionic strength
	mM	*mM*	*mM*	*mM*	*mM*	*M*
Standard	100	10	20	5	4	0.180
2× diluted	50	5	10	2.5	2	0.086
5× diluted	20	2	4	1	0.8	0.038
10× diluted	10	1	2	0.5	0.4	0.019

TABLE III
COMPOSITION OF THE pH-CHANGE SOLUTIONS AT HIGH AND LOW IONIC STRENGTH

pH solution	KCl	$Mg Cl_2$	Citric acid-K_2HPO_4 buffer	Ionic strength
	mM	*mM*		*M*
pH 5.8 low μ	10	0.5	0.8	0.013
pH 4.8 low μ	10	0.5	0.8	0.014
pH 3.95 low μ	10	0.5	0.8	0.014
pH 3.4 low μ	10	0.5	0.8	0.014
pH 5.7 high μ	50	2.5	4	0.066
pH 4.7 high μ	50	2.5	4	0.069
pH 3.7 high μ	50	2.5	4	0.071
pH 3.5 high μ	50	2.5	4	0.073

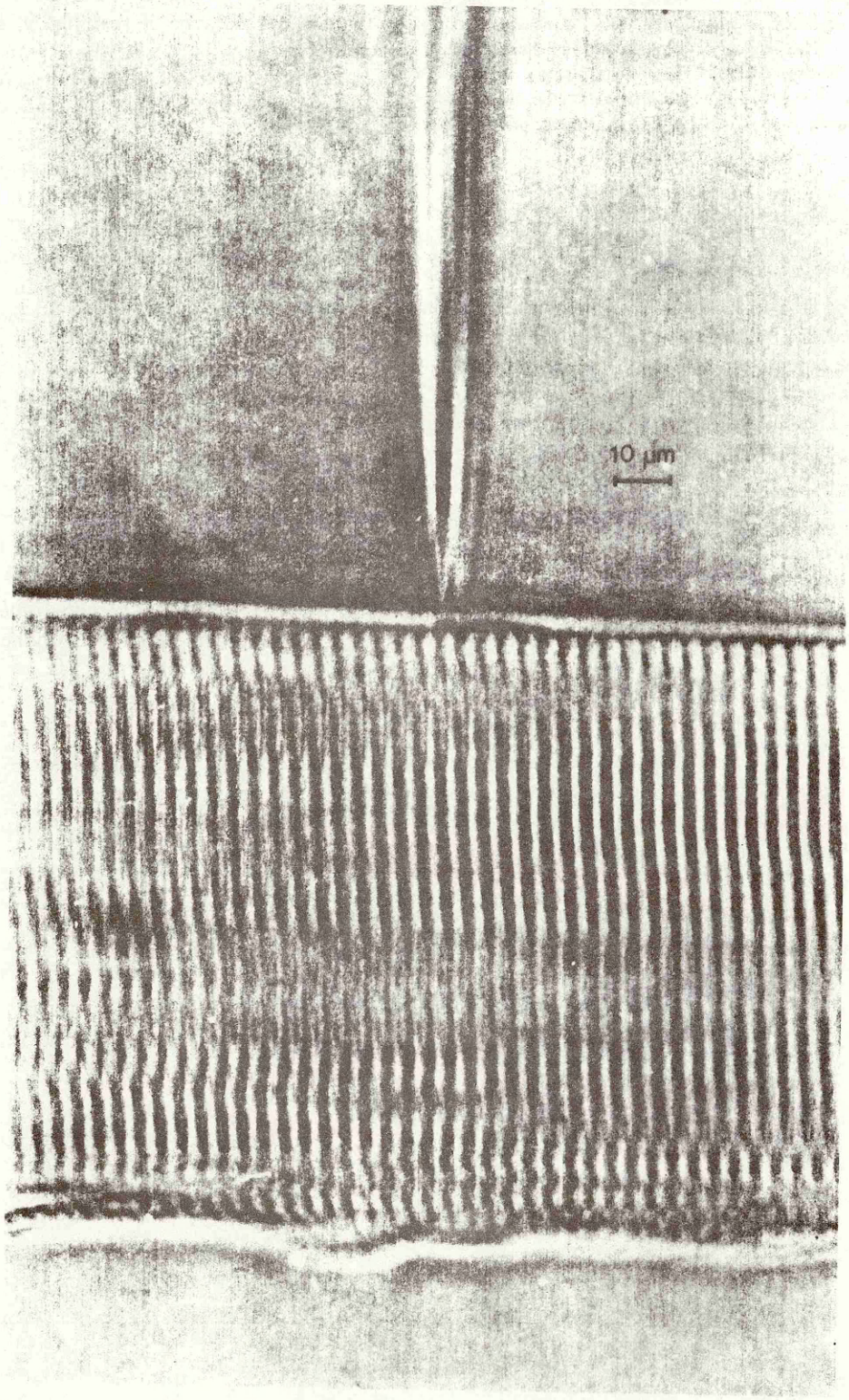

FIGURE 1 Micrograph of bundle of fibers, showing a microelectrode in position in an A-band. The sarcomere length is ~3 µm, the calibration bar is 10 µm.

Theory

The theory was given in Elliott and Bartels (1982), Naylor (1982), and Naylor et al. (1985). The internal concentrations of the free ions were determined from the external concentrations, using the measured Donnan potential and the Nernst equation. A computation of the net internal charge then gave the fixed charge on the protein (filament) matrix, and since the geometry of the A- or I-band was known from the measurements with the diffraction techniques, the charges on the muscle filaments could be determined.

RESULTS

Potential Measurements

In the following account the potential measured in the A-band is called E_A, the potential measured in the I-band is called E_I. The potentials in all experiments were found to be independent of sarcomere length. Experimental data are shown in Fig. 2 for a typical example, chemically skinned rat muscle in rigor and relaxing solutions.

Chemically Skinned Rat Muscle. In random insertion experiments, some of which were made before the set-up was improved with high-power microscopy, two potential peaks were always observed in rigor when 20 readings, taken randomly, were plotted as a histogram. The distribution on the two peaks was dependent on sarcomere length, with fewer readings around the less negative peak at shorter sarcomere lengths and an approximate equal number of readings in each peak at longer sarcomere length (where the A- and the I-band are of similar length), see Fig. 3. Comparing with experiments where the position of the microelectrode is located in the microscope, the less negative potential peak coincides with E_I and the more negative peak coincides with E_A.

In relaxing solutions only one potential peak was found in random insertion experiments. The two potentials E_A and E_I, observed with light-microscope location, were found to be equal in all relaxing solutions. Table IV and V give the data for rat muscle at four ionic strengths, in rigor (IV) and in relaxed (V) conditions. All potential data in the tables are from direct observations under the light microscope. We also made observations in a rigor solution at pH 6 and $\mu = 0.074$ M (see Table III). Data from this solution are included in Table IV and show that in chemically skinned rat muscle, as in glycerinated rabbit muscle, the protein charge concentration in both bands decreases with decreasing pH (above the isoelectric point).

Glycerinated Rat and Rabbit Muscle. There was no significant difference in the potential measure-

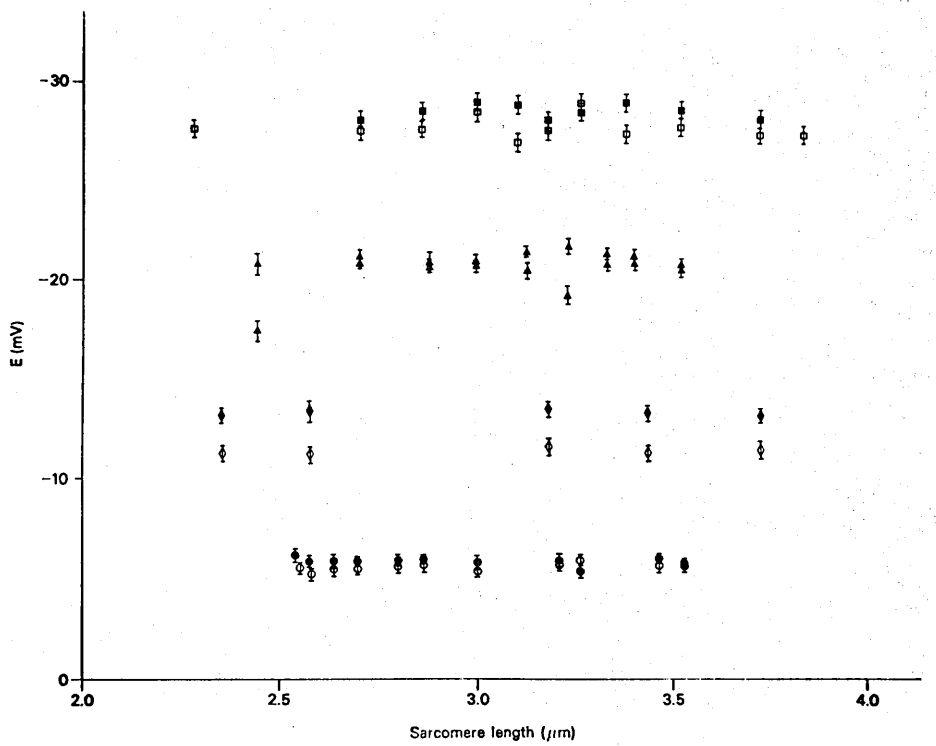

FIGURE 2 Skinned rat muscle, potentials in the various solutions plotted as a function of sarcomere length; standard error shown. Note that in a given solution there is no sarcomere-length variation of potential. These results are from the A-band without Brij treatment and in this band there is no difference between the potentials in relaxation and rigor in these conditions. Solid circles, standard rigor solution; open circles, standard relaxing solution; solid diamonds, 2× diluted rigor solution; open diamonds, 2× diluted relaxing solution; solid triangles, 5× diluted rigor solution; open triangles, 5× diluted relaxing solution; solid squares, 10× diluted rigor solution; open squares, 10× diluted relaxing solution.

ments taken from glycerinated rat fibers and from glycerinated rabbit fibers. E_A and E_I were found to be different and E_A more negative than E_I in all rigor solutions. E_A and E_I were found to be the same in the relaxing solutions. The results are given in Table VI for rat muscle. Notice that in the rigor solution based on 50 mM KCl there was a difference in the values of the potentials between the skinned and the glycerinated muscle. Both the A- and the I-band potentials were significantly more negative in the skinned than in the glycerinated rat preparations. Data for glycerinated rabbit muscle in the relaxing solutions are given in Table VII, and are not very different from the rat data.

In relaxing solution there was a difference between skinned and glycerinated muscle, which was reported in a preliminary communication by Bartels and Elliott (1982). In the glycerinated preparations, E_A decreased from rigor to the relaxed state to a value close to E_I. E_I stayed constant at a given ionic strength. In the skinned muscle E_I increased from rigor to relaxed state to a value close to E_A. E_A stayed approximately constant. We shall return to this point in the Discussion section entitled Rat Muscle—Differences between Skinning and Glycerination.

Naylor et al. (1985) predicted the I-band charge in glycerinated rabbit muscle from experiments on the A-band alone in rigor, varying the ionic strength and the pH. To check these predictions the experiments were repeated measuring the I-band potentials in the solutions used by Naylor et al. (1985). An I-band potential is indeed present (Table VIII) different from the A-band potential in all rigor solutions (compare with Naylor et al., 1985, Tables I and II). The I-band charge decreases with decreasing pH and becomes positive on the acid side of the thin filament isoelectric point.

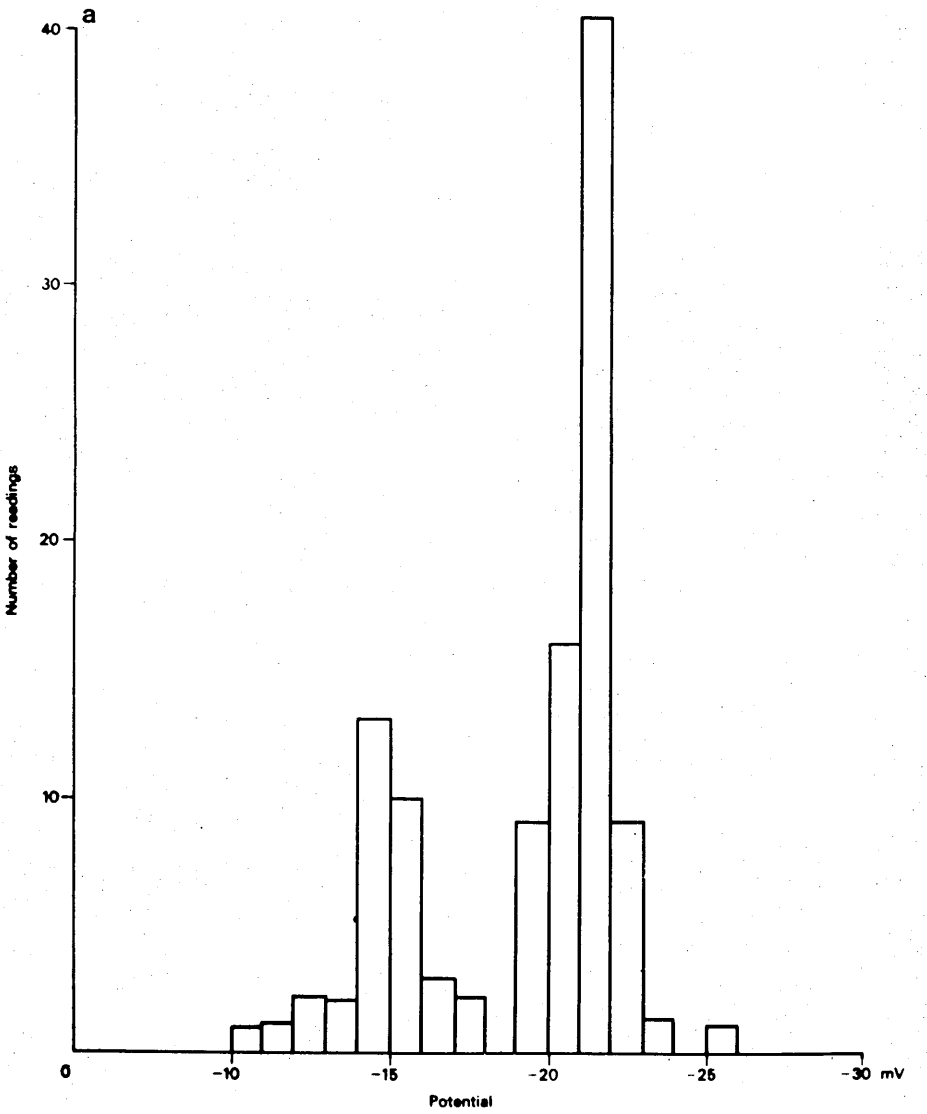

FIGURE 3 Histograms of 20 potentials taken at random (without microscopic observation) in skinned rat muscle in the rigor solution based on 20 mM KCl. Note the different form between long and short sarcomere lengths. (*a*) S = 2.51–2.75 μm; (*b*) S = 3.26–3.50 μm.

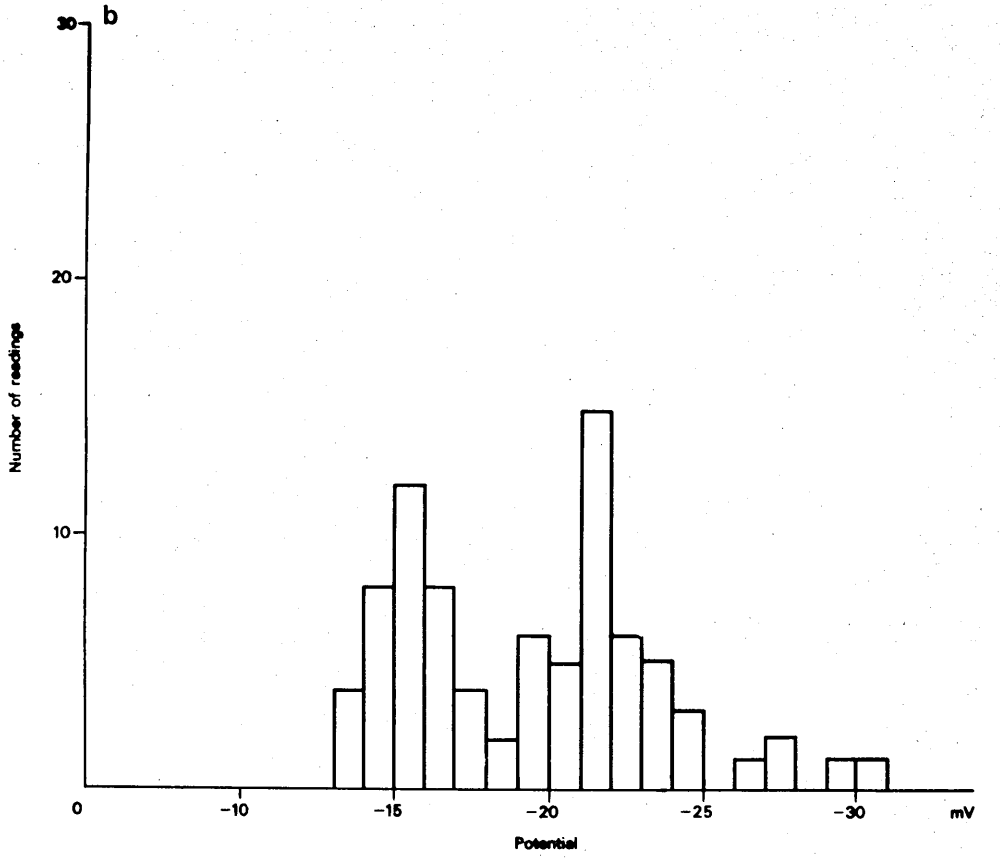

FIGURE 3B

TABLE IV
SUMMARY OF THE RESULTS FROM SKINNED RAT MUSCLE IN RIGOR, INCLUDING ONE SET OF RESULTS AT LOW pH

Solution	E_A	E_I	$[Pr]_A$	$[Pr]_I$	X-ray data	σ_m	σ_a (from x-ray slope)	σ_a (from E_I)	σ_m/σ_a (from x-ray slope)	σ_m/σ_a (from E_I)
	mV	*mV*	*mM*	*mM*		*e/nm*	*e/nm*	*e/nm*		
Standard rigor pH 7 μ = 0.14 M	−5.7 ± 0.6 n = 200	−2.7 ± 0.7 n = 200	−63 ± 7	−30 ± 8	d^* = (50.0 ± 1.0) −(4.4 ± 0.9)S‡ n = 22	51	12	12	4.4	4.2
2× diluted μ = 0.072 M	−11.7 ± 1.0 n = 200	−8.0 ± 0.7 n = 200	−68 ± 6	−46 ± 4	d = (58.1 ± 1.4) −(7.0 ± 1.2)S n=37	47	20	16	2.4	3.0
5× diluted μ = 0.030 M	−19.9 ± 0.9 n = 200	−14.0 ± 0.8 n = 200	−53 ± 3	−35 ± 2	d = (60.3 ± 0.7) −(6.9 ± 1.4)S n=26	43	16	2.7	3.0	
10× diluted μ = 0.015 M	−28.9 ± 1.0 n = 200	−19.6 ± 1.0 n = 200	−44 ± 2	−26 ± 3	d = (59.0 ± 1.2) −(6.2 ± 1.7)S n=15	38	12	11	3.1	3.4
Low pH rigor solution pH 6 μ = 0.074 M	− 8.4 ± 0.5 n = 300	−6.0 ± 0.5 n = 300	−45 ± 3	−32 ± 3	d = (61.1 ± 1.3) −(7.7 ± 2.1)S n=15	32	15	11	2.2	2.8

σ_m and σ_a are the linear charge densities of the thick and thin filaments, respectively. [Pr] is the concentration of protein charge expressed as mM of univalent charge. All potentials and the associated [Pr]s are given as a mean and standard deviation, n is the number of readings. The x-ray data are shown on the least-squares straight line fit to the experimental data, with standard errors calculated in the normal manner. The charge ratio's from the x-ray slope have a precision of about ±50%, the thick filament and thin filament linear charges calculated from the A- and I-band potentials have a precision of about ±20%, and the thin filament linear charge derived from the x-ray slope has much lower precision (see Naylor et al., 1985).

*d is measured in nanometers.

‡S is measured in microns.

X-ray Data

For chemically skinned rat muscle the equatorial (1,0) lattice spacing (d) was determined before the measurement of the potential for 20–25 preparations in each solution. A typical set of data is plotted Fig. 4 for skinned rat muscle in the relaxing solution based on 20 mM KCl.

The spacing shows linear relationships as a function of sarcomere length, decreasing with increasing sarcomere length. For the lowest ionic strength in rigor muscle this is not quite true, however; up to a sarcomere length of 3 μm the regression coefficient for the fitted line fulfills the criteria for a straight line, with d decreasing, but above 3 μm, d stays approximately constant. In this case we have used the equation from the points at or below 3 μm for our present purposes, and we are investigating the phenomenon further. X-ray data for skinned rat muscle, in rigor and relaxed, are given in Tables IV and V.

We are not able to measure stiffness of the fiber in rigor and relaxing solutions because this would have made the apparatus impossibly cumbersome, so as a test for the efficacy of our relaxing solutions we used the relative intensities of the (1,0) and (1,1) equatorial reflections as an index of the state of the muscle (Huxley, 1968; Rome, 1972). Fig. 5 shows the intensity ratio categories (using the scale introduced by Elliott et al., 1963) against sarcomere length for rigor and relaxing solutions. At all ionic strengths the intensity ratio shifts towards the relaxed position of the cross-bridge in the appropriate solution. The value of the lattice spacing, however, did not behave in the same way at all ionic strengths. Comparison of the x-ray data summarized in Table IV and V shows that in the relaxing solution based on 100 mM KCl solution the lattice spacing was generally ~1.5–2.0 nm greater than in the corresponding (rigor) solution, in the solutions based on 50 mM KCl the spacings were about equal, and in the solutions based on 20 and 10 mM KCl the rigor spacing was greater than the relaxed by ~1.0 and 2.0 nm, respectively.

No x-ray data were recorded for glycerinated rat muscles, and the x-ray data for skinned rat muscle in a given solution are used in all calculations where there is no separate set of data. The justification for this is that in our experience, for both rat and rabbit muscles, x-ray equatorial data for skinned and glycerinated preparations are similar in the same solution under all conditions where both sets of data are available.

X-ray data for glycerinated rabbit muscle in rigor are given in Tables I and II of Naylor et al. (1985); for relaxed glycerinated rabbit muscle in our standard relaxing solution we have combined the data of Naylor (1977) and Rome (1972) with the addition of six experimental points taken subsequently. This gives, for the standard relaxing solution based on 100 mM KCl, $d = (56.1 \pm 0.9) - (6.2 \pm 0.7)\ S$ ($n = 74$, units as in Tables IV and V). Notice that the slope of this line is not significantly different from skinned rat muscle in the same solution (Table V) and the difference in the intercepts of the two lines is barely significant.

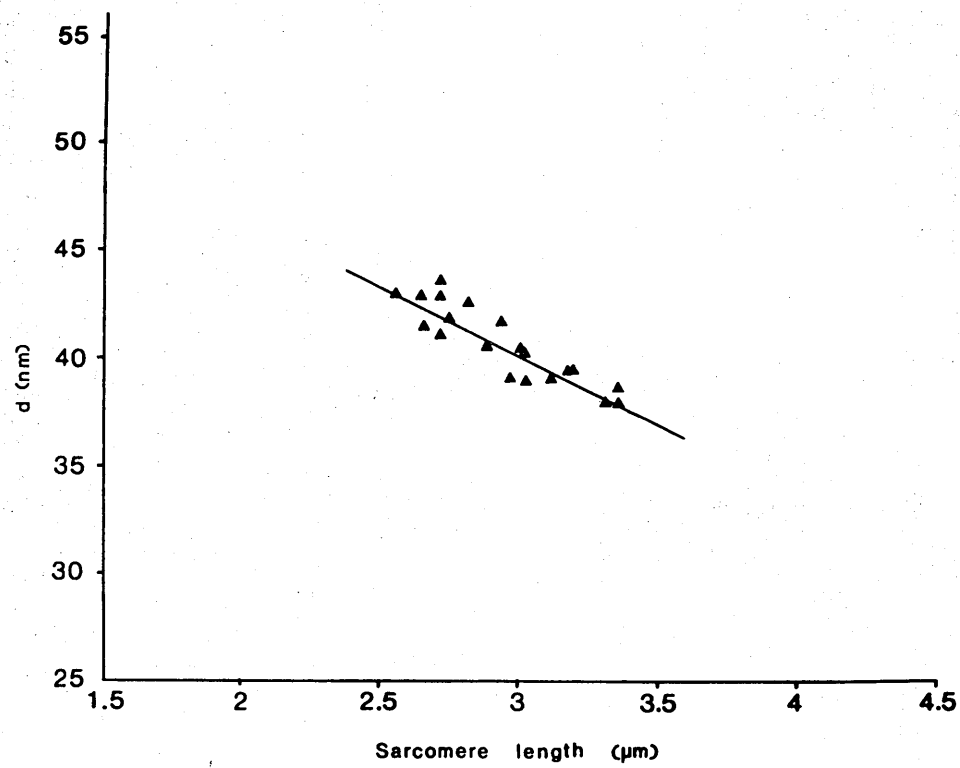

FIGURE 4 A typical set of x-ray data for rat muscle in standard relaxing solution (pH 7, μ = 0.18). The best fit straight line is shown.

TABLE V
SUMMARY OF THE RESULTS FROM SKINNED RAT MUSCLE IN RELAXING SOLUTIONS

Solution	E_A	E_I	$[Pr]_A$	$[Pr]_I$	X-ray data	σ_m	σ_a (from x-ray slope)	σ_a (from E_I)	σ_m/σ_a (from x-ray slope)	σ_m/σ_a (from E_I)
	mV	*mV*	*mM*			*e/nm*	*e/nm*	*e/nm*		
Standard relaxing pH 7 μ = 0.18M	−5.0 ± 0.8 n = 200	−5.0 ± 0.8 n = 200	−70 ± 11		d^* = (59.1 ± 0.9) −(6.4 ± 1.4)S‡ n = 22	(59)	(20)	(30)	3.0	2.0
2× diluted μ = 0.086M	−9.2 ± 0.9 n = 200	−9.1 ± 1.0 n = 200	−65 ± 7		d = (53.0 ± 1.0) −5.5 ± 1.3)S n = 19	(47)	(15)	(24)	3.2	2.0
5× diluted μ = 0.038M	−19.5 ± 1.0 n = 200	−19.6 ± 1.0 n = 200	−62 ± 4		d = (59.9 ± 0.9) −(7.4 ± 1.6)S n = 22	(44)	(19)	(22)	2.3	2.0
10× diluted μ = 0.019M	−27.4 ± 1.0 n = 200	−27.3 ± 0.9 n = 200	−49 ± 3		d = (58.2 ± 1.1) −(6.4 ± 1.4)S n = 24	(39)	(14)	(20)	2.9	2.0

The charge values from the A- and I-band potentials are given in parentheses because it seems likely that these include SR values as well as filament effects (see text). Other details as Table IV.
*d is measured in nanometers.
‡S is measured in microns.

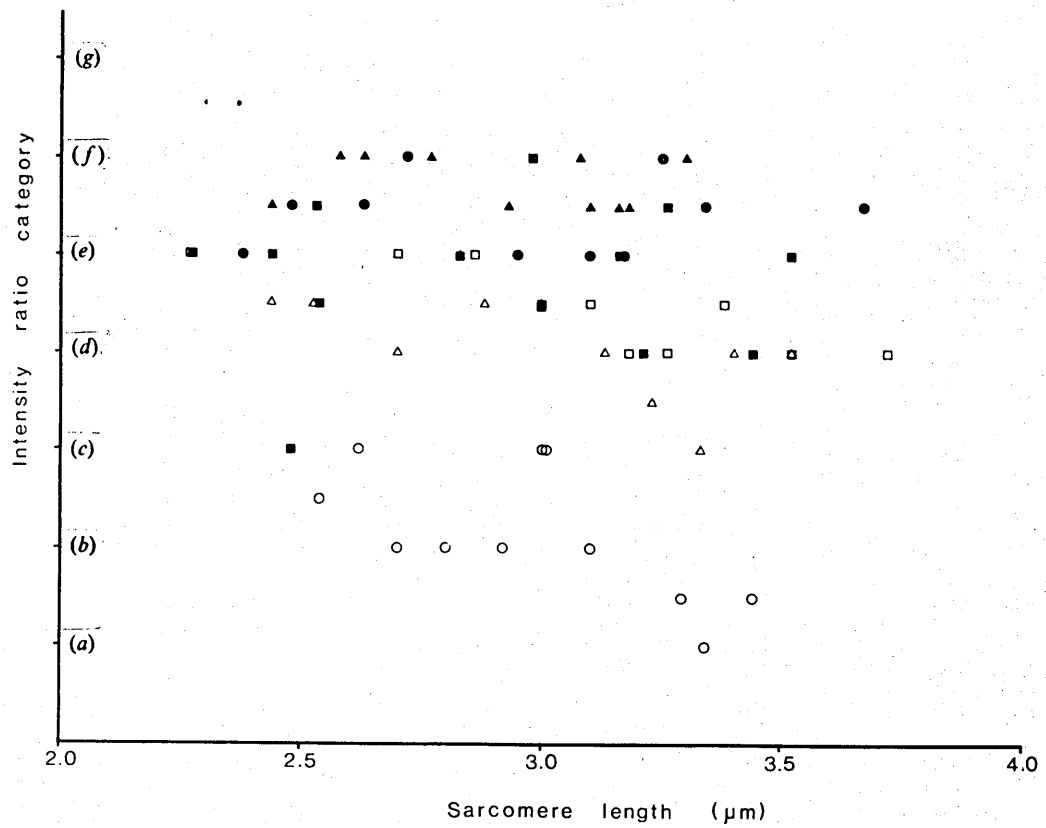

FIGURE 5 The relative intensities of the (1,0) and (1,1) equatorial reflections in relaxation and rigor as a function of sarcomere length. The qualitative scale used is taken from Elliott et al. (1963), and uses the following categories: (*a*) 1,0 seen clearly, no sign of 1,1; (*b*) 1,0 seen clearly, traces of 1,1; (*c*) 1,0 > 1,1, both seen clearly; (*d*) 1.0 ≃ 1.1, both seen clearly; (*e*) 1.0 < 1.1, both seen clearly; (*f*) traces of 1.0, 1.1 seen clearly; (*g*) no sign of 1.0, 1.1 seen clearly. Other symbols as in Fig. 2, open symbols are in relaxed muscle, solid symbols in rigor, circles are standard solutions, triangles 5× diluted, and squares 10× diluted. Notice that the intensity ratio shows appropriate changes between the rigor and relaxing solutions, at all dilutions and at all sarcomere length.

TABLE VI
POTENTIALS AND CHARGE VALUES FROM GLYCERINATED RAT MUSCLE

Solution		E_A	E_I	$[Pr]_A$		$[Pr]_I$
		mV	*mV*	*mM*		*mM*
Standard	rigor	−5.3 ± 0.5	−2.7 ± 0.6	−59 ± 5		−30 ± 6
	relaxing	−2.5 ± 0.5	−2.6 ± 0.6		−36 ± 7	
2× diluted	rigor	−8.6 ± 0.7	−5.2 ± 0.7	−49 ± 4		−29 ± 4
	relaxing	−5.2 ± 0.6	−5.2 ± 0.7		−37 ± 3	
5× diluted	rigor	−20.4 ± 0.9	−13.0 ± 0.9	−54 ± 3		−32 ± 2
	relaxing	−12.9 ± 1.0	−12.9 ± 1.0		−39 ± 3	
10× diluted	rigor	−27.1 ± 1.0	−20.1 ± 1.0	−40 ± 2		−27 ± 2
	relaxing	−20.1 ± 1.0	−19.9 ± 1.0		−32 ± 2	

Standard deviations shown. [Pr] defined as in Table IV.

Calculations of Filament Charge

The protein charge concentration [Pr] was calculated in each case (Elliott and Bartels, 1982) and the results are given in Table IV–VIII.[1] The net charge per nanometer of filament was calculated using the diffraction data to determine the relevant volumes, these charges are also given in Tables IV, V, VII, and VIII. The thin filament charge is seen to be essentially constant over the range of ionic strengths, the thick filament charge increases with ionic strength.

DISCUSSION

Relaxation and Rigor — Thick Filament Charges

In relaxed muscle, an excess of Mg-ATP is present in solution and pCa is held >7 by a chelating agent. The myosin heads are free to move, and are in thermal motion about their equilibrium positions (Poulsen and Lowy, 1983). In rigor muscle there is no free ATP, and the myosin heads are very probably bound to the actin filaments in the overlap zone; the x-ray evidence for this statement is well reviewed in Hanson (1968). It has often been suggested (e.g., Reedy et al., 1965; Hanson, 1968) that the rigor conformation represents a frozen state of the myosin heads in one phase of the contractile cycle. Although Huxley (1973) pointed out that the x-ray pattern of contracting muscle does not resemble that of rigor muscle to any large extent, it is likely that rigor muscle is related to contracting muscle, so that information about muscle in rigor may be relevant to the contraction mechanism.

The first measurements of Donnan potentials in relaxed (glycerinated rabbit psoas) muscle were made by Pemrick and Edwards (1974). In this pioneering study they reported a sarcomere-length effect in relaxation though not in rigor (their Figs. 2 and 3); this sarcomere-length effect is not seen in the present measurements. However, their experimental data are not convincing on this point, because the values of potential that they report do not accord with our own, theirs being considerably more negative both in relaxation and in rigor in the same muscle in similar solutions at similar ionic strengths. Possibly they may have been affected by the microelectrode artefact, which was described in Naylor et al. (1985). Note that the tip size of their microelectrodes (~1 μm) was 5–10 times greater than those used here (Naylor et al., 1985) and it is therefore possible that their electrodes averaged the potentials differently from those used here. Our experience is that there is no sarcomere length effect on the A-band or I-band potentials, either in relaxation or in rigor (i.e., Fig. 2). This statement includes observations made in solutions identical with those used by Pemrick and Edwards (1974).

The explanation for the lack of sarcomere-length effect given by Elliott et al. (1978) and see also the preceding paper, Naylor et al. (1985), is that the volume of the A-band phase increase as extra charge is brought into the A-band by the thin actin-containing filaments, and that this volume change compensates for the extra charge, so that the average charge concentration in the A-band, which will determine the observed potential, stays constant. This explanation is very similar to that given by

[1] Here also it is convenient to express protein charges in millimoles per liter of univalent charge, see Naylor et al. (1985).

TABLE VII
SUMMARY OF RESULTS FROM GLYCERINATED RABBIT MUSCLE IN RELAXING SOLUTIONS

Solution	E_A	E_I	$[Pr]_A$ $[Pr]_I$	X-ray data	σ_m	σ_a (from x-ray slope)	σ_a (from E_I)	σ_m/σ_a (from x-ray slope)	σ_m/σ_a (from E_I)
	mV	*mV*	*mM*		*e/nm*	*e/nm*	*e/nm*		
Standard relaxing pH 7 μ = 0.18M	−2.3 ± 0.6 n = 400	−2.2 ± 0.7 n = 400	−31 ± 9	d^* = (56.1 ± 0.9) −(6.2 ± 0.7)S‡ n = 74	23	8	12	2.8	2.0
2× diluted μ = 0.086M	−6.0 ± 1.0 n = 400	−5.7 ± 1.0 n = 400	−42 ± 7	d = (53.0 ± 1.0) −(5.5 ± 1.3)S n = 19	30	9	15	3.2	2.0
5× diluted μ = 0.038M	−14.8 ± 1.1 n = 400	−14.8 ± 1.1 n = 400	−45 ± 4	d = (59.9 ± 6.9) −(7.4 ± 1.6)S n = 22	32	14	16	2.3	2.0
10× diluted μ = 0.019M	−19.8 ± 1.1 n = 400	−19.5 ± 1.0 n = 400	−32 ± 2	d = (58.2 ± 1.1) −(6.4 ± 1.4)S n = 24	26	9	13	2.9	2.0

Other details as in Table IV.
*d is measured in nanometers.
‡S is measured in microns.

Elliott (1973) to explain the roughly linear behavior of the (1,0) x-ray spacing with muscle length in glycerinated and skinned muscles. The explanation implies that the microelectrode responds to the average ionic concentration (or potential, see Elliott and Bartels, 1982) within the whole A-band, and does not respond to the local concentrations in the H-zone or overlap regions where the tip finds itself. This suggests that the microelectrode tip, although only 0.1–0.2 μm in diameter, nevertheless has a response field that is probably a single order of magnitude larger than this. Certainly, as was pointed out in the previous paper, it has not been possible to detect separate potential regions in the H-zone and overlap regions, see also Fig. 2.

Aldoroty et al. (1985) in their investigation of crayfish muscle fibers, where the A-band is three times longer than rat or rabbit muscle, have observed a small sarcomere-length effect on the A-band potential. In this muscle there are six thin actin-containing filaments for every thick myosin-containing filament, so the charge brought into the A-band as the overlap increases is considerably larger than in rat and rabbit muscle where there are only two thin filaments per thick filament. Possibly in these circumstances the volume change in the A-band is unable to compensate for the extra charge, so that the charge concentration, and thus the A-band potential, does increase with sarcomere length decrease.

The major observation of this paper is that for both rat and rabbit muscle it is possible to record Donnan potentials

TABLE VIII
I-BAND POTENTIALS AND CHARGES FOR GLYCERINATED RABBIT MUSCLE IN RIGOR SOLUTIONS

Solution	E_I	[Pr] (mM) σ_a (e/nm)	Solution	E_I	[Pr] (mM) σ_a (e/nm)	Solution	E_I	[Pr] (mM) σ_a (e/nm)
	mV			*mV*			*mV*	
Rigor series		−29 ± 5	pH series, low μ		−6.3 ± 1	pH series, high μ		−25 ± 3
pH 7.0	−2.6 ± 0.5	13	pH 5.8	−5.8 ± 0.5	2	pH 5.7	−4.6 ± 0.6	9
μ = 0.14 M	n = 400		μ = 0.013 M	n = 80		μ = 0.066 M	n = 80	
pH 7.0	−5.4 ± 1.0	−31 ± 6	pH 4.8	−4.7 ± 0.6	−4.6 ± 1	pH 4.7	4.6 ± 0.6	26 ± 4
μ = 0.072	n = 400	13	μ = 0.014 M	n = 80	1	μ = 0.069 M	n = 80	11
								net positive charge
pH 7.0	−14.5 ± 1.1	−36 ± 3	pH 3.95	6.9 ± 0.6	9 ± 1	pH 3.7	6.8 ± 0.5	42 ± 4
μ = 0.030	n = 400	13	μ = 0.014 M	n = 90	2	μ = 0.071 M	n = 80	19
					net positive charge			net positive charge
pH 7.0	−18.8 ± 1.5	−25 ± 2	pH 3.4	15.1 ± 0.7	27 ± 3	pH 3.5	10.1 ± 0.6	73 ± 6
μ = 0.015	n = 400	9	μ = 0.014 M	n = 80	7	μ = 0.073 M	n = 80	21
					net positive charge			net positive charge

Values are measured for comparison with derived values in Naylor et al., 1985. Other details as in Table IV.

TABLE IX

A- AND I-BAND POTENTIALS, IN STANDARD RIGOR AND RELAXING SOLUTIONS, FROM CHEMICALLY SKINNED RAT MUSCLES TREATED WITH 500 $\mu g\ ml^{-1}$ BRIJ 58 SOLUTION IN THE SKINNING SOLUTION FOR 35 min TO INACTIVATE SR

	E_A	E_I
Standard rigor solution	-5.4 ± 0.7 ($n = 120$)	-2.4 ± 0.6 ($n = 120$)
Standard relaxng solution	-2.5 ± 0.7 ($n = 80$)	-2.4 ± 0.6 ($n = 80$)

The A- and I-band potentials, under these conditions, conform to the pattern seen in glycerinated rat muscle (Table VI) rather than in chemically shinned rat muscle without Brij treatment (Tables IV and V). Standard deviations are shown. n is the number of readings.

from the A- and I-bands separately and directly. In rigor the A-band potential, E_A, is significantly more negative than the I-band potential, E_I. In relaxation the two potentials are equal within the experimental error and their value is close to E_I measured in rigor. (The last part of the second statement does not apply to chemically skinned rat muscle in relaxing solution; we will comment in the next section on the difference between the results for skinned and glycerinated muscle in relaxing solutions.) This clear observation of an A-band potential, which is more negative in rigor than in relaxation, means that the lattice electric charge in the A-band is significantly higher in rigor than in relaxation (after making proper allowance for any observed volume changes).

How much higher is the A-band protein charge in rigor? This depends on the solutions that are compared. Taking the rigor and relaxing solutions, both based on 100 mM KCl, the values are 53 mM in rigor and 33 mM in relaxation, an increase of ~60% in rigor. However, the relaxing solution has a greater ionic strength than the rigor solution (Tables IV and V) because of the added ions. In Fig. 6 the A- and I-band protein charges for rabbit muscle are plotted as a function of ionic strength. At a constant ionic strength of 0.14 M appropriate for mammalian muscle, the A-band charge is 53 mM in rigor and 38 mM in relaxing solution, an increase of ~40% in rigor. Whichever of these increases may be appropriate in the physiological case, the increase is too large to be explained by the binding of two ligands (ATP, for example) to the myosin molecule. Taking the lower of the two figures, if the net myosin charge in relaxation is ~80–90 electrons (e)/molecule (Milhayi, 1950, Jennison et al., 1981, and Karn et al., 1983, all give values close to this range), then the extra charge in rigor is 32–36 e, too large for two ATP molecules (~6–8 e). In addition, in relaxed muscle these ligands are supposed to be bound, and to be released when

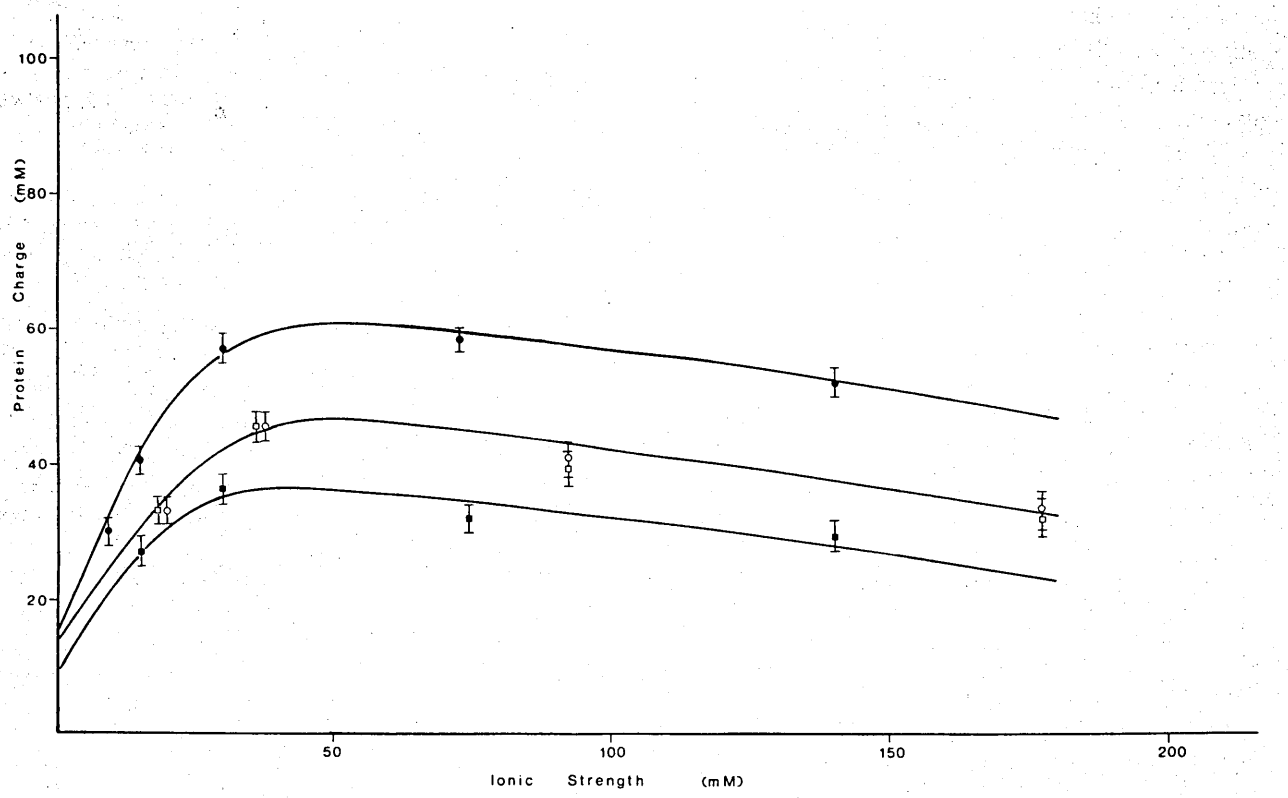

FIGURE 6 The protein charge in glycerinated rabbit psoas muscle, relaxed and in rigor, as a function of ionic strength. Standard deviations shown, number of readings $n = 400$ for each point. Solid circles, A-band, rigor; open circles, A-band relaxed; solid squares, I-band, rigor; open squares, I-band relaxed.

the muscle goes into the contraction cycle and presumably into rigor also, an effect that would be in the reverse direction to our observation. The implication is that the charge effect must be amplified in some way, and we shall return to this point in the section entitled Charge Amplification.

There is a further implication of our results and those of Naylor et al. (1985). Since the extra charge in rigor is not a function of sarcomere length, and thus not a function of filament overlap, the effect cannot depend primarily on actin-myosin cross-linking unless a very few cross-links are sufficient for total charging. It seems then that in rigor there may be two quite separate effects, the myosin-containing filaments charge up throughout the A-band, and they cross-link to the actin filaments in the overlap region. These effects both depend on the absence of free ATP, but the charging effect may occur independently of cross-linking.

Scordilis et al. (1975) used the fluorescent dye CC-6 to serve as an indicator of the potential measured in glycerol-extracted muscle with microelectrodes, and showed that the fluorescence decreased by ~30% on the addition of ATP. They did not then localize this effect, but Scordilis, S. P. (unpublished results), using synthetic thick and thin filaments showed that the effect was primarily due to the myosin-containing filaments. This work correlates closely with the present observations.

Rat Muscle — Differences between Skinning and Glycerination

In chemically skinned rat muscle, different behavior to glycerinated rat muscle was observed. For both preparations in rigor, E_A is significantly greater than E_I and in relaxation the two potentials are equal within experimental error. Except in the solution based on 50 mM KCl (see the section entitled Potential Measurements in Results) the rigor results from the two preparations are not significantly different, but in the glycerinated preparations, E_A decreases in relaxation to E_I (rigor), whereas in the skinned preparations, E_I increases in relaxation to E_A (rigor), see Tables IV–VI. We found this difference puzzling, and it seemed that it could be explained most simply by another structure, in parallel with the whole sarcomere, which charged up (negatively) as the myosin-containing filaments discharged, and vice versa. Since this structure would appear to be effective in skinned preparations but not in glycerinated ones, an obvious candidate is the sarcoplasmic reticulum (SR), because the main difference between the two preparations could be the lack of an effective SR in the glycerinated case. It is therefore suggested that the different behavior of the two preparations might be caused by charging the longitudinal elements of the SR in relaxation, probably by phosphate compounds absorbed to the outer surface. This hypothesis was tested (Bartels and Elliott, 1982) by treating skinned fibers with a 500 μg/ml Brij 58 solution for 35 min to inactivate the SR (Orentlicher et al., 1974). As predicted, these muscles then gave similar results to glycerinated muscle (Table IX). Potential measurements are difficult in the Brij-treated muscles because the electrode tip tends to block, possibly with pieces of SR.

The hypothesis may be made quantitative by considering the fixed charge concentrations in the two bands. In the solutions based on 100 mM KCl, for glycerinated relaxed both are -36 ± 8 mM, and for skinned relaxed both are -70 ± 11 mM, so the SR contribution, according to our hypothesis, is about -34 mM. The total surface area per unit volume of the SR has been estimated (for frog muscle) to be ~2.0 μm^{-1} of fiber (Mobley and Eisenberg, 1975). Combining these figures gives a charge change of ~ 10 e nm^{-2} of SR membrane. This figure seems plausible, but suggests that the hypothetical charging is not simply the binding of ATP at the ATPase sites. This would require about three ATP molecules per square nanometer, while the x-ray studies of Worthington and Liu (1973) show that ATPase particles in SR membranes are ~7 nm apart. It is therefore necessary to invoke some as yet unspecified effect of the Ca-ATP membrane pump, and of the ions that have been pumped into the SR. A very similar behavior to that in the chemically skinned rat muscles has also been observed in mechanically skinned barnacle muscles (Bartels and Elliott, 1981*b*). These barnacle muscles also have a well-developed SR system (Selveston, 1967) and the same considerations probably apply as in rat muscles. Aldoroty and April (1984) have also observed effects that they ascribe to membrane charging. Although the hypothesis has been developed by considering the SR, it remains formally possible that another parallel system might be involved. The cytoskeleton is an obvious alternative candidate.

Thin Filament Charge, the Effects of ATP, Ionic Strength, and pH

The thin filament charge measured in the I-band changes between the ATP-free rigor solution and the ATP-containing relaxing solution. From Fig. 6, at $\mu = 0.14$ M, the change is from about -28 mM (rigor) to about -38 mM (relaxing). This corresponds to an increase of (negative) charge of ~5 e/actin monomer in the thin filament, and might be the binding of two phosphate ions per monomer (in a recent preliminary communications, El-Salch and Johnson [1982] have suggested that actin can bind up to nine phosphate ions noncovalently). The thin filament charge also changes with ionic strength (Fig. 6) and with pH (Tables IV and VIII).

The thin filament charges measured in the I-band can be compared with those predicted from the A-band charge using the method of Naylor et al. (1985). The values in Table VIII, for both ionic strength and pH variation, may be compared with those in Tables I and II of Naylor et al.

(1985). There is reasonable agreement in the ionic strength series, and in the low μ pH series at all pHs except pH 3.5, if it is assumed that because of the uncertainty in Naylor et al.'s method of prediction a factor of two difference between the two figures is acceptable. In the pH series at high μ the agreement is not within this criterion, and the predicted charge is much smaller than that measured in the I-band. This might imply that in such rigor solutions negative ions are lost from the actin-containing filaments when they cross-link to the myosin heads (or alternatively that more positive ions bind). Alternatively, and more likely, the disagreement may indicate that the Naylor et al.'s method is not a good one where the gradient term in the x-ray data is <3.0 (in the units defined by the equation) because the uncertainty in the spacing difference between $S = 2.2$ μm and $S = 3.8$ μm is then too great. In relaxing solutions the thin filament charge in glycerinated rabbit muscle predicted from the A-band spacing variation is in reasonable agreement with that directly measured from the I-band potential (Table VII). This is also true of the results from skinned rat muscle in rigor (Table IV). In both these cases the gradient terms are >3.0. It is concluded that in skinned and glycerinated preparations the gradient of the d vs. S relationship of the x-ray data can be used to indicate the relative charges on the thick and thin filaments, as suggested by Elliott (1973) and Naylor et al. (1985), except when the gradient term is <3.0 in the units defined by the equation.

Charge Amplification

The charge amplification effect, which appears as a firm conclusion from these experiments (see the Relaxation and Rigor — Thick Filament Charges section above) leads immediately to a question, exactly where in the thick filament does this amplification occur? It seems very probable that it must involve the myosin molecules themselves, since these are the major constituent of thick filaments, and since the work of Scordilis, S. P. (unpublished results) also suggests this. We are currently seeking to confirm this with experiments on threads made from purified myosin molecules (Cooke et al., 1984; Bartels et al., 1985). On the assumption that it is so, where in the myosin molecule, or the assembly of myosin molecules, does the charge amplification reside?

At the present time any answer to this question must of necessity be hypothetical. There are, however, a number of clues. The amino acid sequence data of McLachlan and Karn (1982) and Karn et al. (1983) leads to a net charge of 2 e^+ on the heavy chain of each myosin head, if the 21 histidine residues are not ionized. On the rod portion of the molecule the net charge is 94 e, if the 34 histidine residues are not ionized; thus the net molecular charge (excluding the light chains) is 90 e (two heads and one rod). Notice that the major part of the molecular charge is one the rod, the heavy chains of the myosin heads are comparatively neutral at physiological pH. Lowey et al. (1969) observed by chromotographic elution that the head was less negatively charged than the rest of the myosin molecule.

It is possible that the extra charge in rigor appears on the head alone, and that the head charge increases from 2 e^+ to 16 e to accommodate an extra 18 e per head (see the Relaxation and Rigor — Thick Filament Charges section above). This seems a very large increase to be accommodated in a comparatively small globular protein, and no obvious physical model comes to mind. As has already been explained this could not be just the effect of binding one ligand molecule (ATP or ADP) per head.

A second possibility is that the head charge stays the same or nearly the same, and the extra charge is distributed uniformly along the rod. McLachlan and Karn (1982) have shown that in a myosin rod there are 38 repeat sequences of 28 amino acids, showing a similar and pronounced charge pattern in each sequence. The charged state, which has been observed, would on this basis be about one extra electronic charge for each of these 38 sequences. As a third possibility, the change might be confined to the S_2 region of the myosin molecule, the first 12 of these sequences. In this case the extra charge per sequence would be ~3 e, which looks interestingly as though it might be one phosphate ion (though the numerology should not be taken too seriously, for the whole rod only one in three sites might be occupied, each with a phosphate ion).

The latter two models have a common mechanism, the binding of ATP to myosin (which is the major effect in relaxation) causes the release of ions from the myosin rod or at least from part of it. How could this occur? For a possible mechanism, attention may be drawn to the views of Saroff (e.g., Loeb and Saroff, 1964) who considers that ion binding to proteins takes place by hydrogen bonds onto networks of charged side chains clustered along the polypeptide chain (Fig. 7). In myosin such clusters, which have been called "Saroff sites," may be set up between the myosin molecules in the filament (Elliott, 1980) or possibly, in view of the sequence data of McLachlan and Karn (1982), between the two polypeptide chains in one myosin molecule. In either case, mechanical stress transmitted along the shafts of the molecules, or between the two chains in a single molecule, might make small alterations in the structure of the intermolecular, or interchain Saroff sites. Saroff (1973) discussed "linked sites," which give rise to cooperativity in ion binding; we have observed (Elliott, 1980; Bridgman, T. D., E. M. Bartels, and G. F. Elliott, manuscript in preparation) that the ion-binding effects in muscle A-bands do appear to be cooperative.

Extended salt-bridge networks have been demonstrated in crystallographic studies by Bloomer et al. (1978) between the subunits of tobacco mosaic virus (TMV) coat protein, and by Adams et al. (1973) in lactate dehydrogenase. In the latter study the networks were specifically identified as anion binding sites. Perutz (1978) gives other

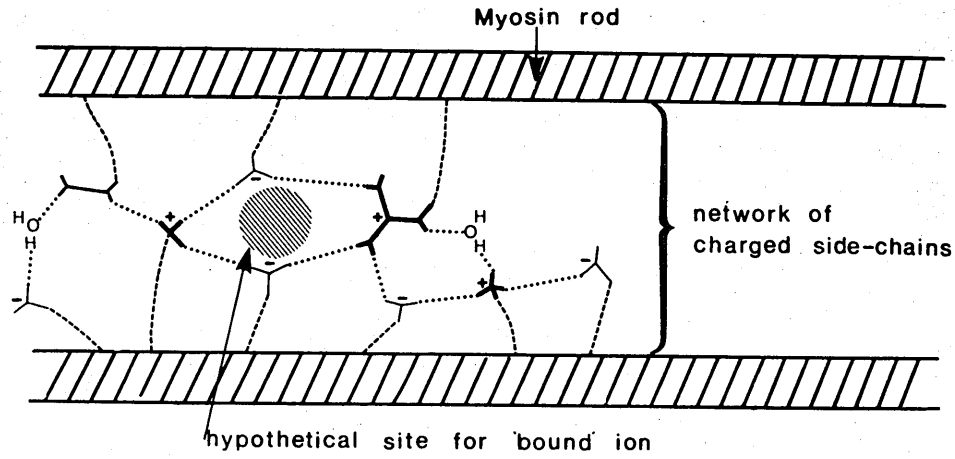

FIGURE 7 A hypothetical Saroff site, a network of charges side chains between two myosin rods (or possibly between two myosin polypeptide chains in a single myosin rod). The binding of some ion to such a site would affect the local charge balance, and this might cause a disseminated mechanical strain in the rod or rods, which might affect the binding properties of a similar neighboring binding site, possibly cooperatively. Notice that the vertical scale between the rods has been much exaggerated to show the network. In all probability the site is much more compact than it appears in this diagrammatic representation.

examples of extended salt-bridge interactions, and draws attention to their probable involvement in the allosteric interactions of hemoglobin. In a recent review of methods of reconstructing myosin filaments from solution, Koretz (1982) stresses the importance of pH and precise ionic conditions, which will control the molecular charge, and probably the ion-binding capacity, of the filaments formed.

It would not be appropriate to go further into these matters in this paper, so we will merely suggest the tentative model shown in Fig. 7. The interactions of myosin with ATP/ADP, by transmitting stress along the rod, controls the ion-binding characteristics of the rods, or of part of them. To explain the present results the binding of ATP would cause the low-charge state, its release would cause the high-charge state. Preliminary experiments have shown (Bartels and Elliott, 1983) that PP_i also gives the low-charge state, while ADP and AMP-PNP give the high-charge one.

This mode of action would fit easily into models of muscle contraction of the type envisioned by Harrington et al. (1979) though it would also fit easily into models of the swelling type (Elliott et al., 1970, see also the discussion after the paper of Elliott et al., 1978). Current work on myosin threads (Cooke et al., 1984; Bartels et al., 1985) is aimed at clarifying the details of the mode of action.

CONCLUSIONS

(*a*) The fixed protein charge is different in the A- and the I-bands of striated muscle in the rigor state. (*b*) The fixed charges are equal in the A- and I-bands of relaxed muscle. (*c*) The largest charge change between relaxation and rigor is on the thick filaments, and occurs whether or not the myosin heads are cross-linked to the thin filaments. (*d*) Possibly an event at one position on the myosin molecule, the binding of ATP (or certain other ligands) causes a disseminated change that modifies the ion-binding capacity of the myosin rods or parts of them.

APPENDIX

Discussion of Postulated Diffusion Potentials in the Presence of ATP

It has recently been suggested that there is a substantial contribution from diffusion potentials, particularly in the presence of ATP, which affect the measured Donnan potential (Godt and Baumgarten, 1984). We have commented already on these experiments (Elliott et al., 1984) but would like to give a quantitative calculation here.

The concentration of myosin heads in a typical A-band is ~0.4 mM and at the height of activation each head hydrolyzes ~35 ATP molecules/s. Therefore in a contracting muscle A-band the turnover of ATP and its product is ~14 mM/s. It is more difficult to know what is the ATP turnover in a relaxed muscle, but it is probably a factor of 10 or 100 times smaller. De Simone (1977) used the Nernst-Planck diffusion equation to calculate the deviations from equilibrium (Donnan) potentials. The deviation potential was governed by a dimensionless coefficient, μ, which he defined in his Eq. 21.

$$\mu = \frac{J_r}{Kc}\left(\frac{1}{D_2} - \frac{1}{D_1}\right).$$

Here J_r is the flux of reactants, K is the Debye-Hückel constant, c is the reservoir ion concentration, and D_1 and D_2 are the diffusion coefficients of the reactant and product.

This equation can be applied to the diffusion of ATP and its products in the muscle case. If cylindrical geometry and radial flow are assumed the flux of the reactants in contracting muscle is $14 \times r/2$ mM·s^{-1} per unit area, where r is the cylinder radius. (For spherical geometry the factor is $r/3$, the difference is trivial.) The diffusion coefficients for ions in muscle were measured by Kushmerick and Podolsky (1969) who gave $\sim 0.2 \times 10^{-5}$ cm^2 s^{-1} for ATP and ~0.4 in the same units for SO_4 (this is probably similar to PO_4, which they did not measure). In our experiments the reservoir ionic strength is 180 mM in standard relaxing solution, and the Debye-Hückel constant at this ionic strength is of the order 10^7 cm^{-1}.

De Simone's coefficient in these circumstances is $\mu \sim (14/10^7 \times 180) \times 10^5 \times (2.5 - 5) \times (r/2)$ (working in centimeters, seconds, and

millimoles) ~ $-1 \times 10^{-3} r$. If r is taken as the myofibrillar radius ($\sim 10^{-4}$ cm), this coefficient is of order 10^{-7}, if as the fiber radius ($\sim 10^{-2}$ cm), the coefficient is of order 10^{-5}. In either event De Simone's analysis shows that the deviations from the equilibrium potential are negligible for contracting muscle, and thus even more so for resting muscle.

We have already demonstrated (Elliott and Bartels, 1982, and in the previous paper, Naylor et al., 1985) that the KCl diffusion potentials are within the experimental error the same inside and outside the muscle lattice, and therefore cancel out in the Donnan potential measurement. It can be concluded that diffusion potentials, either passive diffusion potentials from KCl or active diffusion potentials from metabolically used ATP, are negligible in the experimental measurements of Donnan potential described in this paper.

We are grateful to Professor B. M. Millman, Ms. Katy Jennison, and Drs. Carl Moos, and Mark Shoenberg for help, advice, and useful discussions during the course of this work. We are particularly indebted to Dr. H. A. Saroff for ideas about ion binding to muscle proteins. We thank Mrs. Dawn Collins for cheerful and willing technical assistance. We are also indebted to Dr. E. W. April for showing us his two manuscripts on crayfish muscle before publication.

Some early experiments were carried out in 1980 while one of us (G. F. Elliott) was visiting the State University of New York at Stony Brook. The visit was supported by a National Institutes of Health grant GM26392 to Dr. Maynard Dewey, whom we are very grateful to. Supported by S. E. R. C. Grant No. GRC 26521.

Received for publication 28 March 1984 and in final form 19 November 1984.

REFERENCES

Adams, M. J., A. Liljas, and M. G. Rossman. 1973. Functional anion binding sites in dog fish M_4 lactate dehydrogenase. *J. Mol. Biol.* 76:519–531.

Aldoroty, R. A., and E. W. April. 1984. Donnan potentials from striated muscle liquid crystals. A-band and I-band measurements. *Biophys. J.* 46:769–779.

Aldoroty, R. A., N. B. Garty, and E. W. April. 1985. Donnan potentials from striated muscle liquid crystals. Sarcomere length dependence. *Biophys. J.* 47:89–96.

Bartels, E. M., J. M. Skydsgaard, and O. Sten-Knudsen. 1979. The time course of the latency relaxation as a function of the sarcomere length in frog and mammalian muscle. *Acta Physiol. Scand.* 106:129–137.

Bartels, E. M., and G. F. Elliott. 1980. Donnan potential measurements in the A- and I-bands of cross-striated muscles and calculation of the fixed charge on the contractile proteins. *J. Muscle Res. Cell Mobil.* 1:452.

Bartels, E. M., and G. F. Elliott. 1981*a*. Donnan potentials from the A- and I-bands of skeletal muscle, relaxed and in rigor. *J. Physiol. (Lond.).* 317:85–87P.

Bartels, E. M., and G. F. Elliott. 1981*b*. Donnan potential measurements in the A and the I bands of barnacle muscle fibers under various physiological conditions. *J. Gen. Physiol.* 78:12*a*–13*a*. (Abstr.)

Bartels, E. M., and G. F. Elliott. 1982. Donnan potentials in rat muscle: difference between skinning and glycerination. *J. Physiol. (Lond.).* 327:72–73P.

Bartels, E. M., and G. F. Elliott. 1983. Donnan potentials in glycerinated rabbit skeletal muscle: the effect of nucleotides and of pyrophosphate. *J. Physiol. (Lond.).* 343:32–33P.

Bartels, E. M., P. H. Cooke, G. F. Elliott, and R. A. Hughes. 1985. Donnan potential changes in rabbit muscle A-bands are associated with myosin. *J. Physiol. (Lond.).* 358:80.

Bloomer, A. C., J. N. Champness, G. Bricogne, R. Staden, and A. Klug. 1978. Protein disk of TMV at 2.8 Å resolution showing the interactions within and between the subunits. *Nature (Lond.).* 276:362–368.

Cooke, P. H., E. M. Bartels, G. F. Elliott, and K. Jennison. 1984. Myosin threads. *Biophys. J.* 45 (2, Pt. 2):7*a*. (Abstr.)

De Simone, J. A. 1977. Perturbation in the structure of the double layer at an enzymic surface. *J. Theor. Biol.* 68:225–240.

Elliott, G. F. 1973. Donnan and osmotic effects in muscle fibers without membranes. *J. Mechanochem. Cell Motil.* 2:83–89.

Elliott, G. F., and C. R. Worthington. 1963. A small-angle optically focusing x-ray diffraction camera in biological research. Part I. *J. Ultrastr. Reson.* 9:166–170.

Elliott, G. F. 1980. Measurements of the electric charge and ion-binding of the protein filaments in intact muscle and cornea, with implications for filament assembly. *Biophys. J.* 32:95–97.

Elliott, G. F., and E. M. Bartels. 1982. Donnan potential measurements in extended hexagonal polyelectrolyte gels such as muscle. *Biophys. J.* 38:195–199.

Elliott, G. F., E. M. Bartels, P. H. Cooke, and K. Jennison. 1984. Evidence for a simple Donnan equilibrium under physiological conditions. *Biophys. J.* 45:487–488.

Elliott, G. F., J. Lowy, and C. R. Worthington. 1963. An x-ray diffraction and light diffraction study of the filament lattice of striated muscle in the living staté and in rigor. *J. Mol. Biol.* 6:295–305.

Elliott, G. F., G. R. S. Naylor, and A. E. Woolgar. 1978. Measurements of the electrtic charge on the contractile proteins in glycerinated rabbit psoas using microelectrode and diffraction effects. *In* Ions in Macromolecular and Biological Systems. (Colston Papers No. 29). D. H. Everett and B. Vincent, editors. Scientechnica Press, Bristol, United Kingdom. 329–339.

Elliott, G. F., E. M. Rome, and M. Spencer. 1970. A type of contraction hypothesis applicable to all muscles. *Nature (Lond.).* 226:417–420.

El-Sach, S. C., and P. Johnson. 1982. Non-covalent binding of phosphate ions by striated muscle actin. *Int. J. Biol. Macromol.* 4:430–432.

Godt, R. E., and C. M. Baumgarten. 1984. Potential and K^+ activity in skinned muscle fibers. *Biophys. J.* 45:375–392.

Hanson, J. 1968. Recent x-ray diffraction studies of muscle. *Q. Rev. Biophys.* 1:177–216.

Harrington, W. F., K. Sutoh, and Y. Chen Chia. 1979. Myosin filaments and cross bridge movement. *In* Motility in Cell Function. F. A. Pepe, J. W. Sanger, and V. T. Nachmias, editors. Academic Press, Inc., New York. 69–90.

Huxley, H. E. 1968. Structural difference between resting and rigor muscle; evidence from intensity changes in the low-angle equatorial x-ray diagram. *J. Mol. Biol.* 37:507–520.

Huxley, H. E. 1973. Structural changes in the actin- and myosin-containing filaments during contraction. *Cold Spring Harbor Symp. Quant. Biol.* 37:361–376.

Jennison, K., G. F. Elliott, and C. Moos. 1981. Charge measurements of muscle proteins. *Biophys. J.* 33(2, Pt. 2):26*a*. (Abstr.)

Kensler, R. W., and M. Stewart. 1983. Frog skeletal muscle thick filaments are three-stranded. *J. Cell. Biol.* 96:1797–1802.

Koretz, J. F. 1982. Hybridization and reconstitution of thick-filament structure. *Methods Enzymol.* 85(B):20–31.

Kusmerick, M. J., and R. Podolsky. 1969. Ionic mobility in muscle cells *Science (Wash. DC).* 166:1297–1298.

Loeb, G. I., and H. A. Saroff. 1964. Chloride and hydrogen-ion binding to ribonuclease. *Biochemistry.* 3:1819–1826.

Lowey, S., H. S. Slayter, A. G. Weeds, and H. Baker. 1969. Substructure of the myosin molecule. I. Subfragments of myosin by enzymic degradation. *J. Mol. Biol.* 42:1–29.

McLachlan, A. D., and J. Karn. 1982. Periodic charge distributions in the myosin rod amino acid sequence match cross-bridge spacings in muscle. *Nature (Lond.).* 299:226–231.

Milhayi, E. 1950. The dissociation curves of crystalline myosin. *Enzymologica.* 14:224–236.

Mobley, B. A., and B. R. Eisenberg. 1975. Size of components of frog skeletal muscle measured by methods of stereology. *J. Gen. Physiol.* 66:31–45.

Naylor, G. R. S. 1977. X-ray and microelectrode studies of glycerinated rabbit psoas muscle. Ph.D. thesis, The Open University, Milton Keynes, England. 147 pp.

Naylor, G. R. S. 1978. A simple circuit for automatic continuous recording of microelectrode resistance. *Pfluegers Arch. Eur. J. Physiol.* 378:107–110.

Naylor, G. R. S. 1982. On the average electrostatic potential between the filaments in striated muscle and its relation to a simple Donnan potential. *Biophys. J.* 38:201–204.

Naylor, G. R. S., E. M. Bartels, T. D. Bridgman, and G. F. Elliott. 1985. Donnan potentials in rabbit psoas muscle in rigor. *Biophys. J.* 48:47–59.

Orentlicher, M., J. P. Reuben, H. Grundfest, and P. W. Brandt. 1974. Calcium binding and tension development in detergent-treated muscle fibers. *J. Gen. Physiol.* 63:168–186.

Pemrick, S. M., and C. Edwards. 1974. Differences in the charge distribution of glycerol extracted muscle fibers in rigor, relaxation, and contraction. *J. Gen. Physiol.* 64:551–567.

Perutz, M. F. 1978. Electrostatic effects in proteins. *Science* (*Wash. DC*). 201:1187–1191.

Poulsen, F. R., and J. Lowy. 1983. Small-angle x-ray scattering from myosin heads in relaxed and rigor frog skeletal muscle. *Nature* (*Lond.*). 303:146–152.

Reedy, M. K., K. C. Holmes, and R. T. Tregear. 1965. Induced changes in orientation of the cross-bridges of glycerinated insect flight muscle. *Nature* (*Lond.*). 207:1276–1280.

Rome, E. 1972. Relaxation of glycerinated muscle: low-angle x-ray diffraction studies. *J. Mol. Biol.* 65:331–345.

Saroff, H. A. 1973. Action of hemoglobin. The energy of interaction. *Biopolymers.* 12:599–610.

Scordilis, S. P., H. Tedeshi, and C. Edwards. 1975. Donnan potential of rabbit skeletal muscle myofibrils I: electrofluorochromometric detection of potential. *Proc. Natl. Acad. Sci. USA.* 72:1325–1329.

Selveston, A. 1967. Structure and function of the transverse tubular system in crustacean muscle fibers. *A. Zoologist.* 7:515–525.

Worthington, C. R., and S. C. Liu. 1973. Structure of sarcoplasmic reticulum membranes at low resolution. *Arch. Biochem. Biophys.* 157:573–579.

The Lancet · Saturday 5 April 1986

HISTOLOGICAL ABNORMALITIES IN MUSCLE FROM PATIENTS WITH CERTAIN TYPES OF FIBROSITIS

E. M. BARTELS

Biophysics Group, Open University Oxford Research Unit, Boars Hill, Oxford OX1 5HR

B. DANNESKIOLD-SAMSØE

Department of Rheumatology, Københavns Kommunes Hvidovre Hospital, University of Copenhagen, DK-2650 Hvidovre, Denmark

Summary In muscle biopsy specimens from fibrositis patients and healthy subjects no differences in electrical charges on the contractile proteins were detected with a microelectrode technique. However, microscopical examination of fibrositis muscle showed muscle fibres connected by a network of reticular or elastic fibres which are absent in normal muscle and which may be the cause of the disorder.

Introduction

FIBROSITIS (fibromyalgia)[1,2] is characterised by severe muscle pain without any obvious functional defect, although some pathological changes are seen.[3] As a result, many fibrositis patients, although disabled by the disorder, are wrongly given a psychiatric rather than a physical diagnosis. The disorder presents with varying degrees of severity, and the pattern of symptoms categorised as the fibrositis syndrome has been described by Smythe.[4]

In the present study, a microelectrode technique[5,6] has been used to determine fixed electrical charges on muscle proteins in muscle biopsy specimens from fibrositis patients and healthy subjects. Fibre bundles taken from the same muscle specimens were stained with Van Gieson's stain[7,8] to reveal any histological changes in the fibrositis muscle.

Methods

Preparation of Muscle Samples

Biopsy specimens were taken with a Bergström needle[9] from the quadriceps muscle of 7 healthy subjects and 13 fibrositis patients. The average age of the patients (4 men and 9 women) was 49 years (range 38–59). All the patients fulfilled the criteria for the fibrositis syndrome.[4] All subjects were informed about the nature, purpose, and possible risks of the experiments before giving their consent to participate. The biopsy specimens were transferred directly from the Bergström needle to a glycerination solution to remove the cell membranes and internal membrane systems.[5] The glycerination solution consisted of KCl 50 mmol/l, $MgCl_2$ 1 mmol/l, EGTA 2 mmol/l, and phosphate buffer (pH 7) 10 mmol/l in a 50% glycerol solution.

Bundles of 2 to 4 muscle fibres were then dissected from the glycerinated biopsy specimens and transferred to a petri dish containing a 2–3 mm layer of biologically inert silicone resin (Sylgard-184, Dow Corning Corporation, Midland, Michigan, USA) in which a slot 2 mm wide had been cut to accommodate the fibre bundles. The bundles were stretched between the sides of the slot and held in place by pushing the ends of the fibres into razor-blade cuts in the resin.

Measurement of Electrical Potentials

Measurements were made on muscle fibres soaked in a rigor solution and a relaxing solution, both at two different ionic strengths. Rigor solution I contained KCl 100 mmol/l, $MgCl_2$ 5 mmol/l, and phosphate buffer (pH 7) 20 mmol/l. Relaxing solution I contained KCl 100 mmol/l, $MgCl_2$ 10 mmol/l, EGTA 4 mmol/l, Na_2ATP 5 mmol/l, and phosphate buffer (pH 7) 20 mmol/l. Rigor solution II was half the concentration of rigor solution I, and relaxing solution II was half the concentration of relaxing solution I.

All muscle preparations were soaked in the experimental solution for an hour before any measurements were taken. Donnan potentials were measured from the A and I bands with a microelectrode technique combined with high-power light microscopy with phase and polarisation contrast (magnification ×400), as described by Bartels and Elliott.[6] In each experiment the protein charge concentration was calculated from the Donnan potential.[5] Assuming that the volume of the contractile apparatus is the same for a given ionic strength in the rigor and relaxed state,[5,6] the protein charge concentrations can be compared directly and taken to represent the fixed electric charges on the contractile proteins.

40 to 60 readings were taken from two different fibre bundles from each subject and in each experimental solution.

Histology

Each muscle sample used for electrical measurements was examined under a Zeiss 405 inverted microscope (phase contrast at ×25 and ×400 magnifications), to investigate possible differences between healthy and fibrositis specimens.

Small fibre bundles, containing 3 to 6 fibres, from the glycerinated sample were soaked for an hour in one of the rigor solutions. The preparations were then stained with a modification of Van Gieson's method,[7,8] using 2% acid fuchsin in a saturated picric acid solution. This staining method leaves collagen fibres red and elastic fibres, reticular fibres, myofibrils, and cytoplasm yellow. Since fuchsin (red stain) and picric acid (yellow stain) compete for the stain-binding sites, myofibrils tend to turn slightly red with the destaining time of 5–7 min used here.

Quadriceps Strength Measurements

The maximal isokinetic muscle strength of the knee extensors was measured on all subjects with an isometric dynamometer (Cybex II, Lumex, New York), as described by Danneskiold-Samsøe et al.[10] The isokinetic strength measurements were carried out at various angular velocities—30, 60, 120, 180, and 240 degrees.

Results

Electric Charges

The electric charges on contractile proteins in the A and I bands of muscles from fibrositis patients did not differ significantly from control values (see table).

Histology

The unstained and stained preparations showed the same characteristic differences between fibrositis and healthy

CONCENTRATIONS OF FIXED ELECTRICAL CHARGES IN A AND I BANDS OF GLYCERINATED MUSCLE FIBRES FROM FIBROSITIS PATIENTS AND HEALTHY CONTROLS (MEAN±SD)

Solution*	Charge concentration (mmol/l)†	
	Normal	Fibrositis
Rigor I:		
A band	−60±5	−66±8
I band	−32±6	−37±4
Rigor II:		
A band	−60±4	−61±5
I band	−40±3	−40±2
Relaxation I:		
A band	−45±5	−48±4
I band	−45±5	−47±4
Relaxation II:		
A band	−51±4	−50±3
I band	−51±4	−50±3

*The ionic strength of the I solutions was 0·14 mol/l and that of the II solutions 0·07 mol/l.
†Each data set represents the average value from 7 normal or 13 fibrositis subjects.

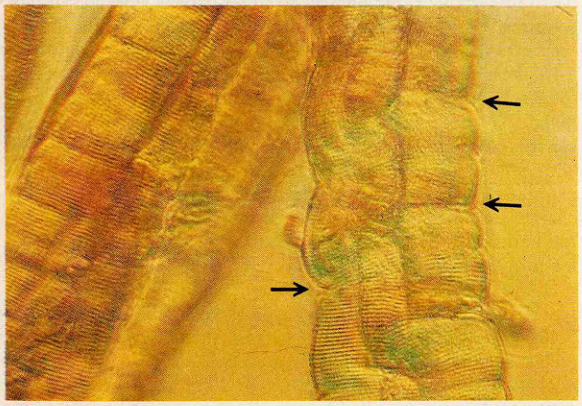

Fig 1—Fibre bundle from a glycerinated quadriceps muscle from a fibrositis patient, showing rubber-band-like structures along the fibres (arrows).

Van Gieson, ×400.

muscles. Although the fibrositis muscles showed a regular sarcomere repeat, the fibres looked as if rubber bands had been placed around the diameter at varying intervals, constricting the fibre at these sites (fig 1). Another difference found in the fibrositis muscle was an interconnecting network of thin threads between the individual muscle fibres which looked as if they connected with the rubber-band structures (fig 2). In normal muscle (fig 3) rubber-band structures are never seen, and interconnections rarely seen. The thin interconnecting threads appeared yellow even after brief destaining, which classifies them as either elastic or reticular fibres.

Quadriceps Strength Measurements

In the fibrositis patients the isokinetic muscle strength at all the measured angular velocities was considerably less (by 36–42%) than that of healthy controls (fig 4). The steepness of the force-velocity curve in patients was similar to that demonstrated in healthy subjects.

Discussion

Measurements of the fixed electric charge in the A and I bands of striated muscle cells with the Donnan potential method is a simple method that has not before been applied to medicine. A difference in the electric charges on the contractile proteins in either the A band or the I band between

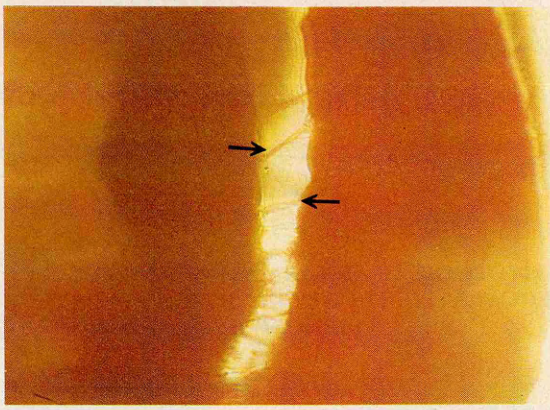

Fig 2—Interconnecting network of thin threads between fibres of fibrositis muscle (arrows).

Van Gieson, ×400.

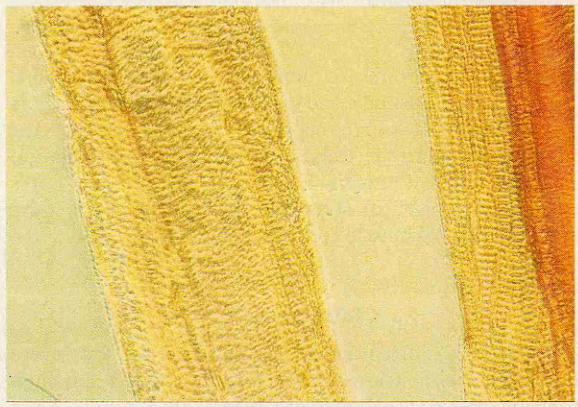

Fig 3—Fibre bundle from a glycerinated healthy quadriceps muscle.

Van Gieson, ×400.

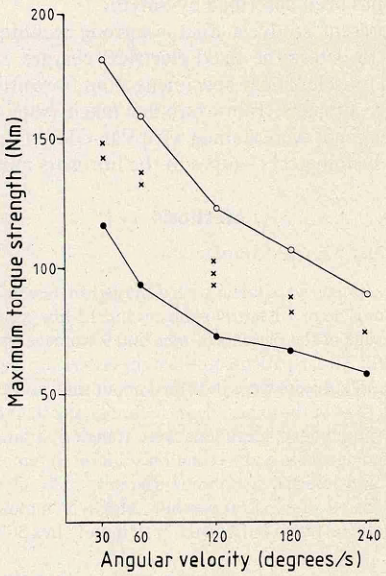

Fig 4—Maximal isokinetic quadriceps strength in fibrositis patients (●——●) and healthy subjects (○——○).

xxx $p<0·01$; xx $p<0·02$; x $p<0·05$ (Mann-Whitney test for unpaired samples).

a healthy and a diseased muscle must be due to a difference in the contractile proteins. Any such difference could affect the contractile processes and appear as a malfunctioning muscle.

Our results, however, show that patients with fibrositis have normal charge values in both A and I bands. They confirm that the contractile processes in the muscle cells of these patients are normal, as are biochemical values such as the level of muscle enzymes in the plasma.[11]

What, then, is wrong with these patients? All fibrositis patients have pains and tenseness in their muscles, and those we examined were from a subgroup of patients who do not respond to massage treatments.[12] Another subgroup, who do respond positively to massage treatments, show a rise in creatine kinase and plasma myoglobin during treatment.[12]

Since our patients were clearly in pain, and this muscle pain was not caused by failure of the contractile system, it must have been caused by something outside the cells. The microscopical appearance of the muscles from our patients was different from that of normal muscle even after glycerination, which removed the membrane structures. The connections between the cells and the rubber-band structures around them may indicate the nature of the disorder. If one muscle cell is stimulated to contract, it will create a pull in all the connecting cells as the contraction progresses. This will cause a passive sideways stretch or pull, which may be painful in itself or may perhaps stimulate the neighbouring cells. This will affect a new area of muscle fibres and start a cascade of contractions, bringing the muscle into a state of exhaustion and pain. This state of exhaustion and pain may account for the muscle weakness in fibrositis demonstrated by a reduction in isokinetic knee extensor strength.

We conclude that a likely cause for the symptoms in our group of patients is a network of elastic fibres connecting the muscle fibres and forming constricting bands around the fibres in a way that creates pulls between neighbouring cells whenever a cell contracts. We suggest that microscopical examination of a muscle biopsy specimen, combined with isokinetic strength measurements, is a reliable method for diagnosing the fibrositis syndrome in patients who do not respond to massage treatments.

We thank Dr A. Young for his support, Prof G. F. Elliott and Dr R. Bach-Andersen for their encouragement, and Salomia Hirschhorn, Anette Nawrocki, and Dawn Collins for technical assistance. This study was supported by the SERC, the Danish Rheumatism Association, the Danish Medical Research Council, and the Foundation of 1870.

Correspondence should be addressed to E. M. B.

REFERENCES

1. Murray GR. Myofibrositis as a simulator of other maladies. *Lancet* 1929; i: 112–16.
2. Yunus M, Masi AT, Calabro JJ, Miller KA, Feigenbaum SL. Primary fibromyalgia (fibrositis): Clinical study of 50 patients with matched normal controls. *Sem Arthritis Rheum* 1981; **11:** 151–71.
3. Henriksson KG, Bengtsson A, Larsson J, Lindström F, Thornell LE. Muscle biopsy findings of possible diagnostic importance in primary fibromyalgia (fibrositis, myofascial syndrome). *Lancet* 1982; ii: 1395.
4. Smythe HA, Moldofsky H. Two contributions to understanding of the "fibrositis" syndrome. *Bull Rheum Dis* 1977–78; **28:** 928–31.
5. Naylor GRS, Bartels EM, Bridgman TD, Elliott GF. Donnan potentials in rabbit psoas muscle in rigor. *Biophys J* 1985; **48:** 47–59.
6. Bartels EM, Elliott GF. Donnan potentials from the A- and I-bands of glycerinated and chemically skinned muscles, relaxed and in rigor. *Biophys J* 1985; **48:** 61–76.
7. Van Gieson J. Laboratory notes of technical methods for the nervous system. *NY Med J* 1889; **50:** 57–60.
8. Lille RD. Histochemical acetylation of hydroxyl and amine groups. Effects on the periodic acid-Schiff's reaction, anionic and cationic dye and Van Gieson's collagen stains. *J Histochem Cytochem* 1964; **12:** 821–41.
9. Bergström J. Muscle electrolytes in man. *Scand J Clin Lab Invest* 1962; suppl 68.
10. Danneskiold-Samsoe B, Kofod V, Munter J, Grimby G, Schnohr P, Jensen G. Muscle strength and functional capacity in 78–81 year old men and women. *Eur J Appl Physiol* 1984; **52:** 310–14.
11. Danneskiold-Samsøe B, Christiansen E, Lund B, Bach-Andersen R. Regional muscle tension and pain (fibrositis). *Scand J Rehab Med* 1982; **15:** 17–20.
12. Danneskiold-Samsøe B, Christiansen E, Bach-Andersen R. Myofascial pain and the role of myoglobin. *J Scand Rheum Physiol* (in press).

PERCUTANEOUS DOUBLE-BALLOON MITRAL VALVOTOMY FOR RHEUMATIC MITRAL-VALVE STENOSIS

MUAYED AL ZAIBAG PAULO A. RIBEIRO
SAAD AL KASAB MOHAMED R. AL FAGIH

Adult Cardiology Division, Riyadh Cardiac Centre, Riyadh Military Hospital, PO Box 7897, Riyadh 11159 Kingdom of Saudi Arabia

Summary Percutaneous transatrial mitral valvotomy with a double-balloon technique produced striking symptomatic improvement in 7 of 9 patients with severe mitral stenosis. In 7 patients the mitral valve area (Gorlin formula) increased significantly and the mitral end-diastolic gradient fell significantly. Similar improvements were noted in follow-up haemodynamic studies at 6 weeks. There were no procedure-related complications. It is concluded that percutaneous double-balloon mitral valvotomy may be an alternative to surgical treatment for mitral stenosis.

Introduction

THE Kingdom of Saudi Arabia, in common with many other parts of the world, still has a high prevalence of rheumatic heart disease.[1] Rheumatic mitral stenosis appears at one end of the spectrum of the clinical manifestations of the disease.

Currently, symptomatic rheumatic mitral stenosis requires surgical intervention. The use of a non-surgical therapeutic alternative was first described in 1984 by Inoue et al[2] in 6 patients, and Lock et al[3] has used the same transvenous single transatrial approach in children. However, Lock et al had to dilate the atrial septal puncture with an 8–10 mm angioplasty balloon catheter, which could interfere with the haemodynamic assessment of mitral stenosis.[4]

We now describe the results obtained with our percutaneous double-balloon mitral valvotomy technique in 9 patients with rheumatic mitral stenosis.

Patients and Methods

Patients

Percutaneous balloon mitral valvotomy was attempted in 9 adults with rheumatic mitral stenosis. (6 women and 3 men, mean age of 25±7 SD years). Patients were selected according to the following criteria: (i) severe symptomatic rheumatic mitral-valve stenosis (A2–OS $\leqslant$80 ms, mitral valve area $\leqslant$1 cm^2); (ii) no previous history of thromboembolic complications or cardiac surgery; (iii) age >15 years; (iv) in sinus rhythm; (v) no mitral regurgitation on auscultation; (vi) absence of mitral calcification on fluoroscopy; (vii) no detectable left atrial clot on cross-sectional echocardiography and absence of extensive mitral subvalvular fusion.

6 patients had symptoms in New York Heart Association (NYHA) class III, 2 in class II, and 1 in class IV. Medication included digoxin (all patients), diuretics (all patients), beta-blockers (patients 1, 3, 4, 6, 7, 9), and verapamil (patient 8). 5 patients had an apical diastolic thrill. Auscultation revealed a palpable first heart sound and a close opening snap, together with a diastolic rumble with presystolic accentuation $\geqslant$grade 3/4 in all cases. Mild aortic regurgitation was detected clinically in 3 patients.

Medication

All patients were anticoagulated with warfarin for 3–4 weeks before the procedure. On admission warfarin anticoagulation was replaced by intravenous heparin infusion, which was continued for

To be published in "Electrical double layers in Biology"
ed Martin Blank, Plenum Publishing Corp.
New York, 1985.

THE MYOSIN FILAMENT; CHARGE AMPLIFICATION AND CHARGE CONDENSATION

G.F. Elliott, E.M. Bartels and R.A. Hughes

Open University, Oxford Research Unit, Foxcombe Hall,
Berkeley Road, Boars Hill, Oxford, OX1 5HR, England.

Current models for the molecular mechanism of muscular contraction are derived largely from structural and biochemical information. Experimental evidence has traditionally been obtained as answers to questions like "where are the various contractile proteins located, what are the physical and chemical properties of the isolated, purified proteins in solution, how do the kinetics of muscle chemistry correlate with structural changes in working muscles?" A detailed picture of many essential events in muscle contraction has been obtained in this manner and has been incorporated into current views of the sliding filament hypothesis, see for example the monographs of A.F. Huxley (1980) and Bagshaw (1982).

A direct physical approach to any working mechanism of microscopic dimensions should include (1) the distribution of matter, and importantly (2) the distribution of electric charge. Some understanding of these two distributions would provide an essential step in defining a working mechanism in physical terms. While the experimental paradigm in the biological sciences usually includes substantial effort to define the distribution of matter in systems which may have been simplified, in solution for example, the distribution of electric charge is often overlooked or ignored in kinetic schemes, largely because of the technical difficulties in obtaining a reliable index of charge patterns at high spatial and temporal resolution. Even in contracting muscle, where finite changes in the distribution of contractile material occur on a measureable time scale, very little effort has been made to analyse the mechanism in the physical terms of charge density and distribution.

Collins and Edwards (1971) showed that Donnan potentials could be observed from vertebrate striated muscle (using 3 M KCl electrodes) after the membrane had been rendered porous by glycerol treatment, and that these potentials could be used to calculate the fixed charge on the contractile proteins. After this pioneering work we combined the same approach with X-ray and light diffraction (Elliott et al 1978, Naylor et al 1985) to derive the linear charges on the thick (myosin-containing) and thin (actin-containing) filaments in the muscle. The theoretical and practical basis of the method of filament-charge measurement is discussed in Elliott and Bartels (1982), Elliott et al (1984) and Naylor (1982).

Using light microscopy to locate the microelectrode tip, we also demonstrated (Bartels and Elliott 1980, 1981, 1985) different Donnan potentials

in the A- and I-bands of glycerinated vertebrate striated muscle (and in mechanically skinned barnacle muscle). In rigor (the absence of ATP) the negative A-band potential is about twice the I-band potential. In relaxing solution (containing ATP) the A-band potential in the glycerinated muscle falls to the same as the I-band potential. This potential fall is also observed in a solution containing pyrophosphate (PP_i) but not one containing ADP or AMP-PNP (Bartels and Elliott 1983), so that it appears to be caused by the pyrophosphate moiety of the ATP molecule. In a contracting solution (Ca^{++} and ATP present) both A-band and I-band potentials exceed resting values in the early phase of tension development, and then fall below resting values during the recovery phase (experiments made with slow muscle fibres, mechanically or chemically skinned, Bartels and Elliott 1984a and b).

There are some differences in the behaviour of the A- and I-band potentials in relaxing solutions between muscles that have been glycerinated and those that have been skinned mechanically or chemically. We have shown (Bartels and Elliott 1982, 1985) that these may arise from the presence in skinned muscles of a parallel system, probably the sarcoplasmic reticulum, which charges up as the thick filaments discharge, and which is not present (or not functional) in glycerinated muscle or in skinned muscle treated with specific detergents to remove the sarcoplasmic reticulum.

The A-band potential change on the addition of ATP is a dramatic effect. In collaboration with Dr. Peter Cooke we have developed threads of purified myosin, the major protein component of a muscle A-band, and have made Donnan measurements on such threads (Bartels et al 1985). Figure 1 shows the results of a typical experiment, the myosin molecular charge falls sharply with the addition of small amounts of ATP, the fall is essentially over by 0.5 mM [ATP]. This is about twice the concentration of myosin molecules in the threads, so that the effect may be stoichiometric, with one or two ATP-binding sites per molecule. The potential (and charge) decrease coincides with the rise of $[MgATP^{--}]$ in the solution, and the charge in this experiment falls from about 75e (electronic charges) $molecule^{-1}$ in the absence of ATP to about 50e in the presence of 0.5 mM $[MgATP^{--}]$, so the change is too large for 2 ATP molecules (~ 4-8e). In a relaxing solution (containing ATP) the ligand is known to be bound, and to be released when the muscle goes into the contraction cycle and into (ATP-free) rigor also; the consequent change due to this alone would be in the reverse direction to our observations. The implication is that the charge effect must be amplified in amount and reversed in sign, and our working hypothesis is that the ion-binding properties throughout the protein are modified as a result of some initiating event.

McLachlan and Karn (1982) have shown that in a myosin rod (the α-helical tail of the myosin molecule) there are 38 repeat sequences of 28 amino acids, each sequence showing a similar and pronounced charge pattern. The charge change would, on this basis, be about one extra electronic charge for each of these 38 sequences. Alternatively, the change might be confined to the S-2 region of the myosin molecule, the first twelve of these sequences. In this case the charge change per sequence would be about 3e, which looks interestingly as though it might be one phosphate ion. The hypothesis is that the binding of ATP/PP_i to myosin (the major effect in muscle relaxation) causes the release of negative ions from the myosin rod, or at least from part of it. Alternatively, positive ions might be bound rather than negative ions released. For a possible mechanism, we favour the ideas of Saroff (Loeb and Saroff 1964), that ion-binding to proteins is by hydrogen bonding onto networks of charged side chains clustered along the polypeptide chain. In myosin such clusters (Saroff sites) may be set up between the myosin rods in the filament or between the two polypeptide chains in one myosin rod (Figure 2). Mechanical stress transmitted through the filament backbone might cause small alterations in the structure of the Saroff sites (Figure 3) giving rise to the co-operativity in effects which we have observed in muscle A-bands

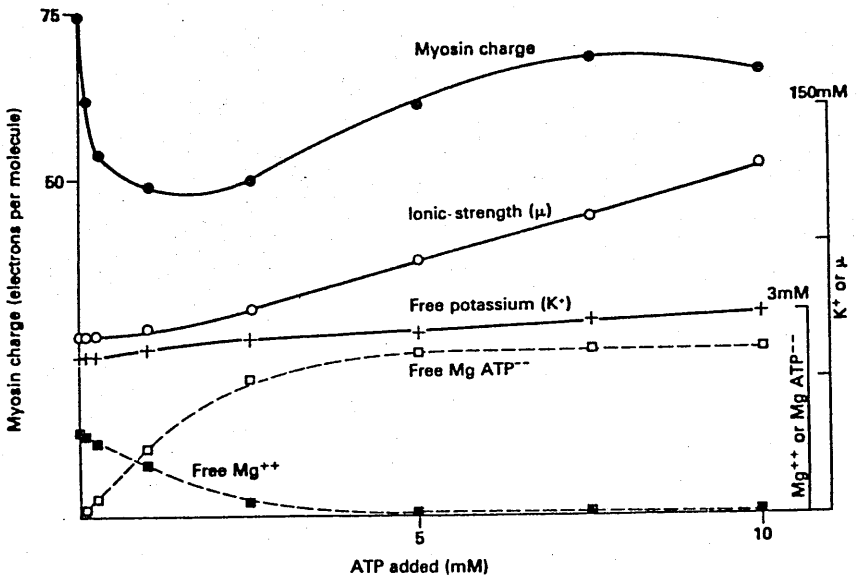

Fig. 1. An ATP titration experiment on threads containing filaments of purified myosin shows that the molecular charge reduction occurs sharply at low values of added ATP, and is maximal by about 0.5 mM [ATP]. The levels of several of the solution constituents are plotted; the fall in charge coincides with the rise in [MgATP^{--}]. The subsequent increase in charge is probably a non-specific ionic-strength effect, since it coincides with the rise in μ and we have observed similar effects in both rigor and relaxing solutions.

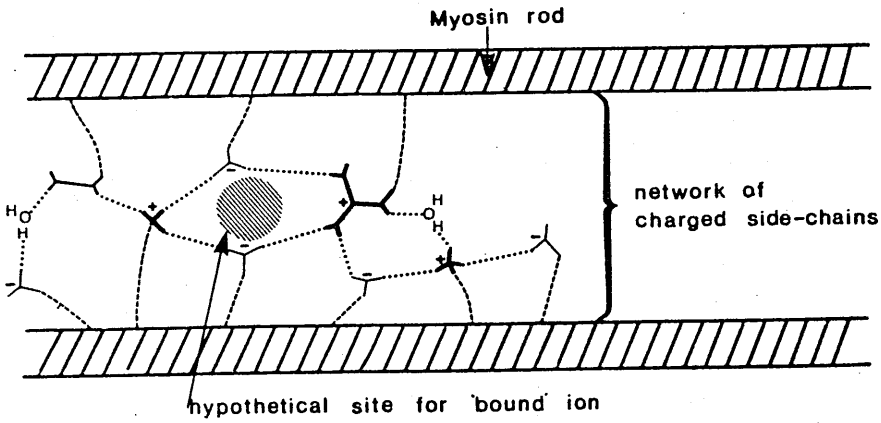

Fig. 2. A hypothetical Saroff site, a network of charged side-chains between two myosin rods. Such networks are apparent from the work of McLachlan and Karn (1982), although the form of this one is taken from tobacco mosaic virus coat protein. Notice that the vertical scale between the rods has been much exaggerated to show the network, in all probability a myosin site is much more compact than appears in this diagramatic representation.

A natural question arises; if the charge reduction that we have observed is initiated by ATP/PP_i binding to a specific site, where is that site on the

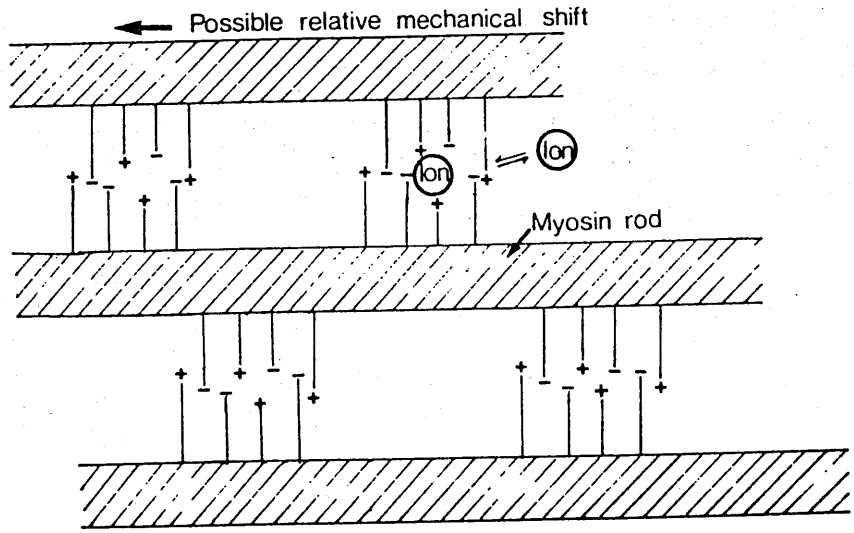

Fig. 3. In a myosin filament, with many identical Saroff sites between adjacent myosin rods, the binding or release of an ion at one site may cause a relative mechanical shift of the two rods, affecting the adjacent sites and giving rise to co-operativity of the ion-binding or release.

myosin molecule? Since the effect is observed in myosin rod gels as well as in whole myosin gels (Bartels et al 1985) it would seem that the effect cannot be caused by ATP/PP_i binding at the primary ATP-ase site on the globular myosin head (S-1). There must, then, be some further ATP-affected site on the α-helical backbone of the myosin rod. Such secondary ATP sites have been observed by a number of previous workers, including Harrington and Himmelfarb (1972), whose studies revealed the presence of one or two binding sites in the rod segment of myosin. They investigated the association/dissociation of myosin filaments at pH 8, and remarked that these rod sites exert a profound effect on the stability of the filaments at low substrate concentrations. They did not, however, find substantially different behaviour between ATP, ADP, AMP-PNP or PP_i. In our experiments, at pH 7 where the filaments are associated, ATP and PP_i do cause the charge decrease, ADP and AMP-PNP do not do so. There seem to be some parallels between our experiments and those of Harrington and Himmelfarb, but the details remain to be explained.

A second question should also be asked. Does the striking decrease in negative charge in the presence of ATP/PP_i stem from the release of negative ions from the protein, or from the binding of positive ions to the protein when the ATP/PP_i initiates some Saroff-type mechanism? Here the clues are contradictory. Experiments in which the anion type is varied (T.D. Bridgman, E.M. Bartels and G.F. Elliott, paper in preparation) show that there are differences between the filament charges measured in different anions. This could imply that anion binding in rigor is the important effect, and that anion release occurs on ATP/PP_i addition. On the other hand, Lewis and Saroff (1957) showed that myosin binds about 20 K^+ ions at pH 7 and $[K^+]$ = 0.1 M, and showed moreover that actomyosin (that is, myosin linked to actin in the rigor configuration) bound less K^+ ions under similar conditions. This work suggests that changes in cation binding might be important, but unfortunately Lewis and Saroff did not investigate the effect of ATP upon K^+ binding. This second question could probably best be answered by equilibrium dialysis experiments using radioactive isotopes, and we intend to carry these out as soon as possible.

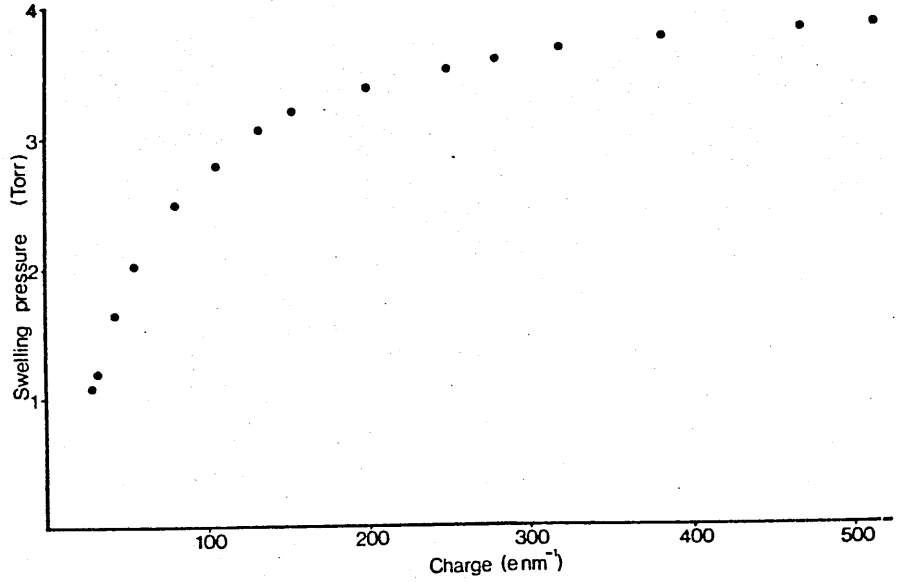

Fig. 4. The swelling pressure in Torr as a function of surface charge, calculated as explained in the text for filaments of charge radius 15 nm, at a Debye length of 1.0 nm. Charge saturation begins at about 100 e nm^{-1} and is advanced by about 200 e nm^{-1}.

We have demonstrated that charge changes can be observed in muscle in situations which are of direct physiological importance. Do these charge changes give rise to effects which are relevant to the function of muscle? The charge changes might affect the electrostatic swelling pressure within the muscle filament lattice, and thus change the transverse force balance that must exist in that lattice (Elliott 1968, April 1975, Millman and Nickel 1980). However, Millman and Nickel (1980) first drew attention to the charge-saturation effect for muscle, that the calculated electrostatic repulsive force between the filaments does not increase beyond a certain level with filament charge; the alternative formulations of Elliott and Bartels (1982) and Naylor (1982) have also shown this effect.

Charge saturation is related to counter-ion charge condensation (Manning 1969, 1978). Manning has shown that for those molecules that may be approximated as a line charge, there is a maximum molecular charge which can affect the field produced by the molecule, because if the molecule charge exceeds this critical maximum, the excess charge is neutralised by the condensation of counter ions in the region of the line charge. The critical charge, in this line charge approximation, is one electronic charge per Bjerrum length, and this length, at 25°C in an aqueous environment, is about 0.7 nm.

The Manning analysis applies to line charges, and has been used successfully to explain experimental effects in systems of small polyion radius such as DNA molecules (e.g. Manning 1978). It is not immediately clear how the analysis may be applied to systems of much larger polyion radius, such as muscle thick filaments. Lampert (1983, see also Lampert and Crandall 1980), has considered this problem theoretically, and gives numerical tables which can be used to estimate the maximum effective charge and confinement radius for an isolated charged cylinder (of finite radius) in an electrolyte. An alternative approach is to derive the swelling pressure saturation as the filament charge increases, and this is shown in Figure 4, calculated using the computer programme described in Elliott and Bartels (1982), based on

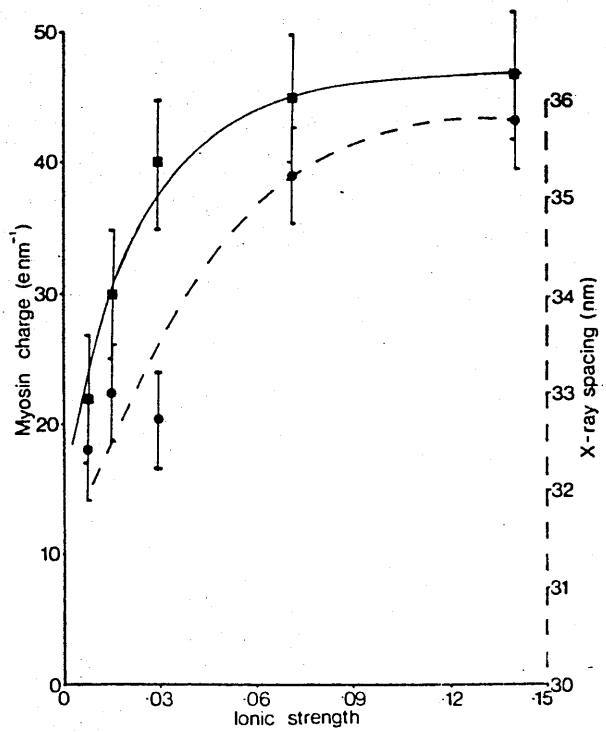

Fig. 5. X-ray-spacing (d_{10}), round points, and myosin filament charge, square points, measured in rigor solution of similar composition obtained by serial dilution of a standard salt solution to different ionic strengths (for details of the solutions see Naylor et al 1985). All were at pH 7, phosphate buffer, and all X-ray spacings were taken at sarcomere lengths of 3.8 μm. Experimental errors are shown. The saturation in myosin filament charge is a real effect, for higher ionic strengths the filament charge falls, but the X-ray spacing is then very difficult to measure because the reflections become very diffuse. The correlation between X-ray spacing and filament charge is clear (curves fitted by eye).

Alexandrowicz and Katchalsky (1963). Figure 4 shows that for filaments of 15 nm charge radius, at a Debye length of 1.0 nm, the charge saturation occurs at between 100 and 200 e nm^{-1}. This agrees with the 100 e nm^{-1} figure given by Millman (1985, this volume). 100 e nm^{-1} on the surface a 15 nm radius filament is about 1 e nm^{-2} of filament surface area, so that the individual charges under these circumstances are on the average separated by rather more than the Bjerrum length, which seems intuitively reasonable.

In view of the agreement between us and Millman (1985), and the intuitive reasonableness of the order of magnitude, it might be hoped that the maximum effective charge derived from Lampert (1983) would also agree. Unfortunately this is not so, and calculation from this paper suggests a maximum effective charge of 14 e nm^{-1} for cylinders of radius 15 nm at a Debye length of 1.0 nm. The table in Lampert's paper which leads to this conclusion is derived by numerical integration, so that we are unable to go further into this discrepancy.

It is possible, however, to demonstrate experimentally that the X-ray

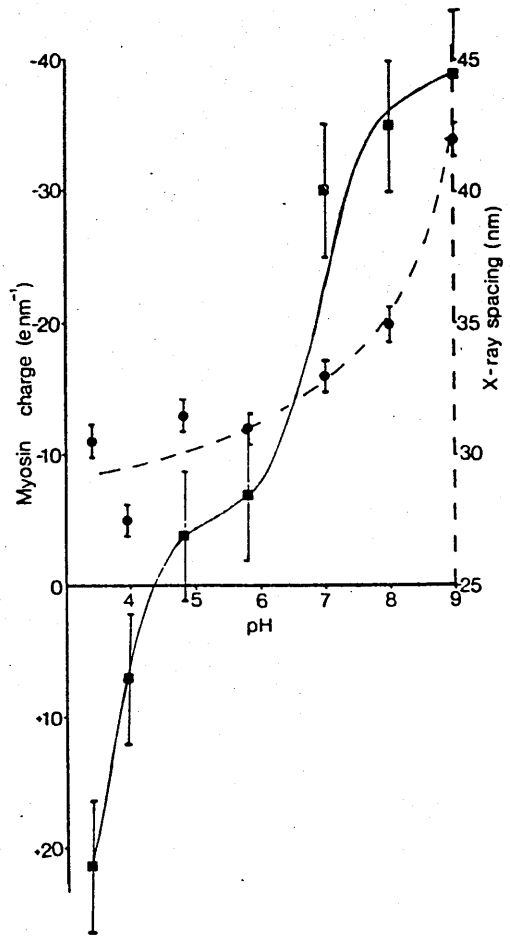

Fig. 6. X-ray spacing (d_{10}), round points, and myosin filament charge, square points, in rigor solutions all at ionic strength ~ 0.014 M, and of different pH's. All X-ray spacings were taken at a sarcomere length of 3.8 μm except for those at pH 8 and 9, which are at 3.45 μm (we are indebted to Mr. R.J. Ward for these two measurements). At pH's below 6.0, citrate buffer was used, at pH 7 and 8, phosphate buffer and at pH 9, borate buffer. Most of the data are from Naylor et at 1985, with the addition of subsequent experiments at pH 8 and 9. Experimental errors are shown. The general correlation between charge and spacing is clear. The curves are fitted by eye, and we have not chosen to suggest a minimum in the X-ray spacing between pH 4 and 5, since the measurements are not convincing although a minimum would be expected at around the isoelectric point, pH 4.4.

spacing between the muscle filaments is sensitive to the myosin charge. This is most easily seen at long sarcomere lengths, where the situation is not complicated by actin-myosin interactions. The results for ionic strength variation are plotted in Figure 5, and for pH variation in Figure 6. The data for these Figures are largely from the results of Naylor et al (1985), and the Figures are plotted for rigor muscle at a sarcomere length of 3.8 μm, which is zero overlap between the thick and thin filaments. These Figures show clearly that the interfilament repulsive forces are not charge saturated in the experimental regime in rigor, and that they certainly will not be so at the lower filament charges seen in relaxed muscle.

Our contracting muscle results, in conjunction with the measurements on relaxed and rigor muscles, would fit naturally into Harrington's (1971) model where the force is generated by some ionic-led phase change within the S-2 link between the myosin head (S-1) and the filament backbone. They would also fit into models where the basic event is ionic swelling in the filament lattice, converted to longitudinal force by the myosin heads acting as dragging anchors (e.g. Elliott, Rome and Spencer 1970 modified as suggested in the discussion following Elliott et al 1978). In either case we may recall the words of Albert Szent-Györgyi (1941), "I was always led in research by my conviction that the primitive, basic functions of living matter are brought about by ions, ions being the only powerful tools which life found in the sea-water where it originated. Contraction is one of the basic primitive functions".

ACKNOWLEDGEMENTS

We are indebted to Ms. K. Jennison, Mr. R.J. Ward and Dr's Peter Cooke, Barry Millman and Carl Moos for enthusiasm and constructive criticism. This work was aided by a grant from the Science and Engineering Research Council.

REFERENCES

Alexandrowicz, Z., and Katchalsky, A., 1960, Colligative properties of polyelectrolyte solutions in excess of salt, J. Polymer. Sci. A., 1:3231.

April, E.W., 1975, Liquid crystalline characteristics of the thick filament lattice of striated muscle, Nature, 257:139.

Bagshaw, C.R., 1982, "Muscle contraction", Chapman and Hall, London and New York.

Bartels, E.M. and Elliott, G.F., 1980, Donnan potential measurements in the A- and I-bands of cross-striated muscles and calculation of the fixed charge on the contractile proteins, J. Musc. Res. Cell Motility, 1: 452.

Bartels, E.M., and Elliott, G.F., 1981, Donnan potentials from the A- and I-bands of skeletal muscle, relaxed and in rigor, J. Physiol., 317:85P.

Bartels, E.M. and Elliott, G.F., 1982, Donnan potentials in rat muscle: Difference between skinning and glycerination, J. Physiol., 327:72P.

Bartels, E.M. and Elliott, G.F., 1983, Donnan potentials in glycerinated rabbit skeletal muscle: the effect of nucleotides and of pyrophosphate, J. Physiol., 343:32P.

Bartels, E.M. and Elliott, G.F., 1984a, Changes in the Donnan potentials from the A- and the I-bands of contracting skeletal muscles, Acta. Physiol. Scand., 121(3):A20.

Bartels, E.M. and Elliott, G.F., 1984b, Donnan potentials from contracting muscle, J. Musc. Res. Cell Motility, 5:227.

Bartels, E.M. and Elliott, G.F., 1985, Donnan potentials from the A- and I-bands of glycerinated and chemically skinned muscles, relaxed and in rigor, Biophys. J., 48:61.

Bartels, E.M., Cooke, P.H., Elliott, G.F. and Hughes, R.A., 1985, Donnan potential changes in rabbit muscle A-bands are associated with myosin, J. Physiol., 358:80P.

Collins, E.W. and Edwards, C., 1971, Role of Donnan equilibrium in the resting potentials in glycerol-extracted muscle, Am. J. Physiol., 221:1130.

Elliott, G.F., 1968, Force-balances and stability in hexagonally-packed polyelectrolyte systems, J. Theoret. Biol., 21:71.

Elliott, G.F., Rome, E.M., and Spencer, M., 1970, A type of contraction hypothesis applicable to all muscles, Nature, 226:417.

Elliott, G.F., Naylor, G.R.S. and Woolgar, A.E. 1978, Measurements of the electric charge on the contractile proteins in glycerinated rabbit psoas using microelectrode and diffraction effects, In:"Ions in Macromolecular and Biological Systems", D.H. Everett and B. Vincent, eds. Scientechnica Press, Bristol.

Elliott, G.F. and Bartels, E.M. 1982, Donnan potential measurements in extended hexagonal polyelectrolyte gels such as muscle, Biophys. J., 38: 195.

Elliott, G.F., Bartels, E.M., Cooke, P.H. and Jennison, K., 1984, Evidence for a simple Donnan equilibrium under physiological conditions, Biophys. J., 45:487.

Harrington, W.F., 1971, A mechanochemical mechanism for muscle contraction, Proc. Natnl. Acad. Sci., 68:685.

Harrington, W.F. and Himmelfarb, S., 1972, Effect of adenosine di- and triphosphates on the stability of synthetic myosin filaments, Biochemistry, 11:2945.

Huxley, A.F., 1980, "Reflections on muscle", Liverpool University Press, Liverpool.

Lampert, M.A., 1983, Maximum effective charge and confinement radius for the Coulomb condensate for an isolated charged sphere or cylinder in an electrolyte, Chem. Phys. Letters, 96:475.

Lampert, M.A. and Crandall, R.S., 1980, Non-linear Poisson-Boltzmann theory for polyelectrolyte solutions: the counterion condensate round a line charge as a delta-function, Chem. Phys. Letters, 72:481.

Lewis, M.S. and Saroff, H.A., 1957, The binding of ions to the muscle proteins, J. Am. Chem. Soc., 79:2112.

Loeb, G.I. and Saroff, H.A., 1964, Chloride and hydrogen-ion binding to ribonuclease, Biochemistry, 3:1819.

McLachlan, A.D. and Karn, J., 1982, Periodic charge distributions in the myosin rod amino acid sequence match cross-bridge spacings in muscle, Nature, 299:226.

Manning, G.S., 1969, Limiting laws and counterion condensation in polyelectrolyte solutions, J. Chem. Phys., 51:924.

Manning, G.S., 1978, The molecular theory of polyelectrolyte solutions with applications to the electrostatic properties of macromolecules, Ann. Rev. Biophys., 11:179.

Millman, B.M. and Nickel, B.G., 1980, Electrostatic forces in muscle and cylindrical gel systems, Biophys. J., 32:49.

Millman, B.M., 1985, Long range forces in cylindrical systems: muscle and virus gels, This volume.

Naylor, G.R.S., 1982, On the average electrostatic potential between the filaments in striated muscle and its relation to a simple Donnan potential, Biophys. J., 38:201.

Naylor, G.R.S., Bartels, E.M., Bridgman, T.D. and Elliott, G.F., 1985, Donnan potentials in rabbit psoas muscle in rigor, Biophys. J., 48:47.

Szent-Györgyi, A., 1941, Discussion, Studies from the Institute of Medical Chemistry, University of Szeged, 1:69.

[*From the Proceedings of the Physiological Society*, 13–14 *February* 1987
Journal of Physiology, **388**, 34*P*, 1987]

Donnan potential measurements from the sarcoplasmic reticulum of rabbit muscle under rigor and relaxed conditions

By E. M. Bartels, G. F. Elliott and R. S. Wall. *The Open University, Oxford Research Unit, Foxcombe Hall, Boars Hill, Oxford OX1 5HR*

Two methods of preparation of rat semitendinosus muscle, glycerination and chemical skinning, give rise to differences in the Donnan potentials recorded in the A and I bands of the muscle (Bartels & Elliott, 1982, 1985); in skinned muscle both the A and I bands are more highly negatively charged in the presence of ATP than in glycerinated muscle. This difference could be due to the presence of an additional parallel system present in the skinned muscle. Sarcoplasmic reticulum (SR) has been suggested as a possibility, as glycerination is thought to remove or inactivate the SR system to a greater extent than mild chemical skinning procedures.

To investigate its effect on charge measurements, SR was prepared as described by Nakamura, Jilka, Boland & Martonosi (1976). The SR vesicle suspension thus obtained was centrifuged at 100000 g_{max} for 1 h to give a densely packed pellet consisting of light and heavy SR which was then used for micro-electrode measurements. The vesicle suspension in sucrose/buffer solution could be frozen and stored at −20 °C for several weeks.

Donnan potentials were measured from the pellets immersed in solutions containing 50 mM-KCl, 4 mM-imidazole/HCl buffer, pH 7·0, 200 mM-sucrose (standard solution), in the presence and absence of 2·5 mM-ATP, using the set-up described by Bartels & Elliott (1985). The results (Table 1) show that addition of ATP increases the protein charge concentration in the pellet. The volume of the pellet does not alter when the ATP solution is added, therefore the charge density of the SR has increased.

Table 1

	Donnan potential (mV)	[Pr] (mM)
Standard solution	−7·9 ± 0·6 S.D.	−33 ± 3 S.D.
Standard solution + ATP	−10·8 ± 0·6 S.D.	−63 ± 4 S.D.

Pooled data from one batch of pellets where the protein concentration of the pellets is known to be ≃ 100 mg/ml (4 experiments, 80 readings in each solution).

These results demonstrate that addition of ATP to pelleted SR vesicles produces an increase in the charge concentration of the vesicles, most likely due to their protein component. This supports the hypothesis that in skinned muscle the SR, which is present in an active form, contributes to the charge measurements, increasing them in the presence of ATP. It seems likely that the charge pattern seen in a skinned muscle preparation is therefore a sum of the contributions from the myofilament system and the sarcoplasmic reticulum.

REFERENCES

Bartels, E. M. & Elliott, G. F. (1982). *J. Physiol.* **327**, 72–73*P*.
Bartels, E. M. & Elliott, G. F. (1985). *Biophys. J.* **48**, 61–76.
Nakamura, H., Jilka, R. L., Boland, R. & Martonosi, A. N. (1976). *J. biol. Chem.* **251**, 17, 5414–5423.

A STRUCTURAL STUDY OF GELS, IN THE FORM OF THREADS, OF MYOSIN AND MYOSIN ROD

P. H. COOKE, E. M. BARTELS, G. F. ELLIOTT, AND R. A. HUGHES
Biophysics Group, The Open University, Oxford Research Unit, Oxford, OX1 5HR, United Kingdom

INTRODUCTION

When a glycerinated, cross-striated muscle cell goes from relaxation to rigor at pH 7, with the removal of ATP, the fixed negative electrical charge in the A-bands increases by ~40% (Bartels and Elliott, 1980, 1981, 1982, 1985). The addition of ATP to the rigor muscle causes the A-band charge to decrease again; the charge change is reversible. The major A-band protein is myosin, and each head of the myosin molecule has a single nucleoside phosphate binding site (Young, 1967; Luck and Lowey, 1968). Possible sites for the initiation of the A-band charge change might therefore be the myosin heads or some other part of the myosin molecule under the influence of ATP binding to the heads.

To find out more about the site of the charge changes in the A-band, a gelled thread of purified myosin, containing oriented filaments, has been developed. In this preparation the protein concentration is comparable to the concentration of A-band myosin. A preparation of gelled purified myosin rod (the myosin molecule without the two globular heads) has also been prepared. Donnan potentials have been measured from these preparations in rigor and relaxing solutions at several ionic strengths (Bartels et al., 1985; and paper in preparation).

This paper and the one that follows (Poulsen et al., 1987) describe the preparation and structure of the threads, as investigated by electron microscopy and x-ray diffraction. The electrical measurements on the threads will be reported in full in a subsequent paper (Bartels, E. M., P. H. Cooke, G. F. Elliott, and R. A. Hughes, manuscript in preparation). Preliminary reports of some of these experiments have appeared previously (Cooke et al., 1984; Bartels et al., 1985, 1986).

METHODS

Preparation of Myosin and Myosin Rod

Back and leg muscles (400–500 g) were excised from rabbits that had been killed by cervical dislocation. Bulk quantities of myosin (2–7 g) were isolated and purified according to the method described by Starr and Offer (1982). There was one modification of their method; the initial precipitation of protein from Guba-Straub solution was allowed to settle overnight at 4°C. About 50–80% of the crude myosin, subjected to anion-exchange (DEAE) chromatography, was eluted, after binding to the column, by the addition of 0.1–0.3 M KCl to the buffer. These KCl fractions contained the purified myosin from which the gelled threads of myosin were prepared.

Myosin rod was prepared from a papain digestion of purified myosin, using the procedures of Margossian and Lowey (1982) for producing heads and rod subfragment. The purified rod fraction was finally re-dissolved in a small volume of a solution containing 0.6 M KCl, 0.05 M potassium phosphate buffer (pH 7.0).

The purity of the myosin and rod subfragment preparations was checked by SDS gel electrophoresis, and no significant contamination by other proteins was observed.

The K^+ EDTA-activated ATPase activity of the purified myosin and myosin threads was estimated in a system containing 0.3 M KCl, 0.1 M Tris/HCl (pH 7.5) with 0.005 M K_2EDTA. The liberated inorganic phosphate was measured at 730 nm after the addition of ammonium molybdate and Fiske and Subbarrow (1925) reagent. The activity of myosin thread samples was also determined in the experimental solutions.

The Manufacture of the Protein Threads

To produce a fixed protein phase suitable for measuring Donnan potentials with microelectrodes, separate methods were devised for handling myosin and myosin rod. For myosin, 1–2 g of the protein at 5–10 mg/ml was induced to form bipolar filaments by dialysis to equilibrium in 0.1 M KCl, 0.005 M $MgCl_2$, 0.02 M potassium phosphate buffer (pH 7). This is the basic rigor solution, which we will call standard rigor solution (see Table I). After 24 h, the suspension of filaments was sedimented by centrifugation in 38-ml tubes at 65,000 *g* for 2 h. The translucent paste containing sedimented filaments, was transferred to a 10-ml syringe equipped with a 4-cm long silicone rubber tubing with an inside diameter of 0.56 mm and a wall thickness of 1.57 mm. The paste of myosin filaments was extruded manually as threads up to 10-cm long into an ice-cold fivefold dilution of the standard rigor solution, at a rate of 1–2 cm s^{-1}. The extruded protein quickly gelled into an opaque thread and settled to the bottom of the container. It was allowed to stand undisturbed for several hours at 4°C, before further manipulation.

For myosin rod, 1–2 g of purified rod subfragment were dialyzed into filamentous tactoids according to the procedure of Margossian and Lowey (1982) and were then sedimented by centrifugation at 16,000 *g* for 40 min. The supernatant fluid was decanted and a small volume of 1.2 M KCl solution, equal to the volume of the precipitated rod, was added to the top of the pellet and mixed using a small magnetic stirring bar. This procedure slowly dissolved the precipitated rod tactoids into ~2 ml of concentrated solution containing 50–100 mg ml^{-1} protein in 0.6 M KCl. The solution was transferred by pipette to a syringe and extruded as a transparent thread, which quickly gelled, into 1–2 liters of an ice-cold solution of the fivefold diluted standard rigor solution. It was then handled in the same way as the threads of myosin.

Dr. Cooke's present address is Integrated Microscope Facility, University of Wisconsin, Madison, WI 53706.

Offprint requests should be addressed to Dr. Elliott.

TABLE I
COMPOSITIONS OF THE SOLUTIONS USED IN THIS STUDY

	KCl	$MgCl_2$	Phosphate buffer, pH 7	Na_2ATP	Na_2ADP	Ionic strength
						M
Standard rigor	100	5	20			0.141
½ Standard rigor	50	2.5	10			0.072
⅕ Standard rigor	20	1	4			0.030
Standard relax	100	5	20	2.5		0.149
½ Standard relax	50	2.5	10	2.5		0.081
⅕ Standard relax	20	1	4	2.5		0.044
Standard ADP	100	5	20		2.5	0.144
½ Standard ADP	50	2.5	10		2.5	0.080
⅕ Standard ADP	20	1	4		2.5	0.039

The amounts are given in millimoles per liter, apart from the ionic strength calculated by the Perrin programme, which is molar.

The myosin and the rod threads that were not used during the week of reparation were stored in a glycerinating solution at −20°C. The lycerinating solution contained 50% glycerol and 50% of a solution with composition of 0.040 M KCl, 0.002 M $MgCl_2$, 0.008 M phosphate uffer, pH 7. The glycerinated threads were soaked for 1 h in fivefold iluted standard rigor solution before experiments were carried out. here were no differences in the measurements of charge-concentration btained from experiments with fresh threads and with glycerinated hreads.

Electron Microscopy

he threads were examined either as thin sections of embedded segments r as small fragments produced by mechanical homogenization. In mbedding, oriented 3–4-mm long segments were treated with 1% lutaraldehyde in an appropriate rigor solution for at least 1 h and then nmersed in a solution of 2% OsO_4 and 0.1 M *s*-collidine at pH 7.2. The hreads were then dehydrated for 2 h by immersion in a graded series of thanol solutions and finally embedded and cured in an epoxy resin ixture. Thin sections of oriented threads were stained with solutions of ranyl acetate and lead citrate.

Filaments were also isolated from segments of the threads by mechanical homogenization in a tissue grinder. The homogenate was adjusted to a rotein concentration of 0.1–0.2 mg/ml by the addition of rigor solution nd drops were applied to Formvar-carbon–coated specimen screens and tained with 2% uranyl acetate after removal of the excess solution by bsorption into filter paper.

X-ray Diffraction

he x-ray data were obtained using the synchrotron radiation source at)aresbury. All recordings were taken on the low-angle scattering camera /ith a specimen-to-film distance of ~2 m; the exposure time on film was 0 min for a meridional pattern and 5 min for an equatorial pattern. Some -ray diffraction patterns were taken on Caeverken AB Reflex 25 film, nd some were recorded using the linear proportional counter. This epended on the configuration that was in use for the parallel x-ray tudies on corneal collagen from this laboratory (e.g., Sayers et al., 982).

The specimens consisted of straight parallel bundles of 5–10 threads. hese were fixed in a circular muscle cell, similar to the perspex cell escribed in Naylor et al. (1985). The distance between the mylar /indows in the cell was 1–2 mm. To use the beam dimensions for aximum resolution, the thread preparations were placed vertically for eridional diffraction and horizontally for equatorial diffraction.

Because the specimen-to-film distance varied from run to run at the ynchrotron, the x-ray spacings were calibrated against the collagen period, assuming that the spacing in wet, freshly dissected, rat-tail tendon in (0.15 M) sodium chloride was 67.0 nm.

Measurement of the Volume and Volume Changes of the Protein Threads

The threads were normally taken to be cylindrical (constant diameter) and their volume was calculated as $\pi l r^2$, where l is the length of the thread and r is the radius. A few rod threads were clearly more ellipsoidal in shape and in those cases the volume was calculated as $\pi\ lab$, where l is the length of the thread and a and b are the two half diameters of the ellipse. The diameter and length of the thread were measured under the microscope using a micrometer scale; 10 measurements were taken over a 1-cm long thread. These measurements were taken on a Zeiss Ultraphot microscope at a final magnification of 68 or on a Zeiss 405 inverted microscope with a final magnification of 25. In no case did we observe any length changes when the experimental solutions were changed.

A swelling factor, S_1, was defined as

$$S_1 = d_2^2/d_1^2,$$

where d_1 is the diameter in the equilibration solution and d_2 is the diameter in a particular experimental solution. This factor was then used to correct for volume changes between the different experimental solutions. The equilibration solution was the fivefold diluted standard rigor solution, at pH 7. The opacity of the threads was also noted during these experiments; some interesting transparency changes were observed.

Determination of the Protein Concentration in the Threads

Protein concentration was determined by the microbiuret methods (Leggett-Bailey, 1967). Threads of known volume were completely digested in a known volume of 3% NaOH before assay. The measurements gave the total amount of protein in a given sample, and the protein concentration in the thread was then calculated in milligrams of protein per milliliter.

Most protein determinations were carried out on samples in the equilibration solution (fivefold diluted standard rigor solution) since all threads are produced and are easy to handle in this solution. When the threads were transferred to the other experimental solutions, it was assumed that there was no diffusion of protein out of the sample, so the protein concentration of a thread in the new solution was P/S_1, where P is the protein concentration in the fivefold diluted rigor solution, and S_1 is the swelling factor, remembering that the threads did not change their length during swelling.

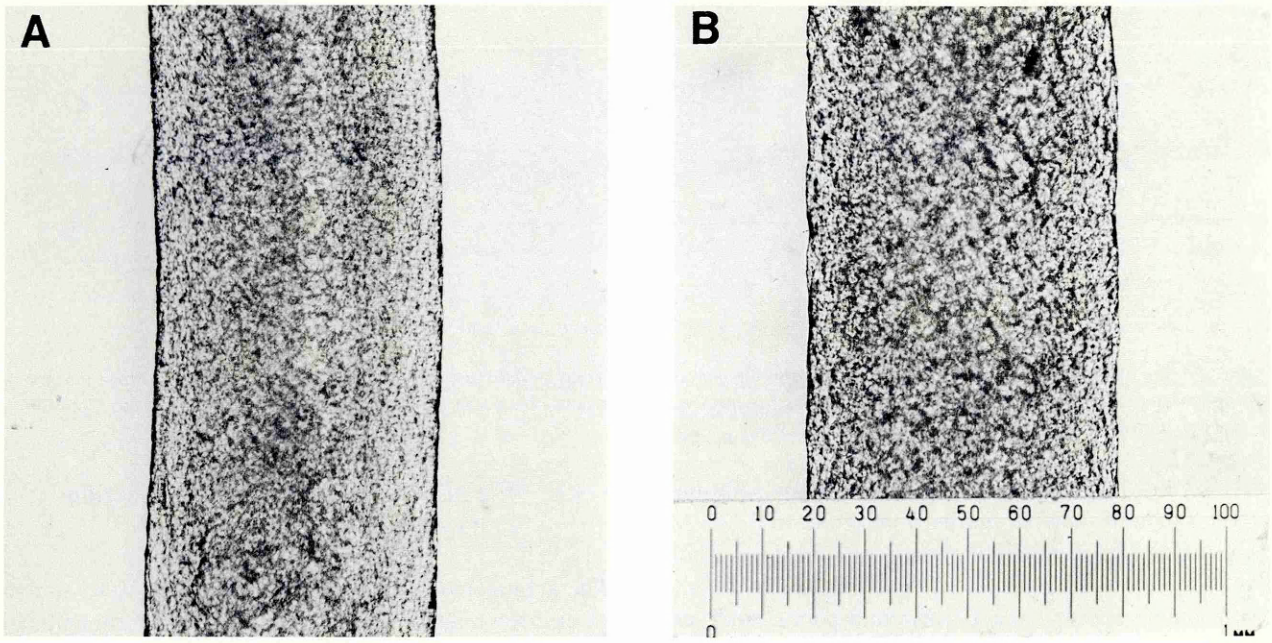

FIGURE 1 Two optical micrographs illustrating changes in diameter of segments of the same gelled thread of myosin in solutions of different ionic strength (the effect of the ligand ATP is similar). In *A*, the thread is condensed at low ionic strength (the fivefold diluted rigor solution, 0.030 M) after extrusion. In *B*, an increase in ionic strength to standard rigor solution (0.141 M) results in a 10% increase in diameter. Scale is 1 mm. 68×.

RESULTS

Morphology and Structure of the Protein Threads

The structure of the threads was designed empirically to provide solid, cylindrical gels of nearly microscopic dimensions at protein concentrations that compare with the density of myosin in the A-bands of muscle.

Light Microscopy

Fig. 1 shows a gelled thread of myosin at equilibrium with two solutions at different ionic strengths. At low ionic strength ($\mu = 0.030$ M) in dilute rigor solution excluding ATP, the diameter of the thread with a protein concentration of 125 mg ml^{-1} was uniformly ~550 μm (Fig. 1 *A*).

After (*a*) the addition of 0.0025 M ATP and adjusting the pH back to 7, (computed $\mu = 0.044$ M) or (*b*) increasing the ionic strength by substitution with standard rigor solution ($\mu = 0.141$ M), the diameter of the threads increase to 580–600 μm, which is an increase of ~10% (Fig. 1 *B* shows rigor, $\mu = 0.141$ M). A further addition of 0.0025 M ATP to the standard rigor solution at physiological ionic strength ($\mu = 0.149$ M) resulted in a >30% increase in diameter of the thread, to over 700 μm. These changes in diameter were essentially complete in 10–15 min and were reversible for up to 5 h of exposure to the solutions at ionic strengths <0.15 M. Table II gives the average changes in the swelling factor calculated from the diameter changes.

Electron Microscopy of Whole Filaments

The microscopic structure of the threads made from myosin were based on typical reconstituted filaments (Huxley, 1963). Fig. 2 shows an electron micrograph of a single, isolated filament from the homogenate produced by liquid shearing of a gelled thread. For dilute suspensions

TABLE II

Solution	N. of experiments	S_1	$\pm\sigma$
Myosin			
Standard rigor	30	1.64	0.18
½ Standard rigor	66	1.27	0.16
⅕ Standard rigor	58	1	—
Standard relax	28	2.06	0.39
½ Standard relax	46	1.50	0.24
⅕ Standard relax	40	1.33	0.19
Standard ADP	14	1.73	0.22
½ Standard ADP	22	1.33	0.20
⅕ Standard ADP	20	1.15	0.20
Myosin rod			
Standard rigor	26	1.02	0.06
½ Standard rigor	26	1.02	0.06
⅕ Standard rigor	26	1	—
Standard relax	24	1.06	0.06
½ Standard relax	22	1.05	0.04
⅕ Standard relax	20	1.08	0.06

The number of experiments, and the swelling factors with their standard deviations in the various solutions, for threads of myosin and of myosin rod. With myosin rod the swelling factor is not significantly different from unity in any solution.

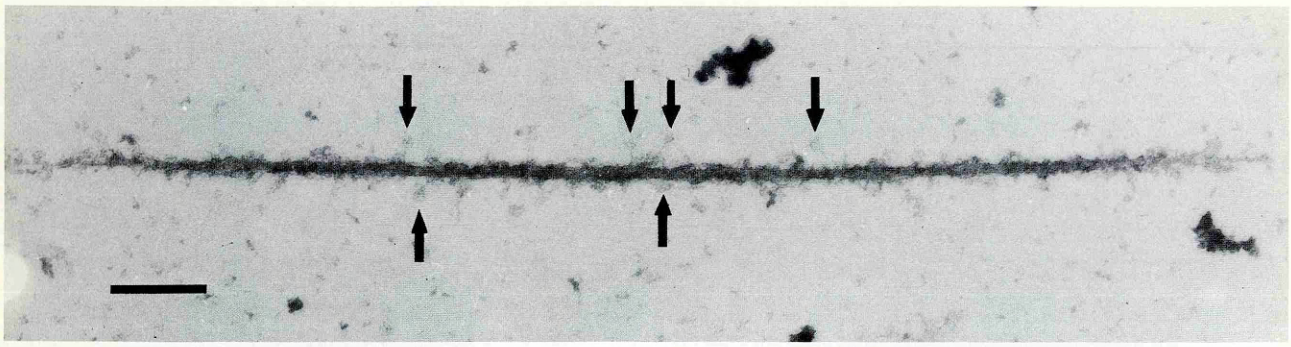

FIGURE 2 Electron micrograph of an isolated myosin filament obtained from a dilute suspension, made by homogenizing a thread in rigor solution at an ionic strength of 0.072 M. Projections (*arrows*) with dimensions of the size and shape of myosin molecules extend from the tapered, bipolar shape. Bar, 100 nm. 128,000×.

~0.1–0.2 mg ml^{-1} protein) in standard rigor solutions, over the range of ionic strengths from 0.072 to 0.141 M, nearly all of the isolated filaments examined as whole mounts by electron microscopy were between 1- and .5-μm long, ~15-nm wide at their mid-points, and very gradually tapered along both ends. A central bare zone was not always observed; instead, irregular projections extended from the filament shafts along the entire length (see Fig. 2).

Electron Microscopy of Thin Sections of Threads

The arrangements of filaments in threads were analyzed by electron microscopy of thin sections cut from embedded segments. A set of results, corresponding to the series of swollen threads studied by light microscopy, is illustrated in Fig. 3.

In cross-sections of threads that were fixed at low ionic

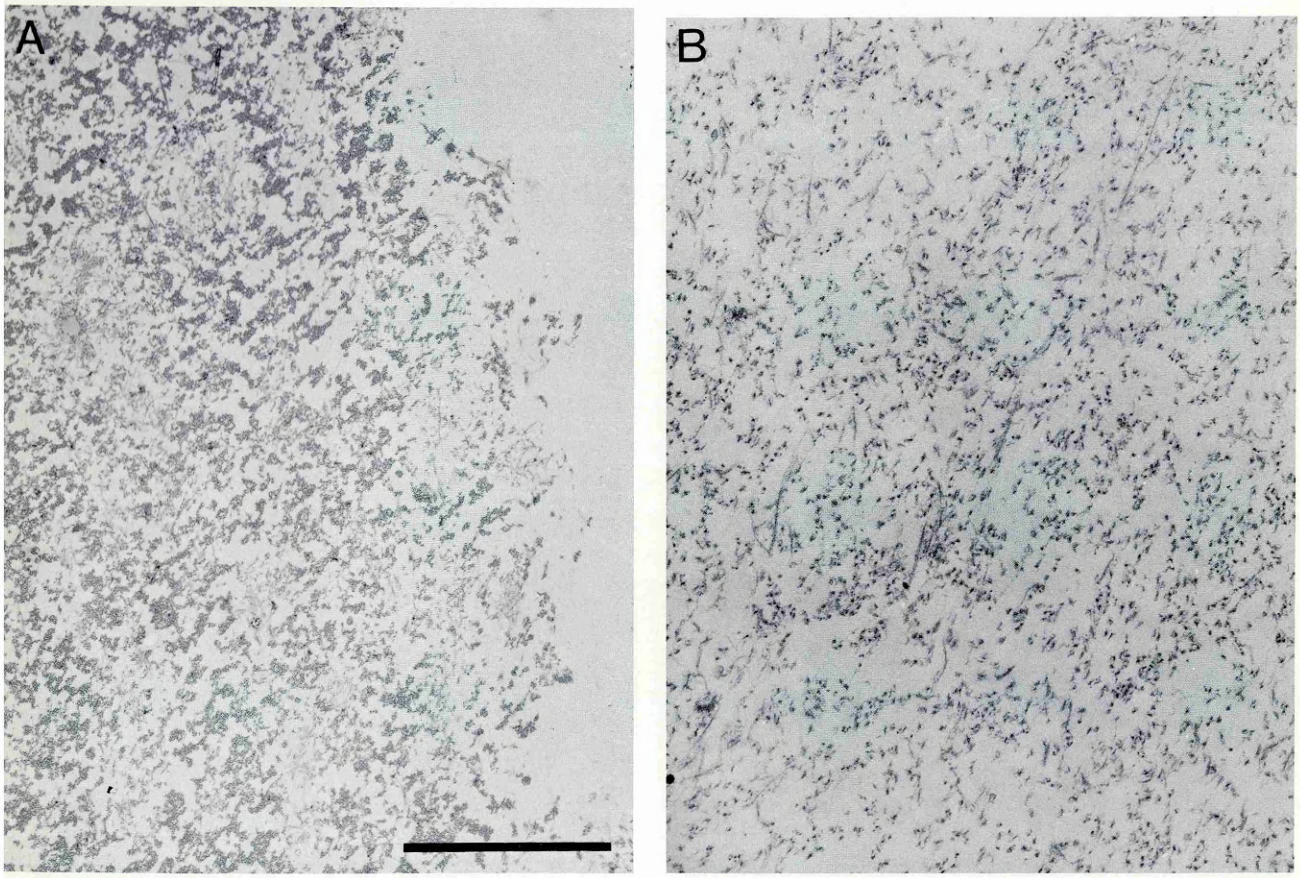

FIGURE 3 Electron micrographs illustrating thin sections of a fixed embedded series of swollen threads. *A* indicates an area of the edge and a cortical area (25-μm deep) of a thread. Irregular bundles of close-packed filaments in nearly exact cross-section and resembling muscle A-bands in size are seen. The filament bundles are separated by clear regions of comparable areas. *B* demonstrates the effect of 0.0025 M ATP in a relaxing solution of low ionic strength (0.044 M). Bar, 1 μm. 28,000×.

strength (0.030 M) and viewed at low magnifications, nearly all the filaments appeared in cross-sectioned profile, indicating mainly axial orientations, and were tightly packed into irregular groups, with intervening clear areas of comparable and irregular size (Fig. 3 *A*). This pattern of arrangement and orientation among the filaments was uniform over large areas in cross-sections, primarily in its cortical 50 or 60 μm, or 25% of the thread diameter.

When the cross-sectional profiles of the filaments were clearly resolved, differences in the packing arrangements in swelled threads were evident. At low ionic strength, bundles contain irregular groups of 50 to over 100 compact filament-profiles with an average near-neighbor spacing of ~34 nm, as determined by optical diffraction (Fig. 3 *A*). The morphological effects resulting from addition of the ligand ATP, causing a relatively minor increase in ionic strength from 0.030 to 0.044 M, are shown in Fig. 3 *B*.

In the presence of 0.0025 M ATP, the profiles of filaments appeared to be widely dispersed and retained no evidence of a uniform interfilament spacing or close packing into bundles separated by clear spaces. Similarly, a significant increase in total ionic strength of the solution phase (a shift from 0.030 to 0.141 M) appeared to disperse the bundles of filaments, and a broad distribution of distances between filament profiles were seen.

High-power transverse sections of the threads (Fig. 4) show that the myosin filaments are quasi-regularly packed, that they have a solid back bone, and are surrounded by a continuous halo, which probably consists of disordered heads. The interstitial spaces are clearly seen in this micrograph, which is of a thread in the fivefold diluted rigor solution. It is, however, difficult to judge the degree of regularity in the filament packing from such micrographs; there are some regions where the packing appears roughly hexagonal but on the whole the order appears liquid-like, with perhaps a nearest neighbor spacing (see the x-ray results, below).

The shape of the filaments seen in cross-section is very variable, probably because the range of alignments means that the cross-section is rarely precise. Sometimes the cross-sectioned filament appears more circular, with a hint of fine subfilaments (or projection origins).

In longitudinal sections of plastic-embedded threads at low ionic strengths, the filaments were grouped into an axially oriented trabecular network of bundles. Each bundle contained a staggered arrangement of filaments, numbering from 5 to 10 filaments in a section of the small bundles to upwards of 50 filaments in large bundles. The bundles were roughly aligned with the fiber axis. This alignment varied from bundle to bundle, however, with most filaments in most bundles within ~ ±15° of the fiber axis. Occasional bundles, or single filaments, were at greater angles to the axis, and there are also electron-dense dots, some of which are probably cross-sections of such

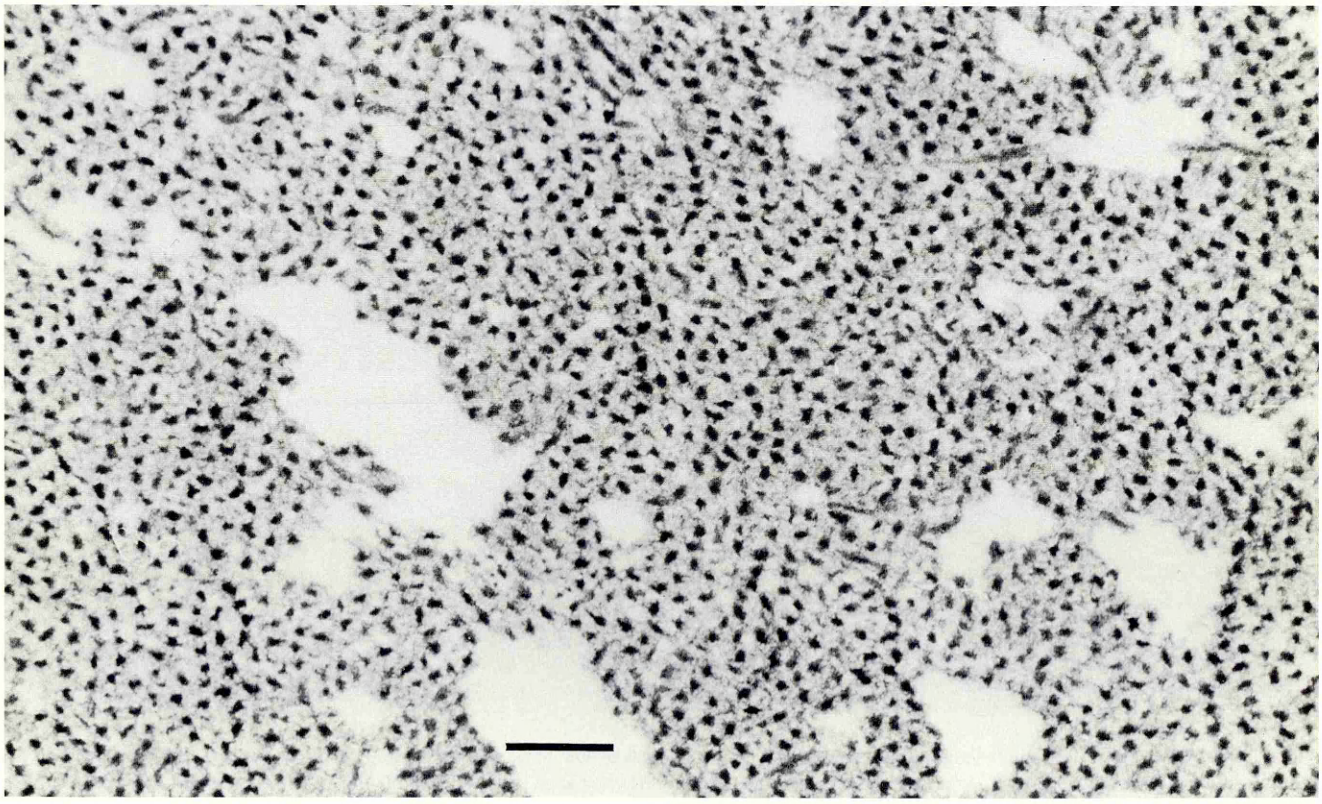

FIGURE 4 Higher power transverse section at 0.030 M ionic strength, showing details of the cross-sectional profiles of the filaments, and the surrounding halo, which represents the myosin head region. Bar, 250 nm. 59,000×.

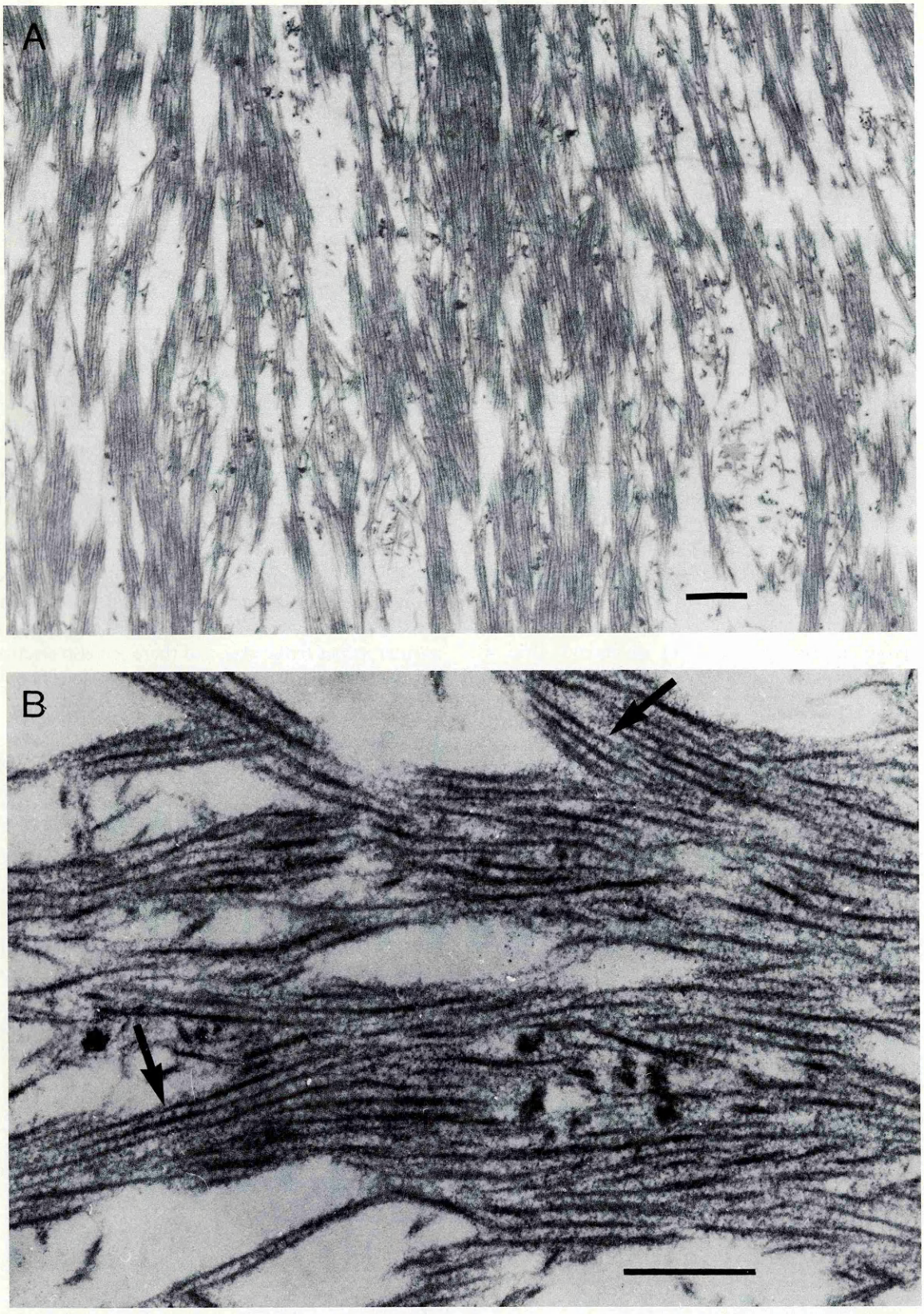

FIGURE 5 *A* shows low-power longitudinal section of a myosin thread at low ionic strength (0.030 M). The orientation of the bundle directions, and the intervening clear regions, can be seen. The fiber axis is vertical on the page. Bar, 500 nm. 20,000×. *B* shows higher power longitudinal section showing a single myosin filament bundle. The arrows show the cross connections, arranged like the rungs of a ladder. The fiber axis is horizontal on the page. Bar, 250 nm. 88,000×.

misaligned filaments. The interstices of the filamentous network were clear and comparable in size to the filament bundles. These interstitial spaces appeared to contain little or no electron dense materials. All these features can be seen in low power micrographs of longitudinal sections (Fig. 5 *A*).

In higher magnification longitudinal sections (Fig. 5 *B*), the filaments appear to have a dense shaft, ~10–12 nm in diameter, and wispy projections can be seen from these shafts. In adjacent filaments these projections often give a ladder-like effect (see the arrowed regions in Fig. 5 *B*). The spacing of the rungs on these ladders could not be measured with any precision, but it seemed to be in the range 13–20 nm.

Electron Microscopy of Myosin Rod

When aliquots of concentrated tactoids made from aggregated myosin rod subfragments in the standard rigor solution were extruded over the same ionic strength gradient that was used for myosin filaments, stable gelled threads did not form. Instead, the threads dissociated into a suspension of rod filaments or tactoids within a few hours (Fig. 6 *A*), presumably because the aggregates of rod were unable to cross-link into a network of bundles.

To induce soluble rod subfragments to gel in extruded threads, very concentrated solutions of rod were extruded into a large volume of low ionic strength salt solution (see Manufacture of Threads). The structure of the resulting gels in thin section was unusual (Fig. 6 *B*): one component was identical to the filamentous tactoids, but another major component was unique. It consisted of stellate or elongated clusters of fine radially oriented strands, possibly molecules or small aggregates of rods, ~200-nm long, mutually linked into a geodesic network extending throughout the longitudinal and transverse axes of the gelled threads. This geodesic network encloses rod filaments or tactoids, which look very much like those in the suspension seen in Fig. 6 *A*, taking account of the different staining conditions of the two micrographs. Probably these tactoids are identical in the two preparations.

X-ray Diffraction Patterns

Myosin. The electron micrographs of the myosin gels showed regular, roughly parallel, myosin filaments. The x-ray pattern, as would be expected, shows a merid-

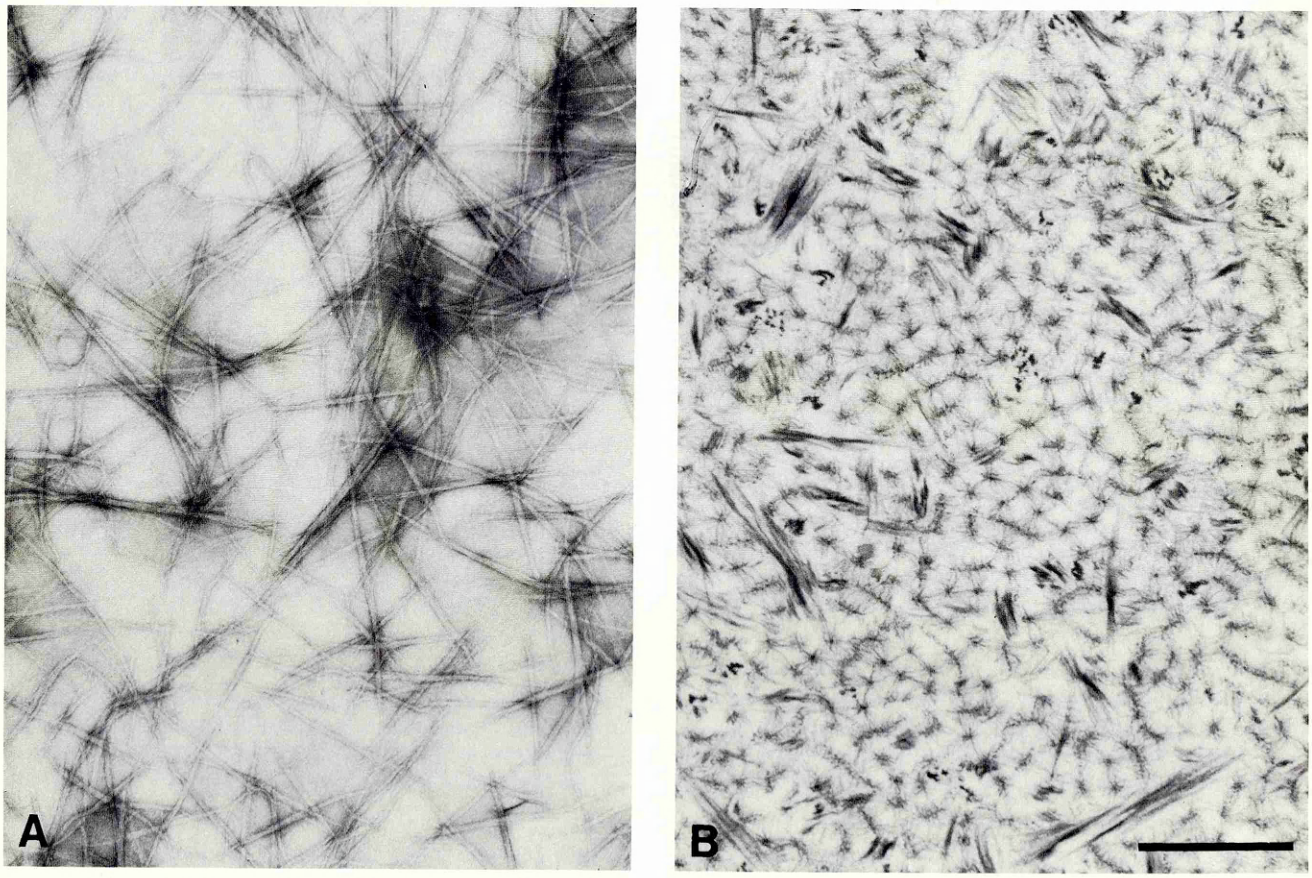

FIGURE 6 In *A*, typical tactoidal filaments of purified myosin rod subfragment are shown in a negatively stained preparation. These filaments did not form a solid gelled thread. In *B*, rod subfragments in a gelled thread are shown, organized as a mixture of filamentous tactoids and cross-linked stellate clusters, in a thin-sectioned, embedded preparation. Bar, 1 μm. 20,000×.

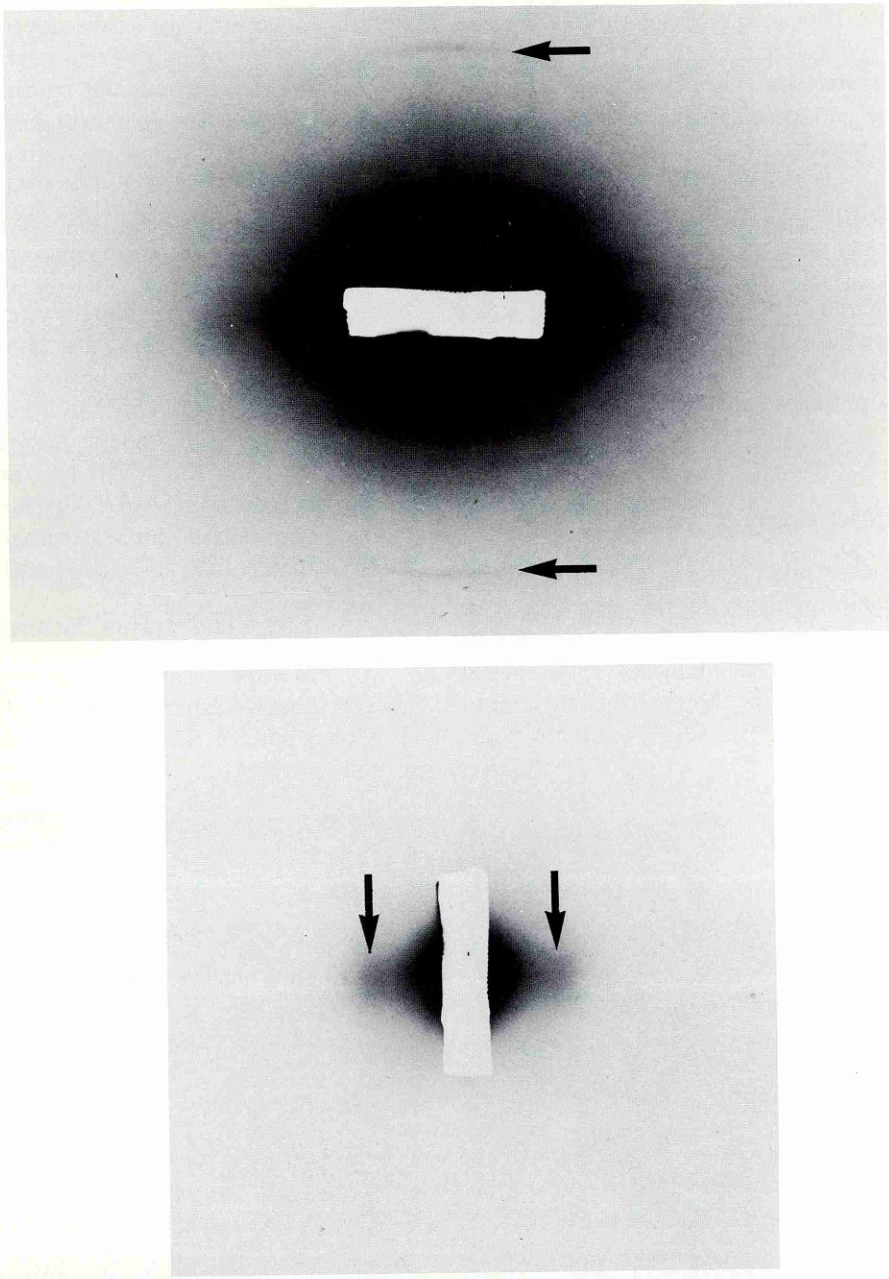

FIGURE 7 X-ray diagrams from myosin threads, fiber axis vertical, in the fivefold diluted (0.030 M) rigor buffer. (*Top*) The meridional pattern, showing the clear, arced, 14.4-nm meridional reflection (marked by an arrow) and the continuous low-angle scattering. (*Bottom*) The equatorial pattern, showing the single diffuse equatorial reflection at 38.0 nm, marked by arrows.

ional spacing of 14.4 ± 0.7 nm (SD, 12 observations, four on film and eight using the proportional counter). Fig. 7 *A* shows a meridional x-ray pattern of a myosin thread taken on film. The 14.4-nm meridional reflection is seen clearly, but compared with an intact muscle it shows considerable arcing across the meridian. The 14.4-nm meridional reflection must come from a relatively well-ordered component and this is likely to be the filament backbone, probably consisting of the light meromyosin subfragment of the myosin molecules. Occasionally there were traces of other meridional reflections, particularly on the counter spectra, but these could not be measured with any precision, and might have been artifacts of the apparatus. No off-meridional layer lines, which could have been interpreted as an organized state of the myosin heads, were seen in any of our patterns.

In the equatorial direction, a single reflection is seen (Fig. 7 *B*). This looks too diffuse to be the (1, 0) spacing of a hexogonal lattice, and by analogy with the cornea (Sayers et al., 1982), it is probably the nearest neighbor distance in a packing that is essentially like a two-dimensional liquid. The spacing of this reflection is ~39

nm both in the fivefold and the twofold diluted rigor solution.

A strong diffuse scatter is seen in the central region, similar to the scatter reported in intact muscles (Poulsen and Lowy, 1983) as arising from the myosin head subfragments, scattering in a disordered mode. A full analysis of this diffuse scatter is described in the paper that follows (Poulsen et al., 1987).

Myosin Rod. Only a few x-ray patterns were recorded from myosin rod threads, and these were taken with the camera operating with the counter, because this was the mode that was operative when rod specimens were available. As might be expected from the electron micrographs, the spacings are different from those of the myosin threads and spacings recorded from intact muscles. In both the meridional and equatorial directions these preparations gave a diffuse spacing at ~19.0 nm. There is, then, some regularity in the structure of these threads, and this is probably related to the cluster and sheet appearance seen in Fig. 6. We intend to follow up on these observations in future experiments at the Daresbury synchrotron.

ATPase Activity of Myosin

With myosin threads solubilized in the assay reagents, typical K^+ ATPase values were 0.1–0.2 μM mg protein^{-1} min^{-1}. This is similar to classical values under these conditions. In the fivefold diluted rigor solution used in the thread experiments, these values were reduced to 6 nM mg^{-1} min^{-1}, showing that the ATPase is largely inhibited under our experimental conditions.

Protein Concentration

The protein concentration in the threads of whole myosin ranged from 60 to 170 mg ml^{-1}, and in the threads of the rod subfragment the concentration ranged from 60 to 120 mg ml^{-1}, all measured in the fivefold diluted standard solution. Most myosin threads in our experiments had a concentration of ~120 mg ml^{-1}, and most rod threads had a concentration of ~90 mg ml^{-1}.

Volume Changes between Different Conditions

The myosin threads swell with increasing ionic strength, with ATP, and to some extent with ADP, as seen in Table II where the swelling factors are given. In contrast, myosin rod preparations show negligible swelling.

DISCUSSION

Morphology of the Threads

Myosin. The electron micrographs show that the myosin threads are composed of typical reconstituted myosin filaments (Huxley, 1963), which are packed roughly parallel to the axis of the thread and are sufficiently well aligned to give both equatorial and meridional x-ray diffraction. The meridional 14.4-nm x-ray reflection arises at least in part from the backbone of the myosin filaments (Elliott and Worthington, 1959; Worthington, 1960; Elliott, 1964), since it is also seen from oriented preparation of light meromyosin (Szent-Györgyi et al., 1960). This reflection is not accompanied by the myosin layer lines, which have been attributed to the regular helical arrangement of the myosin heads or cross-bridges on the surface of the myosin filaments (Elliott, 1964; Huxley and Brown, 1967). This must mean that the myosin heads are not regularly arranged in these myosin threads but extend out randomly to form the halos that are apparent in the cross-sections. The appearance of these halos seems to depend on ionic strength and the presence of nucleotides. The halos are most extended and evident at low ionic strength. At higher ionic strength the halos are not so diffuse or so extended. Possibly this is related to the low ionic strength "cross-bridges" observed by Brenner et al. (1982), in mechanical experiments on single rabbit fibers, and also characterized structurally by Brenner et al. (1984).

A further point may be noted. The myosin threads do not disappear into solution on gentle agitation, as do the rod threads made by a similar technique. This suggests that there must be some mechanical interaction between neighboring filaments, since it is now generally agreed that the Van der Waals attractive forces between myosin filaments are insufficient to account for the cohesion of the myosin filament lattice against the disruptive effect of electrostatic repulsion between the filaments (see, for example, Millman and Nickel, 1980) so that extra elastic forces must exist. In our myosin threads, which contain only purified myosin, these elastic forces certainly involve the myosin heads. It may be sufficient to involve a "tangling" of the heads between neighboring myosin filaments. In contrast, there may perhaps be more specific head–head interactions, as has been suggested from electron micrographs of smooth muscle myosin by Sobieszek (1972) and Cooke (1975) and of striated myosin by Suzuki and Pollack (1986). Furthermore, in the low-resolution x-ray analysis of myosin subfragment 1 in tannic acid–embedded crystals (Winkelmann et al., 1985), there appears to be head–head subfragment 1 dimers, with a close interaction between the two larger regions of the tadpole-shaped myosin molecules, at the crystallographic twofold axes in the [100] planes (see Fig. 6 of Winkelmann et al.). Such dimers might also occur in our gels. In solution studies, Morel and Garrigos (1982) observed that dimers of (skeletal muscle) S-1 were predominant in the analytical ultracentrifuge at low ionic strengths and in the presence of Mg-(nucleotide). Under the conditions of their experiments, however, the EDTA light chain was missing, so that a different interaction might have been predominant (see, for example, Pastra-Landis and Lowey, 1986). The continuous low-angle scattering from these threads, arising from

he myosin heads, is discussed in the paper that follows Poulsen et al., 1987).

Myosin Rod. Threads made from myosin rod id not cohere except under conditions where the three-imensional geodesic network was formed (see Methods). his network has not been reported before for rod prepara-ions, though a similar open-mesh packing was sometimes een in negatively stained preparations of light meromyo-in by Huxley (1963), Phillpott and Szent-Gyorgyi (1954), nd King and Young (1970). Yagi et al. (1981) have hown that light meromyosin (LMM), which undergoes low dialysis from 0.35 to 0.1 M KCl, forms an extensive hree-dimensional network of strands, crossing at 64.4-nm ntervals. They suggest that in these nets the LMM nolecules pack antiparallel, with the NH_2-terminal end of he subfragment molecule starting at a node in the lattice nd the COOH-terminal end finishing in an overlap region nidway between nodes. If a similar packing occurs in the od nets seen in our threads, the extra length introduced by wo S-2 subfragments, each ~70-nm long, would simply ıccount for the difference between the figures of 64.5 nm n the LMM nets and the ~200 nm, which we observe in he rod nets (see Fig. 6 *B*).

The Swelling of Myosin and Myosin Rod

nspection of the swelling coefficients of the myosin rod ;els (Table II) show that these swell very little, <10% by 'olume, under any of the conditions examined. This proba-)ly reflects the three-dimensional nature of the geodesic ıetwork, which is likely to constrain, with strong elastic 'orces, any volume changes that might otherwise be gener-ıted by charge changes. The myosin gels are a different natter; in the phosphate buffer the volume in the standard 'igor solution is 64% greater than in the fivefold diluted :quilibration solution. The addition of ATP to the fivefold liluted equilibration solution, to give the equivalent relax-ng solution, causes a 33% volume increase, and standard :elaxing solution causes the largest increase, a 100% ncrease by volume over the equilibration solution. The rigor and relaxed series, and indeed the ADP series as well, ıll swell with increasing ionic strength, but at a given ionic ;trength the relaxed series is more swollen than either the rigor or the ADP series, by about an extra 10% (volume) at low ionic strengths and by as much as an extra 30% (volume) at the highest ionic strengths. It is thus clear the volume of these gels is not simply related to the charge. In general the charge increases with ionic strength (Bartels, E. M., P. H. Cooke, G. F. Elliott, and R. A. Hughes, manuscript in preparation; see also Bartels and Elliott, 1985) and the volume increases with ionic strength in both the absence and the presence of ATP, so the increased swelling could be a function of the extra charge. However, in the presence of ATP the charge is lower than in its absence (Bartels et al., 1985), so the increased volume in the presence of ATP must be due to other effects of the nucleotide. Perhaps ATP decreases the head–head interaction between different filaments (see Myosin in Discussion), which would constrain the gel from swelling. This conflicts with the observations of Morel and Garrigos (1982), who observe extra dimerization of myosin heads in the presence of Mg ATP. It does, however, agree with our own electron microscope observations (Fig. 3, *A* and *B*), where the addition of ATP at constant salt concentration appears to decrease the clumping of the myosin filaments and to make them distribute more evenly in the available space. This phenomenon is also in accord with the qualitative interpretation of the transparency changes. These interesting effects warrant further study.

We thank Mr. Austin Elliott for expert assistance with some of the protein preparations, and Dr. Carl Moos and Ms. Katy Jennison for ready biochemical advice and enthusiastic interest in the project. We are grateful to Ms. Dawn Collins for help with the photography and diagrams and to Ms. Jill Uttley for word-processing of the manuscript.

We are also grateful for Science and Engineering Research Council grants GRC-26521 and GRB-66776 to G. F. Elliott and E. M. Bartels.

Received for publication 11 July 1986 and in final form 21 December 1986.

REFERENCES

Bartels, E. M., and G. F. Elliott. 1980. Donnan potential measurements in the A- and I-bands of cross-striated muscles and calculation of the fixed charge on the contractile proteins. *J. Muscle Res. Cell Motil.* 1:452.

Bartels, E. M., and G. F. Elliott. 1981. Donnan potentials from the A- and I-bands of skeletal muscle, relaxed and in rigor. *J. Physiol. (Lond.).* 317:85–87P.

Bartels, E. M., and G. F. Elliott. 1982. Donnan potentials in rat muscle: difference between skinning and glycerination. *J. Physiol. (Lond.).* 327:72–73P.

Bartels, E. M., and G. F. Elliott. 1983. Donnan potentials in glycerinated rabbit skeletal muscle: the effect of nucleotides and of pyrophosphate. *J. Physiol. (Lond.).* 343:32–33P.

Bartels, E. M., and G. F. Elliott. 1985. Donnan potentials from the A- and I-bands of glycerinated and chemically skinned muscles, relaxed and in rigor. *Biophys. J.* 48:61–86.

Bartels, E. M., P. H. Cooke, G. F. Elliott, and R. A. Hughes. 1985. Donnan potential changes in rabbit muscle A-bands are associated with myosin. *J. Physiol. (Lond.).* 358:80P.

Bartels, E. M., P. H. Cooke, G. F. Elliott, and R. A. Hughes. 1986. Donnan potentials in muscle A-bands and in myosin gels. *J. Muscle Res. Cell Motil.* 7:74.

Brenner, B., M. Schoenberg, J. Chalovich, L. Greene, and E. Eisenberg. 1982. Evidence for cross-bridge attachment in relaxed muscle at low ionic strength. *Proc. Natl. Acad. Sci. USA.* 79:7288–7291.

Brenner, B., L. C. Yu, and R. J. Podolsky. 1984. X-ray diffraction evidence for cross-bridge formation in muscle fibers at various ionic strengths. *Biophys. J.* 46:299–306.

Cooke, P. H. 1975. Filamentous aggregates of purified myosin from smooth muscle. *Cytobiologie.*11:346–357.

Cooke, P. H., E. M. Bartels, G. F. Elliott, and K. Jennison. 1984. Myosin threads. *Biophys. J.* 45:7a. (Abstr.)

Elliott, G. F. 1964. X-ray diffraction studies on striated and smooth muscles. *Proc. R. Soc. Lond. B Biol. Sci.* 160:467–472.

Elliott, G. F., and C. R. Worthington. 1959. Low angle X-ray diffraction patterns of smooth and striated muscle. *J. Physiol. (Lond.).* 149:32–33P.

Fiske, C. H., and Y. Subbarow. 1925. The colorimetric determination of phosphorous. *J. Biol. Chem.* 66:375–400.

Huxley, H. E. 1963. Electron microscope studies on the structure of natural and synthetic protein filaments from striated muscle. *J. Mol. Biol.* 7:281–308.

Huxley, H. E., and W. Brown. 1967. The low-angle x-ray diagram of vertebrate striated muscle and its behaviour during contraction and rigor. *J. Mol. Biol.* 30:383–434.

King, M. V., and M. Young. 1970. Selective non-enzymatic cleavage of the myosin rod. Electron microscope studies on crystals and paracrystals of light meromyosin-C. *J. Mol. Biol.* 50:491–507.

Leggett-Bailey, J. 1967. Miscellaneous analytical methods: estimation of protein. *In* Techniques in Protein Chemistry. 2nd ed., Elsevier, New York. Chapter 1. 341.

Luck, S. M., and S. Lowey. 1968. Equilibrium binding of ADP to deaminase-free myosin. *Fed. Proc.* 27:519.

Margossian, S. S., and S. Lowey. 1982. Preparation of myosin and its subfragments from rabbit skeletal muscle. *Methods Enzymol.* 85(B):55–71.

Millman, B. M., and B. G. Nickel. 1980. Electrostatic forces in muscle and cylindrical gel systems. *Biophys. J.* 32:49–63.

Morel, J. E., and M. Garrigos. 1982. Dimerization of the myosin heads in solution. *Biochemistry.* 21:2679–2686.

Naylor, G. R. S., E. M. Bartels, T. D. Bridgman, and G. F. Elliott. 1985. Donnan potentials in rabbit psoas muscle in rigor. *Biophys. J.* 48:47–59.

Pastra-Landis, S. C., and S. Lowey. 1986. Myosin subunit interactions. *J. Biol. Chem.* 261:14811–14816.

Philpott, D. E., and A. G. Szent-Györgyi. 1954. The structure of light meromyosin, an electron microscope study. *Biochim. Biophys. Acta.* 15:165–173.

Poulsen, F. R., and J. Lowy. 1982. Small-angle x-ray scattering from myosin heads in relaxed and rigor frog skeletal muscles. *Nature (Lond.).* 5913:146–152.

Poulsen, F. R., J. Lowy, P. H. Cooke, E. M. Bartels, G. F. Elliott, and R. A. Hughes. 1987. Diffuse x-ray scatter from myosin heads in oriented synthetic fibers. *Biophys. J.* 51:959–967.

Sayers, Z., M. H. J. Koch, S. B. Whitburn, K. M. Meek, G. F. Elliott, and A. Harmsen. 1982. Synchrotron x-ray diffraction study of corneal stroma. *J. Mol. Biol.* 160:593–607.

Sobieszek, A. 1972. Cross-bridges on self-assembled smooth muscle myosin filaments. *J. Mol. Biol.* 70:741–744.

Starr, R., and G. Offer. 1982. Preparation of C-protein, H-protein, X-protein and phosphofruktokinase. *Methods Enzymol.* 85(B):130–138.

Suzuki, S., and G. H. Pollack. 1986. Bridgelike connections between thick filaments in stretched skeletal muscle fibers observed by the freeze fracture method. *J. Cell Biol.* 102:1093–1098.

Szent-Györgyi, A. G., C. Cohen, and D. E. Philpott. 1960. Light-meromyosin fraction 1: a helical molecule from myosin. *J. Mol. Biol.* 2:133–142.

Winkelmann, D. A., H. Meekel, and I. Rayment. 1985. Packing analysis of crystalline myosin sub-fragment 1. *J. Mol Biol.* 181:487–501.

Yagi, N., M. J. Dickens, P. M. Bennett, and G. Offer. 1981. Electron microscopy and X-ray diffraction of a hexagonal net of light meromyosin. *J. Mol. Biol.* 149:787–803.

Young, D. M. 1967. On the interaction of ADP with myosin and its enzymatically-active subfragments. *J. Biol. Chem.* 242:2790–2792.

Patients with Polymyositis Show Changes in Muscle Protein Charges

ELSE MARIE BARTELS, SØREN JACOBSEN, LARS RASMUSSEN, and BENTE DANNESKIOLD-SAMSØE

Abstract. **Polymyositis (PM) appears with indolent proximal muscle weakness and is an inflammatory disease with breakdown of muscle cells. In our study the protein charge concentrations of the contractile proteins in the A and I bands were determined, applying a microelectrode technique. Patients with PM show a lower protein charge concentration than healthy control subjects which may be caused by the breakdown and removal of the proteins in the contractile filaments. A tool to judge the state of the disease as well as an aid in diagnosis may have been found in this method. (*J Rheumatol 1989;*16:1542–4)**

Key Indexing Terms:
POLYMYOSITIS MUSCLE PROTEINS MICROELECTRODE DERMATOMYOSITIS

Polymyositis (PM) is an idiopathic myopathy causing mainly skeletal muscle inflammation and subsequent breakdown of muscle cells and showing its appearance by indolent proximal muscle weakness. The progression of the disease can be more or less acute and even lethal, due to involvement of the heart or respiratory muscles. The muscle weakness is caused by the breakdown of muscle cells. Often the disease is accompanied by rashes and is then called dermatomyositis (DM)[1].

The cause of the disease is unknown. Electrical measurements of the protein charge concentration of the contractile proteins have been carried out to see if PM is associated with changes in the contractile filaments.

MATERIALS AND METHODS

Patients. The patient group consisted of 3 male and 4 female patients with definite PM diagnosed according to the criteria[2] shown in Table 1. In addition, Patient 3, a 48-year-old man, had characteristic rashes, fulfilling the criteria for definite dermatomyositis (DM). He was reexamined after 15 months. The mean age of the patients was 60 years (47–78). The mean duration of disease was 2.2 years (1 month–4 years). All patients had started treatment with prednisone shortly after PM had been diagnosed. All subjects were informed about the nature, purpose and possible risks of the experiments before giving their consent to participate.

They were compared with a group of healthy subjects investigated under similar experimental conditions[3].

From the Department of Rheumatology, Frederiksberg Hospital, Copenhagen, Denmark.

Supported in part by an SERC grant to E.M. Bartels, The Danish Medical Research Council, The Foundation of 1870, the John and Birthe Meyer Foundation, P. Carl Petersens Foundation and The Danish Rheumatism Association.

E.M. Bartels, PhD, Research Fellow at Biophysics Group, The Open University, Oxford, UK; S. Jacobsen, MD, Research Associate, Department of Rheumatology, Frederiksberg Hospital; L. Rasmussen, MD, Research Associate, Novo-Nordisk A/S; B. Danneskiold-Samsøe, MD, DM, Head of Department of Rheumatology, Frederiksberg Hospital.

Address requests for reprints to Dr. E.M. Bartels, The Open University, Oxford Research Unit, Foxcombe Hall, Berkeley Road, Boars Hill, Oxford, UK.

Submitted May 15, 1989 revision accepted September 25, 1989.

Muscle samples. Biopsy specimens were taken from the vastus lateralis of the quadriceps muscle using a Bergström needle[4–6]. The biopsy specimens were transferred directly from the Bergström needle to a glycerinated solution to remove the cell membranes and internal membrane systems[7]. After a preparation period of 3 days where the glycerinated solution was changed every 8 h, the glycerinated specimens were stored in the freezer at -25°C in the glycerinated solution. After 3 weeks the preparations were ready for measurement. The glycerinated solution was a 50% glycerol solution buffered at pH 7.0 with 10 mM phosphate buffer and containing 50 mM KCl, 1 mM $MgCl_2$ 2 mM EGTA.

Electric charge measurements. The protein charge concentration in the A and the I bands of the muscles was determined by measuring the Donnan potentials with a microelectrode technique and calculating the protein charge concentrations using Donnan theory as described[8]. About 100 readings were taken from each muscle fiber bundle. All measurements were performed under high power light microscopy (400 x) with phase and polarization contrast which allowed localizing the electrode tip (diameter 0.1–0.2 μm) in either the A or the I bands.

The muscle specimens were measured in 2 rigor and 2 relaxing solutions. Rigor solution 1 contained (mM) KCl 100, $MgCl_2$ 5 and phosphate buffer (pH 7) 20. Relaxing solution 1 contained (mM) KCl 100, $MgCl_2$ 10, EGTA 4, Na_2ATP 5 and phosphate buffer (pH 7) 20. Rigor solution 2 was half the concentration of rigor solution 1 and relaxing solution 2 was half the concentration of relaxing solution 1. Muscle preparations were soaked in the experimental solution 1 h before any measurements were taken to assure an equilibrium condition.

Statistics. Differences between means were tested for significance by Student's unpaired 2-tailed t test. A value of $p < 0.05$ was considered significant.

RESULTS

Protein charge concentrations. Table 2 shows the average protein charge concentrations in PM muscles and in normal

Table 1. *Diagnostic criteria in PM/DM*[2]

1. Proximal muscle weakness of the limbs.
2. Raised muscle enzymes.
3. Myopathic EMG.
4. Microscopic signs of myositis.
5. Characteristic skin rashes.

Definite PM: criteria 1–4 must be satisfied.
Definite DM: 3 of the first 4 criteria and criterion 5 must be satisfied.

Table 2. *Protein charge concentration (mmol/l) in the A and I bands of PM and normal muscle in Rigor solution 1 and 2 and in Relaxing solution 1 and 2*

	Control Group (n=7)	PM Group (n=7)	Reduction in Protein Charge Concentration*
	Mean ± SD	Mean ± SD	(%)
Rigor 1			
A band	−60 5	−45 8	25.7
I band	−32 6	−26 5	18.3
Rigor 2			
A band	−60 4	−45 5	25.7
I band	−40 3	−26 1	34.3
Relaxing 1			
A band	−45 5	−34 3	23.9
I band	−45 5	−34 3	24.4
Relaxing 2			
A band	−51 4	−35 1	30.8
I band	−51 4	−36 1	29.7

* The column at the right hand side shows the charge drop between the protein charge concentration in normal subjects and in patients with PM.

muscles. The patients with PM showed a significantly lower protein charge concentration, with a relative drop in protein charge concentration ranging from 18.3 to 34.3% ($p < 0.001$ for all differences). The average reduction in charge concentration was 27%.

The patient who had been reexamined after 15 months showed a further substantial reduction in protein charge concentration between the 2 tests (Table 3). At the higher ionic strength a further reduction of 29–40% was seen while the lower ionic strength gave a reduction of 4–14%. The clinical state of the patient had seriously worsened during the 15 months that had passed between the 2 samples.

DISCUSSION

A new and interesting finding in patients with PM/DM is a significantly reduced protein charge concentration inside the muscle fibers compared to muscle fibers from healthy subjects. The presence of high serum values of creatine phosphokinase and myoglobin in PM is known to be due to breakdown of muscle cells. Microscopically, muscle fiber degeneration and infiltration of lymphocytes is seen[9]. The reduced protein charge concentration discovered in our study is probably due to this breakdown and the following loss of charged contractile proteins from the filaments. The patient in this study who had been reexamined after 15 months had lower protein charge concentrations as his disease had become worse. Even though one cannot draw any conclusions from one patient, this points towards a link between the clinical state of PM and the protein charge concentration.

Table 3. *Protein charge concentration (mmol/l) in the A and I bands of Patient 3 (DM) reexamined after one year*

	First Sample	Second Sample 15 Months Later	Reduction in Protein Charge Concentration
Rigor 1			
A band	−58	−35	40%
I band	−28	−20	29%
Rigor 2			
A band	−50	−43	14%
I band	−27	−26	4%
Relaxing 1			
A band	−38	−26	32%
I band	−37	−25	32%
Relaxing 2			
A band	−35	−32	9%
I band	−34	−32	6%

The lower charges on the contractile proteins of the patients with PM in this study might also have been induced by the steroid treatment. However, in 2 groups of patients with rheumatoid arthritis, one that did not receive steroids and one that did, no difference in protein charge concentration was found (unpublished observations). We would therefore not expect any glucocorticoid effect in patients with PM either, or if any, patients with PM not treated with glucocorticoid steroids ought to have even lower protein charge concentration than those observed in our study, since steroid treatment diminishes the breakdown of muscle cells in PM. We hope to investigate muscle biopsies from patients with PM before and after steroid treatment in the near future. Furthermore it would be interesting to investigate a possible correlation between the disease severity (e.g., extent of muscle weakness, enzyme levels and degree of inflammation) and the protein charge concentration.

Whether the low protein charge concentrations are specific to PM is not yet known, but at present we have also measured protein charge concentrations in muscle fibers from patients with myotonia congenita[10], which have shown no divergence from normal values (unpublished observations). Other disease entities which have been investigated are rheumatoid arthritis where some divergence from normal protein charge concentrations was seen at lower ionic strengths[10] and primary fibromyalgia where normal protein charge concentrations were found[3].

This microelectrode technique has been in common use for the last 30 to 40 years and the method can be set up easily by a well trained laboratory technician. Further research in other myopathic entities is necessary for determining the sensitivity and specificity of the protein charge concentration measurement technique, but it may prove to be a new aid in diagnosing PM and in judging the severity of the disease in a particular patient.

ACKNOWLEDGMENT

The authors would like to thank Professor G.F. Elliott for helpful advice and laboratory technicians Salomea Hirschorn and Jette Nielsen for technical assistance.

REFERENCES

1. Bohan A, Peter JB: Polymyositis and dermatomyositis. *N Engl J Med 1975;*292:344–7.
2. Bohan A, Peter JB, Bowman RL, Pearson CM: A computer assisted analysis of 153 patients with polymyositis and dermatomyositis. *Medicine 1977;*56:255–86.
3. Bartels EM, Danneskiold-Samsøe B: Histological abnormalities in muscle from patients with certain types of fibrositis. *Lancet 1986;*1:755–7.
4. Bergström J: Muscle electrolytes in man. *Scand J Clin Lab Invest 1962;*suppl 68.
5. Edwards RHT: Percutaneous needle biopsy of skeletal muscle in diagnosis and research. *Lancet 1971;*1:593–5.
6. Edwards RHT, Young A, Wiles M: Needle biopsy of skeletal muscle in the diagnosis of muscle function and repair. *N Engl J Med 1980;*302:261–71.
7. Naylor GRS, Bartels EM, Bridgman TD, Elliott GF: Donnan potentials in rabbit psoas muscle in rigor. *Biophys J 1985;*48:47–59.
8. Bartels EM, Elliott GF: Donnan potentials from the A- and I-bands of glycerinated and chemically skinned muscles, relaxed and in rigor. *Biophys J 1985;*48:61–76.
9. Henriksson KG, Hallert C, Norrby K, Walan A: Polymyositis and adult coeliac disease. *Acta Neurol Scand 1982;*65:301–19.
10. Crews J, Kaiser KK, Brooke MH: Muscle pathology of myotonia congenita. *J Neurol Sci 1976;*28:449–57.